MSci Andrew M. Kelly

Poly(2-oxazoline)s for Biomedical and Hygienic Applications

PhD Thesis

Dissertation

Zur Erlangung des akademischen Grades eines

Doktors der Naturwissenschaften

eingereicht an der

Technischen Universität Graz

Betreuer:

Priv.-Doz. Dipl.-Chem.Univ. Dr.rer.nat. Frank Wiesbrock

Univ.-Prof. Dipl.-Ing. Dr.techn. Franz Stelzer

Institut für Chemische Technologie von Materialien (ICTM)

September 2013

Deutsche Fassung:

Beschluss der Curricula-Kommission für Bachelor-, Master- und Diplomstudien vom 10.11.2008

Genehmigung des Senates am 1.12.2008

EIDESSTATTLICHE ERKLÄRUNG

Ich erkläre an Eides statt, dass ich die vorliegende Arbeit selbstständig verfasst, andere als die angegebenen Quellen/Hilfsmittel nicht benutzt, und die den benutzten Quellen wörtlich und inhaltlich entnommenen Stellen als solche kenntlich gemacht habe.

Graz, am …… ……..

(Unterschrift)

Englische Fassung:

STATUTORY DECLARATION

I declare that I have authored this thesis independently, that I have not used other than the declared sources / resources, and that I have explicitly marked all material which has been quoted either literally or by content from the used sources.

…… ……..

date (signature)

Publication List

Publications in a Journal

A.M. Kelly, V. Kaltenhauser, I. Mühlbacher, K. Rametsteiner, H. Kren, C. Slugovc, F. Stelzer, F. Wiesbrock, **Poly(2-Oxazoline)-Derived Contact Biocides: Contributions to the Understanding of Antimicrobial Activity**, *Macromolecular Bioscience* **2013**, *13*, 116.

A.M. Kelly, V. Kaltenhauser, I. Mühlbacher, K. Rametsteiner, H. Kren, C. Slugovc, F. Stelzer, F. Wiesbrock, **Poly(2-Oxazoline)-Derived Contact Biocides: Contributions to the Understanding of Antimicrobial Activity**, Back Cover *Macromolecular Bioscience* **2013**, *13*.

A.M. Kelly, T. Bodner, L. Ellmaier, V. Schenk, J. Albering, F. Wiesbrock, **Initiation Selectivity During CROP: Effect of π-Electrons in 2-Oxazoline Rings**, *Polymer Preprints* **2012**, *53*, 312.

F. Wiesbrock, A.M. Kelly, K. Rametsteiner, V. Kaltenhauser, F. Stelzer, **Microwave-Assisted Syntheses and Applications of Poly(2-Oxazoline)-Derived Contact Biocides**, *Polymer Preprints* **2012**, *53*, 321.

A.M. Kelly, A. Hecke, B. Wirnsberger, C. Wappl, F. Wiesbrock, **Poly(2-Oxazoline)-Based Hydrogels: Influence of the Monomers on the Swelling Degrees**, *Polymer Preprints* **2012**, *53*, 362.

A.M. Kelly, A. Hecke, B. Wirnsberger, F. Wiesbrock, **Synthesis of Poly(2-oxazoline)-based Hydrogels With Tailor-Made Swelling Degrees Capable of Stimuli-Triggered Compound Release**, *Macromolecular Rapid Communications* **2011**, *32*, 1815.

A. Hecke, B. Wirnsberger, A.M. Kelly, F. Stelzer, F. Wiesbrock, **Oxazoline-Based Hydro-, Amphi- and Lipogels from Microwave-Assisted Synthesis**, *Scientia Pharmaceutica* **2010**, *77*, 660.

Publications in a Book

F. Wiesbrock, A.M. Kelly, **Poly(2-Oxazoline)s as Additives in Polyolefin Compounds with Antimicrobially Active Surfaces**, *Advances in Polymer Science and Technology*. **2013**, 21.

F. Wiesbrock, A.M. Kelly, V. Kaltenhauser, K. Rametsteiner, F. Stelzer, **Microwave-Assisted Fabrication of Novel Polymer Contact Biocides,** *14th Austrian Chemistry Days* **2011**, 67.

A.M. Kelly, A. Hecke, B. Wirnsberger, F. Wiesbrock, **Swelling Degrees and Stimuli-Responsive Degradation of Poly(2-Oxazoline)-Based Hydrogels,** *14th Austrian Chemistry Days* **2011**, 74.

Research Reports

A.M. Kelly, F. Wiesbrock, **Microwave-Assisted Scale-up of Polymerizations and Polymeranalogous Reactions, 2013.** (Anton Paar Appliction Note.)

A.M. Kelly, F. Wiesbrock, **Scale-up of Ionic Liquid Synthesis, 2012.** (Anton Paar Appliction Note.)

Poster Presentations

A.M. Kelly, B. Wirnsberger, F. Wiesbrock, **Crosslinked Poly(2-Oxazoline)s as Membranes with High Li^+ Ion Conductivity**, *Austrian-Slovenian Polymer Meeting - ASPM* **2013**, Bled, SIovenia, 03.04.2013.

A.M. Kelly, A. Hecke, B. Wirnsberger, F. Wiesbrock, **Poly(2-Oxazoline)-Hydrogels as Matrices for Stimuli-Triggered Substance Release**, *Austrian-Slovenian Polymer Meeting - ASPM* **2013**, Bled, SIovenia, 03.04.2013.

M. Fimberger, A.M. Kelly, F. Wiesbrock, **Microwave-Assisted Scale-Up: Synthesis of OCs**, *Microwave & Flow Chemistry* **2013**, Napa, California, 20.07.2013.

A.M. Kelly, T. Bodner, L. Ellmaier, V. Schenk, J. Albering, F. Wiesbrock, **Initiation Selectivity During CROP : Effect of pi-Electrons on 2-Oxazoline Rings**, *ACS Spring Meeting* **2012**, San Diego, California, 25.03.2012.

A.M. Kelly, V. Kaltenhauser, F. Stelzer, F. Wiesbrock, **Microwave-Assisted Synthesis of Poly(2-Oxazoline)-Derived Contact Biocides**, *Microwave & Flow Chemistry Conference* **2012**, Lanzarote, Spain, 28.02.2012.

Oral Presentations

F. Wiesbrock, A.M. Kelly, V. Kaltenhauser, I. Mühlbacher, **Poly(Ethylene Imine)-Derived Contact Biocides: Fabrication of Antimicrobially Active Surfaces**, *Austrian-Slovenian Polymer Meeting - ASPM* **2013**, Bled, Slovenia, 03.04.2013.

F. Wiesbrock, A.M. Kelly, V. Kaltenhauser, **Microwave-Assisted Synthesis of Contact Biocides**, *Microwave & Flow Chemistry* **2013**, Napa, California, 20.07.2013.

F. Wiesbrock, A.M. Kelly, K. Rametsteiner, V. Kaltenhauser, F. Stelzer, **Microwave-Assisted Synthesis and Applications of Poly(2-Oxazoline)-Derived Contact Biocides**, *ACS Spring Meeting* **2012**, San Diego, California, 25.03.2012.

A.M. Kelly, A. Hecke, B. Wirnsberger, C. Wappl, F. Wiesbrock, **Poly(2-oxazoline)-based hydrogels: Influence of the monomers on the swelling degrees**, *ACS Spring Meeting* **2012**, San Diego, California, 25.03.2012.

A.M. Kelly, V. Kaltenhauser, F. Stelzer, F. Wiesbrock, **Microwave-Assisted Synthesis of Poly(2-Oxazoline)-Derived Contact Biocides (Poster Highlight)**, *Microwave & Flow Chemistry Conference* **2012**, Lanzarote, Spain, 28.02.2012.

F. Wiesbrock, A.M. Kelly, A. Hecke, B. Wirnsberger, **Libraries of non-cytotoxic hydrogels with tailor-made properties from microwave-assisted syntheses**, *Microwave & Flow Chemistry Conference* **2012**, Lanzarote, Spain, 28.02.2012.

F. Wiesbrock, A.M. Kelly, V. Kaltenhauser, F. Stelzer, **Novel Poly(2-Oxazoline)-Derived Contact Biocides**, *Advanced Polymers Through Macromolecular Engineering* **2011**, Cappadocia, Turkey, 05.09.2011.

F. Wiesbrock, A.M. Kelly, B. Wirnsberger, **Crosslinked Poly(2-Oxazoline)s: Degradable Hydrogels for Medical Applications**, *European Polymer Conference EUPOC* **2011**, Gargnano, Italy, 29.05.2011.

F. Wiesbrock, A.M. Kelly, A. Hecke, B. Wirnsberger, **Poly(2-oxazoline)-Based Non-Cytotoxic Hydrogels with Tailor-Made Swelling Degrees for Drug Delivery**, *European Polymer Congress EPF* **2011**, Granada, Spain, 26.06.2011.

A.M Kelly, A. Hecke, B. Wirnsberger, F. Wiesbrock, **Swelling Degrees and Stimuli-Responsive Degradation of Poly(2-Oxazoline)-Based Hydrogels**, *14. Österreichische Chemietage* **2011**, Linz, Austria, 26.09.2011.

F. Wiesbrock, A.M. Kelly, V. Kaltenhauser, K. Rametsteiner, F. Stelzer, **Microwave-Assisted Fabrication of Novel Polymer Contact Biocides**, *14. Österreichische Chemietage* **2011**, Linz, Austria, 26.09.2011.

Acknowledgments

Above all, I want to thank Priv.-Doz. Dipl.-Chem.Univ. Dr.rer.nat. Frank Wiesbrock and Prof. Dipl.-Ing. Dr.techn. Franz Stelzer for their outstanding commitment towards the preparation of the presented work, their sage advice, and many productive discussions. Importantly, I must thank the Polymer Competence Center Leoben GmbH for their outstanding contributions to this work both financial and academic.

Moreover, I want to thank all former and present colleagues of the working group Thomas Bodner, Clemens Ebner, Verena Schenk, Elisabeth Rossegger, Martin Fimberger, Angela Hecke, Bianca Wirnsberger, Lisa Ellmaier, Claudia Loher, Inge Mühlbacher, Hannes Offenbacher, Verena Kaltenhauser, Stefan Kalin, Stephan Nestl, Andreas Oesterreicher, Volkan Kumbaraci, László Ólah, Julia Tschische, Birgit Six, Florian Bangerl, Katrin Niegelhell, Maria Ritter, Thomas Schlatzer und Claudia Payerl for both their contributions to the work and to the ethos of the group. My special thanks go in addition to Karl Rametsteiner and Christian Slugovc for their valuable collaboration on the biocide work.

Furthermore, I owe thanks to all my colleagues at the Institute for Chemistry and Technology of Materials for the welcoming working environment. I also thank Renate Trebizan and Liane Hochgatterer for their help with organizational concerns. For his help with all technical challenges, I thank Johann Schlegl, for the SEM-EDX measurements Harald Kren and for the GPC measurements and NMR spectroscopy, I want to thank Josefine Hobisch and Petra Kaschnitz.

I feel I must thank the IAESTE organisation for giving me the opportunity to come to Austria in the first place and in particular Natalia Proskurnia, Teresa Flock and Luciana Vieira for helping me settle in. I would also like to thank Dr. Debbie Willison of Strathclyde University who has been a constant source of support throughout my entire academic career. In the same vein I would like to thank Dr. Lesley Fraser and Dr. Norbert Reinbacher for their much needed suport.

Finally I must thank those closest to me, my family and friends. My grandparents, to whom this work is dedicated, for their example in how to lead a life. My brother Luke for keeping me (relatively) sane in a Rimmer-eque manner. My mother for always steering me in the right direction even when I haven't been the easiest person to deal with. My father for always pushing me to achieve what I can, especially one April morning when I had just about given up. And lastly to you Selma for both amazing and frustrating me in equal measures but somehow getting me to exactly where I needed to be.

In memory of my grandparents

"Highly organized research is guaranteed to produce nothing new."

Frank Herbert, Dune

Table of Contents

1 Introduction

The modern world faces increasing challenges in both treatment of illness and in fighting ever more resilient bacteria. Polymer scientists stand at the forefront in the battle against these problems utilising increasingly advanced materials to deliver outstanding results.

As the population ages, restriction in the number of healthcare professionals limits the access of patients to regular treatment. Additionally, the number of people suffering from disorders causing a reduction in cognitive performance is steadily on the rise.[1] With reduced mental capacity it is often difficult to administer medications effectively and safely.[2] With complicated drug dosages at various times of the day and given the small size of many prescription medications, traditional methods of pharmaceutical intake cause problems for the older populace. It also forces strict schedules on drug taking where, for combined dosages, the time might not be optimal.

To combat both of these issues ever more sophisticated technologies need to be developed, particularly in the field of drug delivery in order to overcome many of the shortcomings facing our medical system. Delivery can be achieved either through patches on the skin (dermal delivery) or in implants under the skin (trans-dermal).[3] Dermal treatments are limited in that the drugs themselves must be modified to pass through the skin and this can often reduce or completely eliminate the effectiveness of the medication. Subsequently, methods which implant the drug delivery systems inside the body receive much interest and may represent the best chance to combat the existing shortcomings. To date, delivery matrices based on biodegradable nanoparticles,[4] micelles[5] and carbon nanotubes,[6] among others, have been reported.

As in all fields of modern life, polymers provide numerous benefits also in this field and have been reported extensively as potential candidates for this purpose.[7] The development of hydrogels in particular for drug delivery has spawned much research in recent years due to their various benefits such as mechanical flexibility, ability to absorb aqueous solutions and biocompatibility.[8]

Another field where advanced polymeric materials are being investigated for their application is on the treatment of surfaces for antimicrobial properties. Over the last few decades, there has been a dramatic increase in infections from so called “super-bugs” of which MRSA (methicillin resistant *Staphylococcus aureus*) is perhaps the most prominent.[9] Traditional treatments such as antibiotics are not feasible in dealing with

these bacteria and alternatives must be found. In hospitals, in particular, disinfection of surfaces is paramount in order to halt the spread of this disease.

Until now, disinfection of surfaces has been achieved mostly via small molecule compounds either free or encapsulated.[10] Such compounds suffer from the fact that they must be replaced on a fairly regular basis and that they can be harmful to mammalian bodies. Recent research has focused on the development of polymeric materials which can kill bacteria on contact and require little to no maintenance.[11] The lack of compound release not only eliminates any potential toxic effects to humans but also means that biocidal activity is retained over an extended period of time.

Poly(2-oxazoline)s represent a class of polymer compounds with many applications across various biomaterials fields.[12] Their rapid and controlled synthesis along with the wide variety of monomers available make them excellent candidates for applications where tailor made properties are required. The ease with which they can be modified or crosslinked additionally suggests that they may play an important role in overcoming challenges in both drug delivery and biocidal surface design.

2 Scope and Motivation

The current and presented work summarizes the scientific output of a collaboration of the Institute for Chemistry and Technology of Materials (ICTM) of the Graz University of Technology, the Polymer Competence Center Leoben GmbH (PCCL) and, for the biocide development, KE KELIT GmbH in Linz, Austria. It is comprised of two main areas, namely the development of crosslinked poly(2-oxazoline)s as potential drug delivery matrices and the synthesis of polymer contact biocides for use in hygienic applications such as surfaces in hospital environments and water pipes. In both cases, the cationic ring-opening polymerization CROP of 2-oxazolines has been the basis for all syntheses and subsequent modification and processing. The usage of 2-oxazolines is selected due to numerous advantages to name but a few, the living or pseudo-living nature of the polymerizations, the renewable nature of many of the reactants involved in monomer synthesis and the existing FDA approval of the polymer poly(2-ethyl-2-oxazoline) p**EtOx**.

When designing drug delivery matrices, many problems with current products must be considered. These are chiefly mechanical problems such as stiffness of the implants causing discomfort within the body and degradation concerns. Hydrogels seemingly answer the first of these problems as their swollen nature typically produces flexible, non-brittle materials. The second concern is of key importance as the presence of toxic by-products and/or their accumulation in the body must be avoided. Additional concerns such as the uptake of medication into the polymer network, ability of the gel to release compounds and modification of hydrogel properties to make them as widely applicable as possible must be taken into consideration.

By varying the 2-oxazoline monomers employed in hydrogel synthesis as well as the amount of crosslinker used, this work aims to answer many of these issues. Variance of the mono-functional species in the synthesis allows for fine tuning of arguably the most important hydrogel property: the swelling degree. Control of the swelling degree allows for the uptake of various compounds to be tailored and additionally will cause different rates and methods of release. Investigations of the correlation of mono-functional variance, crosslinking variance or a combination of both with the swelling degree and subsequent properties have been carried out. The ability of the synthesized hydrogels to take up model organic compounds has been examined as well as the conditions which trigger their release from the polymer network.

Regarding the issue of toxicity and retention of hydrogel degradation products, the degradation products of the chosen monomers and crosslinkers must be removed from the body as rapid as possible and exhibit low or no cytotoxic effects. Degradation of the hydrogels synthesized via hydrolysis has been investigated, aiming to show that degradation products allowing for excretion through the renal system for instance, are formed. Cytotoxicity tests have been carried out to determine the effect of the gel itself on normal cell growth. The monomer 2-ethyl-2-oxazoline has been utilized due to its current FDA approval, thus limiting the chances of the hydrogel being unsuitable for use in mammalian bodies. Additionally, the kinetics of both, degradation and subsequent release, have been investigated to give some indication of the lifetime of the hydrogel within the body.

The second part of the work focusses on using poly(2-oxazoline) derived materials in the synthesis of polymer contact biocides. The ever growing resilience of bacteria towards conventional antibiotic medications is an increasing problem and the design of ever more effective materials to deal with them is of increasing prominence. It has been aimed that materials can be developed which will follow simple and scalable synthetic protocols whilst additionally providing the much needed antimicrobial activity. Hydrolysis of poly(2-oxazoline)s to polymers bearing cationic charges, essential to antimicrobial activity, has been carried out, and the kinetics have been investigated. Two series have been examined – one with a hydrophobic and one possessing a hydrophilic side chain – to determine the effect of side chains on biocidal activity. Syntheses have been carried out under microwave irradiation in order to ensure as rapid as possible fabrication of the materials.

Following synthesis, the materials have been compounded with PP due to its prominent role as construction material in many modern-life applications. Characterization has not merely been carried out on the antimicrobial polymers themselves, but also on blends with PP. The investigation of the surface characteristics of such materials has been of prime importance, as it is by mere contact surface that cell lysis is aimed for. Techniques including surface energy measurements and SEM-EDX (among others) have been utilized to ensure that any observed antimicrobial effects can be attributed to poly(2-oxazoline) based copolymers near the surface. Biocidal tests have been carried out over the complete set of materials and against all types of microbes: gram positive bacteria, gram negative bacteria, and fungal species, aiming at the establishment of a correlation between increasing cationic charge density and the presence of side groups with the

biocidal activity. Based on the correlation, the best candidates possible for further antimicrobial application development can be chosen. Further work has been carried out on a selected candidate in order to best illustrate its potential in this field. The test of its long term retention of biocidal activity particularly in aqueous environments is paramount, as well as its efficacy against some of the most difficult to kill bacteria currently causing problems around the world. Finally, indication has been given not only of the scale-up of the reactions but also of the minimum amount of antimicrobial material required to retain activity.

Overall, the aforementioned ideas and strategies aim to synthesize and characterize poly(2-oxazoline) based materials for two distinct applications within the biomaterials field. The outcome should ideally involve the development of tailor made materials applicable to a wide variety of situations such as drug delivery in case of the hydrogels and biocides providing sufficient activity against many microbes.

3 State of the Art

3.1 Poly(2-oxazoline)s

Poly(2-oxazoline)s represent a polymer class with ever growing interest and potential applications. Over the last decade, their numerous benefits have resulted in extensive research towards their applications in all sorts of fields. Synthesized via cationic ring-opening polymerizations CROP (Scheme 3-1), the living nature enables for the synthesis of homopolymers, copolymers and block copolymers with low polymer dispersity indices. Control over the molecular weight is essential in polymer science when considering applications of the polymers in the biomedical and biomedicinal fields. Indeed, poly(2-oxazoline)s have been classified by the Food and Drug Administration as biocompatible.[13,14] Many 2-oxazoline monomers are currently commercially available owning to varied synthetic strategies. The arising versatility in synthesizing a wide range of materials with tailor-made properties makes this class of polymer incredibly interesting.

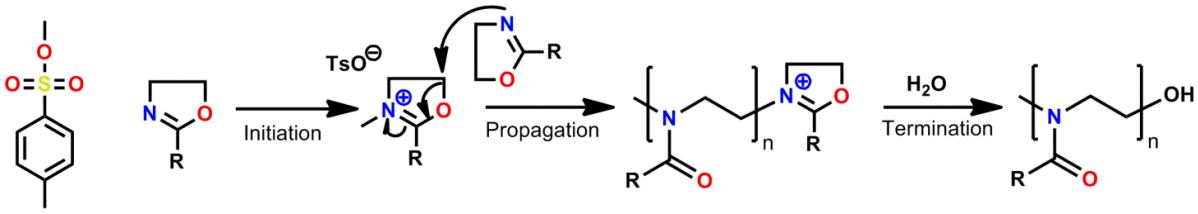

Scheme 3-1: Polymerization of 2-oxazolines initiated by methyl tosylate.

This class of polymers has recently received renewed attention due to the advent of microwave reactors. However, they have been known of since the sixties of the lst century when four research groups “discovered” them almost simultaneously:

In 1966, Tomalia and Sheetz reported on the successful synthesis of acyl and aryl substituted poly(aziridine)s from 2-oxazolines in the presence of a boron trifluoride initiator.[15] Additional intitators such as methyl tosylate or an oxazoline macroinitiator were also considered. Monomers were synthesized from the reaction of nitriles and chlorohydrins. Notably, both 2-methyl- **MeOx** and 2-phenyl-2-oxazoline **PhOx**, which are still utilized and investigated today, were successfully polymerized by the group. The reactions were carried out over a day or more yielding glassy, yellowish resins.

The work of Fukui et al. at this time focused more on establishing the mechanism for the polymerization.[16] Again, both **MeOx** and **PhOx** were polymerized, this time utilizing

species such as stannic chloride and boron trifluoride etherate as initiators and acetonitrile as a solvent. Additionally, they showed that the hydrolysis of either polymer resulted in the formation of poly(ethylene imine). They concluded that due to the nature of the initiators the polymerization proceeded in a cationic manner with the opening of the ring occurring between the 1 and 5 positions of the oxazoline ring.

Hellman and co-workers focused on polymerizations of 2-oxazolines obtained by the gas-phase dehydration of carboxylic acids and 2- or 3-amino acids.[17] Initially, polymerizations were carried out using the established set of initiators at room temperature. However, the polymeriztion was proven to be very slow and temperatures were increased to the region of 120 °C. It is suggested that even at these elevated temperatures it is required to leave the reaction for many hours in order to achieve high conversion. Notably, the syntheses were carried out in bulk without additional solvent.

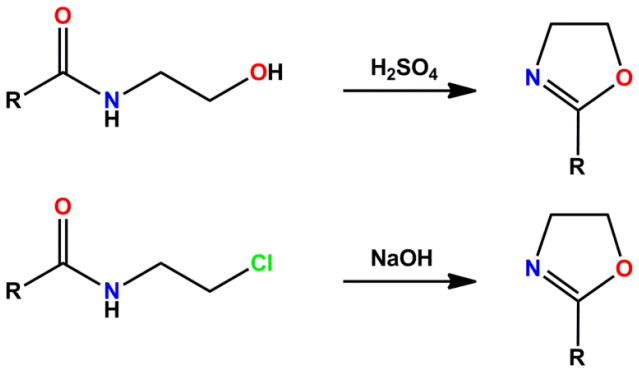

Scheme 3-2: Synthesis of 2-oxazoline monomers by cyclodehydration of *N*-hydroxyethylamides (top) and cyclodehydrohalogenation of *N*-chloroethylamides (bottom).

Contemporary work by the research group of Litt described the preparation of a 23 membered library of 2-oxazoline monomers and their subsequent polymerization (Scheme 3-2).[18] Solids of high molecular weight were obtained from polymerizations utilizing among others fluorinated Lewis acids and mineral acids as initiators. When the monomers were substituted with an aromatic group, the corresponding polymers were synthesized with a chain length reproducing the ratio of monomer to initiator. When an alkyl group was present in the monomers, however, some deviation was noticed, which was attributed to chain transfer reactions. Notably, whilst most other initiators initiated living polymerizations, fluorinated Lewis acids enabled for the monomer to attack the anion and terminate the polymerization.

Whilst poly(2-oxazoline)s were under-utilized for many decades until the advent of microwave chemistry allowed for the significant shortening of reaction times, the work in the sixties laid the foundation for the work done today. The cationic nature of the polymerization was identified, and many of the initiators used are still considered today. Recently, the group of Schubert investigated the reactivity of various initiators finding that methyl triflate followed by methyl tosylate provided by far the most rapid polymerization rates. The use of methyl or benzyl bromide was still beneficial.[19] Also metal cations including bismuth salts and metallocenes can be used to initiate the CROP of 2-oxazolines.[20]

This wide range of initiators, monomers and the living nature of the polymerization make poly(2-oxazoline)s an interesting and thanks to increased reaction rates relatively simple material to investigate.

3.1.1 Monomers

Despite the relatively recent developments in the polymerization of 2-oxazolines, the initial successful monomer synthesis dates from before the beginning of the last century.[21] In the decades since, the synthetic methods to produce new, ever more sophisticated monomers has continued yielding many possible routes. By far the two most common strategies utilized today involve one-pot syntheses utilizing amino acids and either carboxylic acids or nitriles. Today, much commercial production is carried out via these methodologies.[22,23] For 2-oxazolines with up to six carbons in the chain (including aromatics), the work of Witte and Seeliger is frequently considered for synthesis, whilst for longer chains, the methods of the Henkel Patent are more suitable.[24,25] In case of the Witte and Seeliger method, nitriles are involved compared with carboxylic acids described by the Henkel Patent.

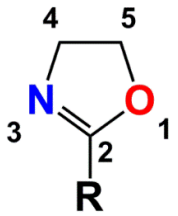

Figure 3-1: General structure of 2-oxazoline monomers.

3.1.1.1. Witte and Seeliger

During the seventies, Witte and Seeliger published work concerning the synthesis of 2-oxazolines from amino alcohols and nitriles under catalytic conditions (Scheme 3-3).[22] For the catalyst, metal salts such as cadmium acetate dehydrate and zinc chloride were commonly recommended. Typically, this synthetic route is chosen to prepare monomers with side chains of up to six carbons. It is also possible to synthesize bis(2-oxazoline)s via this route if dinitriles are utilized along with the amino alcohols. Due to the liquid or molten nature of the reactants at the reaction temperature of 130 °C, solvents can be eliminated from the synthesis. Normally, the nitrile and catalyst are heated under argon atmosphere with the amino alcohol being added dropwise over time forming ammonia gas. The reaction is allowed to run for over a day, after which the monomer is recovered under reduced pressure via distillation.

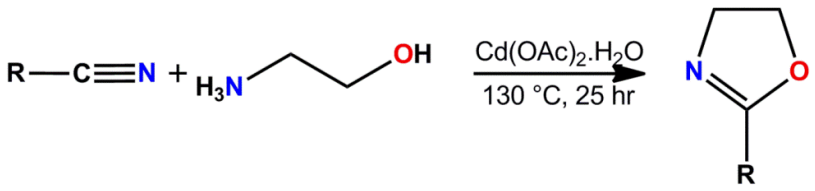

Scheme 3-3: Synthesis of 2-oxazoline monomers from nitriles and ethanol amine. In this synthesis, the R group typically contains less than seven carbon atoms.

3.1.1.2. Henkel Patent

As stated before, the Henkel patent differs from the previously described method in that it utilizes a carboxylic acid or an ester as opposed to a nitrile.[23] The catalyst used in the reaction is typically a metal butoxide, with zirconium and titanium commonly used as metals. From this procedure, alkyl and alkenyl substituted oxazolines with chain length of the substituents of seven or greater can be synthesized. In the presence of the catalyst, the carboxylic acid and amino acids are reacted at between 100 and 250 °C for over 24 hours. A reactive distillation is required to not only remove any unreacted educts, but also drive the equilibrium away from the linear product and towards the cyclic oxazoline. Such distillations often take significantly longer than the Witte and Seeliger method, and, consequently, yields are typically lower.

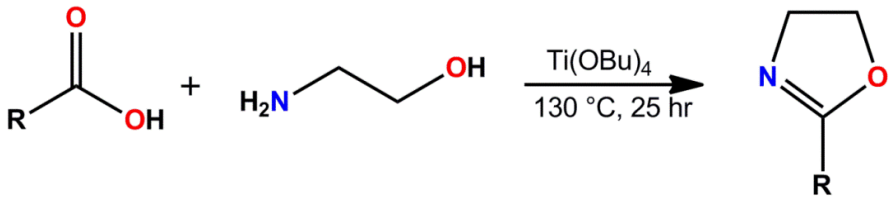

Scheme 3-4: Synthesis of 2-oxazoline monomer from carboxylic acid and ethanol amine. The R group typically contains seven or more carbon atoms.

3.1.1.3. X-Ray Structures

Despite the long understood cationic nature of the living polymerization of 2-oxazolines, the reason why the reaction was highly selective even when utilizing highly reactive cations was lacking experimental proof. Wiesbrock et al. reported a solution to this issue:[26] By investigating crystal structures of 2-oxazolines bearing aliphatic and aromatic substituents, the π-electron delocalization in 2-oxazoline rings could be identified.

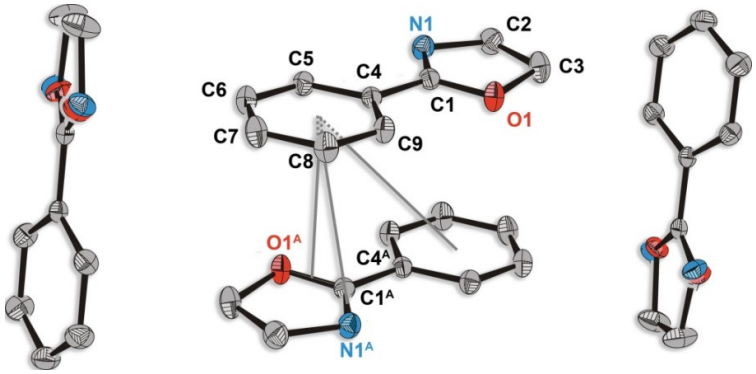

Figure 3-2: Excerpt of the crystalline phase of the **PhOx** monomer.

NonOx, **TMBOx**, and **PhOx** were investigated for their crystal structure and were shown to share the common motif of π-electron delocalization along the N-C-O segment. The 2-oxazoline pentacycles were slightly twisted. Substituents in the 2-position were shown to affect the stabilization by positive inductive effects in **PhOx**, in addition to normal resonance stabilization. Delocalization of the π-electrons was illustrated by the two different C-O bond lengths in the 2-oxazoline pentacycles as well as the C-O and C-N π-arene interactions in the crystalline phase of **PhOx** (Figure 3-2). This imparts a partial negative charge at the nitrogen atom and likewise a partial positive charge on the oxygen atom (Scheme 3-5). Such charge distribution explains why initiation of the polymerization occurs exclusively at the nitrogen atom even when utilizing highly reactive cations.

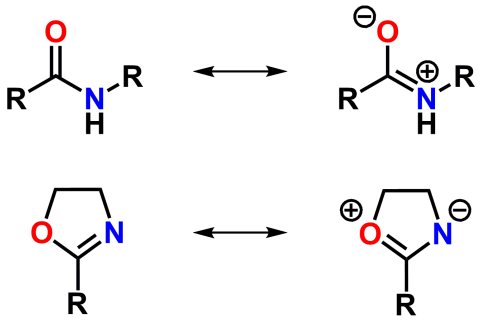

Scheme 3-5: Resonance delocalization of π-electrons of the C=X double bonds involving the adjacent Y heteroatom in amides (top; X = O, Y = N) and 2-oxazolines (right; X = N, Y = O).

3.1.2 Microwave-Assisted Polymerization of 2-Oxazolines

The long reaction time for the polymerization of 2-oxazolines has been a limiting factor in the synthesis of these materials for a long time. However, the last decade has seen a vast increase in interest in this field coinciding with the growth in microwave assisted polymer chemistry. Microwave assisted chemistry allows for the more rapid and controlled synthesis of general organic compounds and polymers.[27-29] The increased polymerization times afforded by microwave assisted synthesis has aided the research into 2-oxazolines and allowed for their benefits to be properly exploited.

Microwave assisted chemistry works on the principles of direct heating, as microwaves can cause excitation in molecules resulting in rotations and oscillations, which raises the temperature. Today, dedicatedly designed reactors allow for the usage of this technology in the lab. Due to employment of temperature and pressure probes, the parameters can be monitored during the reaction providing greater control over the reactions. For instance, the reactor can automatically shut down if the temperature or pressure exceed certain thresholds, thus reducing the chances of explosions.

Sealed microwave vials allow for autoclave conditions, concomitant with increased pressures. In the case of 2-oxazolines, this allows reactions to be carried out at temperatures exceeding the solvent boiling point and to greatly increase the reaction rate. Additionally, the direct heating of the reactants means that the heating profile is constant throughout the reaction mixture (if efficient stirring is provided at larger volume scales). In conventional heating, this is not the case as areas closer to the heat source are typically much hotter. This heterogeneous temperature profile can lead to unwanted side products and lower product yield. Microwave reactors eliminate this problem and

pave the way to higher yields.[30,31] As a result of these improvements, numerous poly(2-oxazoline)s, their properties and their applications have been reported.[13, 32-43]

The group of Schubert conducted a number of kinetic studies on poly(2-oxazoline) syntheses in a microwave reactor.[31,32] Utilizing methyl tosylate as initiator, 2-oxazolines substituted with methyl, ethyl, phenyl and nonyl side groups were investigated. It was determined that polymerizations could be accelerated up to a factor of 400. Investigation of the activation energies of both, conventional and microwave assisted heating, revealed that they followed the Arrhenius law and had identical activation energy. It was postulated that the acceleration of the reaction in the microwave reactor was purely due to thermal effects and not to “non-thermal microwave effects”. Further work by the group showed the possibility to synthesize di-, tri- and tetra-block copolymers of this series in microwave reactors.[33-35]

3.2 Crosslinked Poly(2-oxazoline)s

Crosslinked polymer networks can be defined as hydro-, lipo-, or amphigels based upon their properties such as solubility and swelling in various liquids. Materials described as hydrogels are of a highly hydrophilic character. They possess not only the ability to absorb water and many biological fluids, but do so in a manner not too dissimilar from living tissue. Numerous applications have been reported in the medical field due in part to their insolubility in water but also to their pore structure.[44] Significant interest has been shown towards development of novel hydrogel networks since the synthesis of HEMA hydrogels was reported.[45,46] Up until now, numerous applications for the gels have been both utilized and suggested including use in cosmetic surgery and additionally more key medical functions such as tissue imaging and engineering and as drug delivery matrices.[47-49]

Biocompatibility has been investigated in this field for some time now as has pH-based degradation.[50] Following these reports, there has been much research on both the biocompatibility and biodegradability of hydrogels with encouraging results.[51-54] Both degradation and diffusion release mechanisms are possible as is a combination of both. These factors indicate that hydrogels could be a significant step in developing polymer based drug delivery matrices carrying not only different drugs but allowing them to be used in multiple types of treatments, for example in providing combined drug dosage.[55]

Poly(2-oxazoline)s possess many of the characteristics required by a polymer network not only for hydrogels in general but also as drug delivery matrices. Numerous hydrogels have been synthesized over the past 30 years and a brief outlook over the results is illustrated below.

3.2.1 In-situ CrossLinking During the Cationic Ring-Opening Polymerization of 2-Oxazolines

3.2.1.1. Initiation of the Polymerization by Mono-Functional Initiators

Early work in the field of poly(2-oxazoline) based hydrogels by Saegusa et al. involved the copolymerization of 2-methyl-2-oxazoline **MeOx** and 2,2'-tetramethylenebis(2-oxazoline) **TMBOx** utilizing a methyl triflate initiator.[56] An almost quantitative yield was achieved from this one pot reaction. Significant swelling of the gel was observed for both

water and 5% sodium chloride solution, with swelling degrees of up to 45 in water when the ratio of mono- to bis-functionalized 2-oxazoline monomers was 60:1. Utilization of other alkyl-2-oxazoline monomers allowed for the swelling properties to be varied: Hydrogels from **EtOx** exhibited high swelling in water and polar organic solvents, whereas greater swelling in less polar solvents was shown for 2-oxazolines with longer chain substituents.

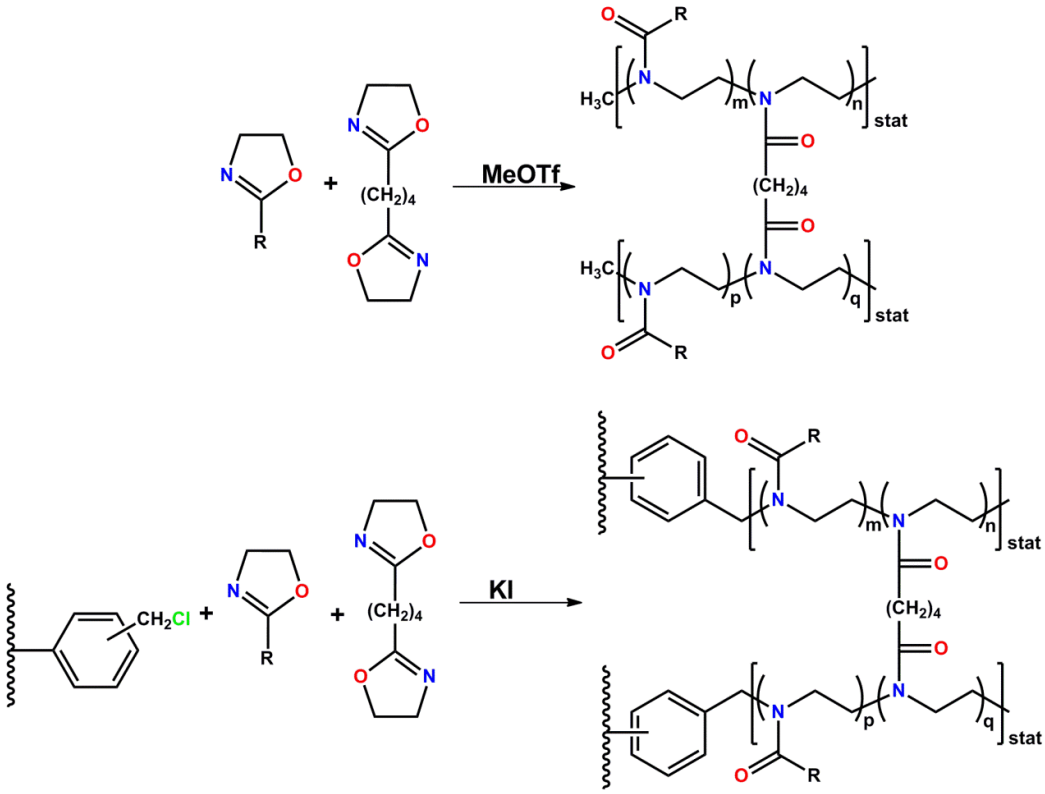

Scheme 3-6: Synthesis of poly(2-oxazoline)-based networks via the copolymerization of mono- and bis-functional 2-oxazolines utilising both (a) a mono-functional initiator (top) and (b) an oligo-functional macroinitiator (bottom).

3.2.1.2. Initiation of the Polymerization by Macroinitiators

MeOx based **TMBOx** crosslinked hydrogels were prepared by Rueda, Voit and co-workers via polymerizations initiated by macroinitiators with yields between 42 and 95% (Scheme 3-6).[57] Random copolymers of chloromethylstyrene and methyl methacrylate or chloromethylstyrene and styrene with dedicated functionalization patterns, were employed as initiators. p**MeOx** was in-situ crosslinked with **TMBOx** subsequent to grafting from the macroinitiators. Hydrogels with a **MeOx**:**TMBOx** ratio of 44:1 showed

maximum swelling degrees of 18 in water, while those with a **MeOx**:**TMBOx** ratio of 138:1 showed highest swelling degrees of 40 in methanol. This macroinitiator method was also used for the copolymerization of **MeOx** and **NonOx** with **TMBOx** as crosslinker.[58] Polar sorbents could be more readily absorbed in gels with a greater ratio of **MeOx** to **NonOx**. The amphigels exhibited highest swelling of 20 mL/g in methanol for a **MeOx**:**NonOx** ratio of 9:1 and 14 mL/g in chloroform for a **NonOx**:**MeOx** ratio of 11:1.

p**MeOx** based hydrogels were also studied by Lim and coworkers who used an iodosilane-functionalized AFM tip as macroinitiator.[59] p**MeOx** was surface-immobilized on the AFM tip whereafter mere contact of the tip with aqueous solutions resulted in the swelling of the hydrogel. This approach enabled for the investigation of patterning applications subsequent to loading of the hydrogel with a solution containing viruses: When the tip came into contact with an amine-modified substrate, the virus solution could be printed on the surface following diffusion induced release from the hydrogel.

Schubert et al described in detailed manner the cellular uptake of poly(2-oxazoline)-based particles.[60] **EtOx** could be copolymerized with 2-9'-decenyl-2-oxazoline **Dc=Ox** in a statistical manner; the polymerization was terminated by addition of fluorescein. Nano precipitation of polymer solution allowed for the preparation of particles of sizes in the range of 200-800 nm. Cellular uptake of the nanoparticles was shown to be viable in mouse fibroblasts with uniform distribution throughout the cytosol.

3.2.2 Crosslinking of Poly(2-Oxazoline)s and PEIs by Complex Formation

3.2.2.1. Crosslinking via Hydrogen Bonds

Kim et al. described the complexation via hydrogen bonds between the amide groups of p**EtOx** and the carboxylic acid groups of poly(methacrylic acid) or poly(acrylic acid).[61] Above pH values of 5.4, no complexes were formed and both polymers were soluble, while for pH values below 5.0, complexes were precipitated from solution as a powder. The complexes were molded into disks and subsequently swollen in a solution of pH 5.1 as part of a series of swelling studies. An equilibrium swelling degree of 30% was determined. The model drug insulin, incorporated into the complex via solution, was selectively released upon application of electric current. Birkinshaw and Collins reported the degradation of complexes of poly(ethylene imine) and hyaluronic acid within 2.5 h.[62]

Despite this, the complex retained a swelling character within the first hour with a swelling degree of 5.

Blends of water-soluble and water-insoluble polymers that formed supramolecular hydrogel networks via hydrogen bonds were reported by Percec and Bera (Figure 3-3).[63] By adjustment of the ratio between the two polymers, glass-transition temperatures and mechanical properties could be tailored to requirement, suggesting that the hydrogels are excellent candidates in fields such as membrane technology. Water-soluble p**EtOx** was blended with water-insoluble poly(2,4,4-trimethylhexamethylene terephthalamide) or aromatic poly(ether sulfone) to yield gels, of which the water uptake increased with the content of the hydrophilic polymer in the mixture: The blend of p**EtOx** and poly(2,4,4-trimethylhexamethylene terephthalamide) possessed a maximum swelling degree of 2.3 for the 80/20 blend (for the 90/10 blend, p**EtOx** dissolved in less than an hour).

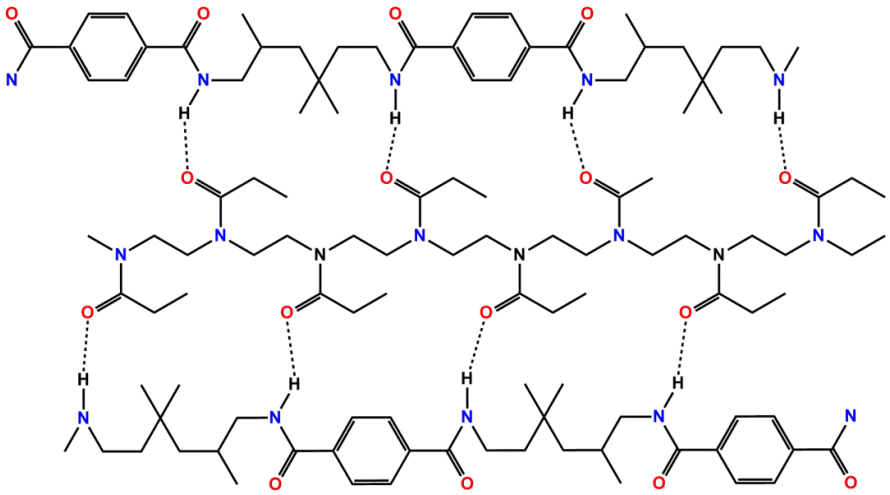

Figure 3-3: Hydrogel formation through complexation via hydrogen bonding.

Kobayashi and coworkers synthesized poly-pseudorotaxanes utilising linear p**EI**s in phosphate-buffered solutions along with α-cyclodextrins in high yields.[64] The p**EI**s and α-cyclodextrin solutions were mixed at 60 °C before being cooled down. The solutions could be shown to display turbidity and form a gel-like network once the gelation temperature had been reached. The gelation temperature was dependent upon the molecular weight of the p**EI**s and was shown to be 56 °C for M_w = 87 kDa and 24 °C for M_w = 3.2 kDa. Such compounds are candidates in gene carrier applications.

3.2.2.2. Crosslinking by Metal Complexation

Much work in the field of metal complexed poly(2-oxazoline) based hydrogels was carried out by Saegusa et al. Statistical p**MeOx**-co-p**EI** was reacted with 3-[4-(4'-methyl-2-2'-bipyridyl)]-propanoic acid to form bipyridyl-bearing copoly(2-oxazoline)s (Scheme 3-7).[65] Concentrated solutions of these polymers formed stable hydrogels via the coordination of metals to the bipyridyl pendant groups following addition of metal salts such as $FeSO_4$ and $RuCl_3$. Redissolution occurred when the material was stored in ethanol. Fe^{2+}-based gels could be reversibly treated with solvents by this method to switch between the hydrogel and solution state. Additionally, the stability of the hydrogel complexes could also be tailored by changes in pH and temperature. Such reversible conversions are the result of ligand exchange reactions in the hydrogel and solution.

The thermal switching of these gels was in detail investigated for Co^{3+}- and Fe^{2+}-complexed networks.[66,67] Co^{3+}-linked gels could be dissolved quantitatively and reversibly upon heating within thirty minutes in contrast to their stability for a number of days under ambient conditions. High swelling of the gel in water with degrees of up to 46.2 indicated that the swelling itself was the rate determining step. Reduction of the cobalt ion could be shown to induce hydrogel solubility; subsequent re-oxidization reverted the process from the solution back to the gel state. Fe^{2+}-complexed hydrogels displayed similar properties to their cobalt analogues regarding their thermal reversibility: By adjusting the temperature, the time required for complete dissolution could be varied from 9 h at 40 °C to less than 5 min at 100 °C. Hence, the Fe^{2+}-linked hydrogels were of a medium stability compared to the Ru^{2+}-based ones (which even at 100 °C took more than a day to dissolve) and Ni^{2+}-based derivatives (which rapidly dissolved even at 40 °C). The properties of the Fe^{2+}-linked hydrogels, on the other hand, identified them as ideal candidates for thermally reversible hydrogels.

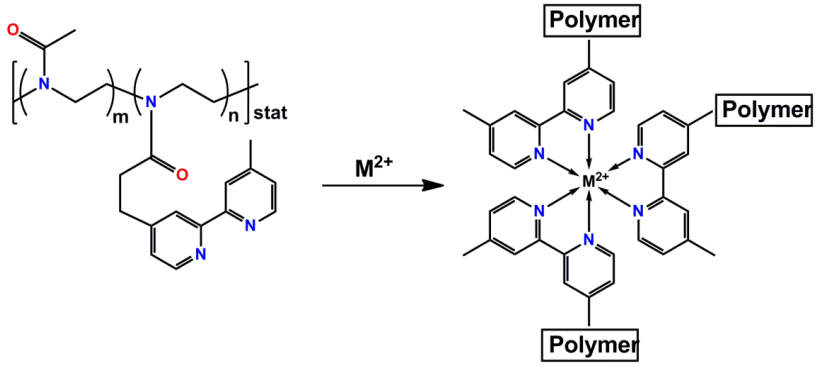

Scheme 3-7: Formation of hydrogels due to crosslinking caused by metal complexation.

Kudaibergenov et al. focused on a number of semi-interpenetrating networks, including hydrogels of poly(acrylic acid) containing linear p**EI**/metal complexes which had been immobilized.[68] The highest swelling degrees of 25 were shown in the case of p**EI**/Fe^{3+} complexes and lowest swelling with degrees of 11 for p**EI**/Pd^{2+} complexes, whilst the poly(acrylic acid) hydrogel itself had a swelling degree of 14.3. Immobilized p**EI**/Cu^{2+} complexes were shown to retain good catalytic activity in the oxidation of cyclohexane to cyclohexanone and cyclohexanol.

Geckeler and Mohan synthesized semi-interpenetrating polyampholytic hydrogels composed of p**EI** and poly(N-isopropylacrylamide-co-sodium acrylate).[69] The content of p**EI** could be varied such that the hydrogel composed of 0.05 g of p**EI** (per 0.87 g of N-isopropylacrylamide and 0.20 g of sodium acrylate) had the highest swelling degree of 337. A decrease in the swelling degrees was noted when cationic additives were present as opposed to when the additives were anionic and non-ionic where the swelling increased.

3.2.2.3. Crosslinking by the Quarternization of Amines

Velichkova and coworkers performed the synthesis of p**PhOx** and p**MeOx**, respectively, which were terminated by iodine at both ends prior to use as a crosslinker for poly(dimethylaminoethyl methacrylate) (Scheme 3-8).[70] Studies of the swelling characteristics indicated that hydrogels containing a larger amount of **MeOx** showed greater swelling in aqueous environments than those with high **PhOx** content. This allowed for the hydrophobic/hydrophilic tuning of the hydrogels.

Studies on the absorption of metal ions such as Cu^{2+}, Mn^{2+}, Ni^{2+} and Fe^{3+} revealed that the amino groups of the crosslinkers allowed for small amounts of sorption, which increased along with pH (range of pH = 1-7). Extraction of up to 70% of anions from aqueous solutions resulted from the large number of ammonium groups present within the networks, illustrating the possibility of utilizing these materials in anion exchange.

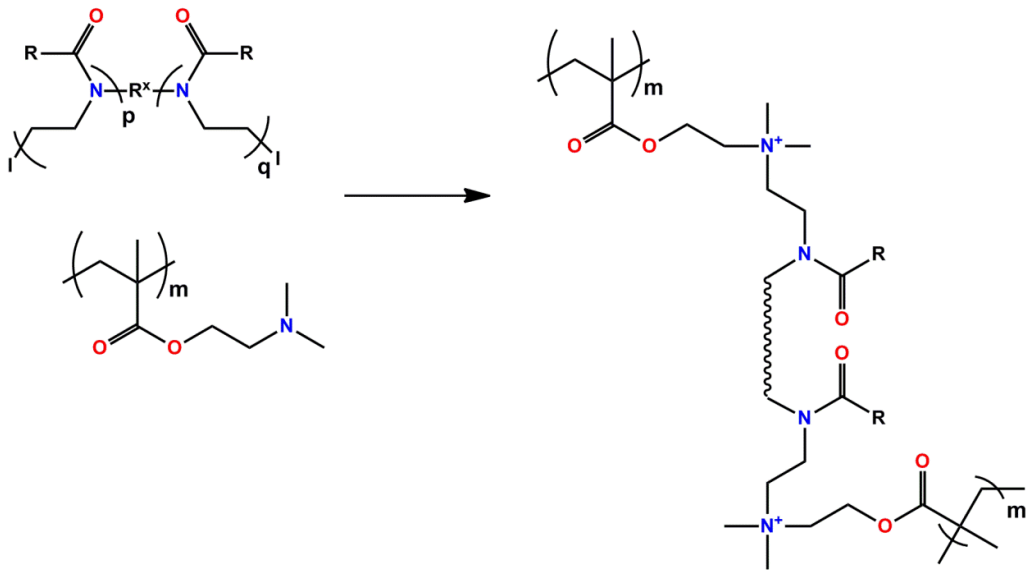

Scheme 3-8: Amine quaternization of a poly(methacrylate) resulting in hydrogel formation.

3.2.3 Crosslinking of Poly(2-Oxazoline)s and PEIs by Physical Processes

3.2.3.1. Plasma Treatment

Immobilization of thin hydrogel films on various substrates was carried out by Werner and co-workers utilizing low-pressure argon plasma.[71] p**EI** was immobilized on poly(tetrafluoro ethylene) and poly(ethylene terephthalate) surfaces by plasma treatment. The lowest p**EI** swelling degrees of 4/1/1 were exhibited in water at pH-values of 3/6.5/11 (compared to poly(*N*-vinyl pyrrolidone) and poly(acrylic acid)). The plasma immobilization was nonetheless shown to be an effective method in producing various polymer films on numerous substrates allowing for more flexible tuning of properties in biomedic(in)al applications.

3.2.3.2. Gamma-Ray Induced Crosslinking

Ali and Al Arifi published work detailing the gamma-ray radiation-induced polymerization and crosslinking of acrylic acid and p**EtOx**.[72] By varying the compositions, 100% gelation could be obtained when the p**EtOx** content in the feed solution reached 65%. The p**EtOx** content in the feed was shown to affect the swelling degree: Swelling degrees in water in the range of 4 for 10% p**EtOx** content decreased to less than 2 for 60% p**EtOx** content. The apparent relative hydrophobicity, despite of the hydrophilic character of both reactants involved, was referred to the engagement of the hydrophilic groups in complex formation. The hydrogels exhibited pH-dependent swelling: The hydrogel with 10%

p**EtOx** content, for example, exhibited swelling degrees of 0 at pH = 3, 10 at pH = 5, and 60 at pH = 7. Ibuprofen could be loaded into the hydrogel; release amounts and release rates strongly depended on the hydrogel compositions (p**EtOx** content) and pH value. These various characteristics make these materials candidates as delivery matrices for colon drug delivery.

Varshney et al. published work on the gamma-ray radiation-induced synthesis and crosslinking of p**EI**/acrylamide hydrogels.[73] Formation of hydrogels was shown to occur primarily by grafting of acrylamide onto the p**EI** backbone and subsequent crosslinking. A maximum content of 1.5% of p**EI** could be used in successful hydrogel syntheses. The swelling degrees of the gels, regardless of the feed mixture, were in the range of 20-30. The hybrid hydrogels showed enhanced metal uptake compared to pure poly(acrylamide) gels. Lead/cadmium uptake was shown to achieve values of up to 19/13 mg/g hydrogel (from 100 ppm solutions of the metal ions).

3.2.3.3. Temperature-Induced Hydrogel Formation

p**EI** hydrogels possessing linear or star architectures, the latter as six-armed p**EI** from corresponding benzenes and as four-armed p**EI** from porphyrin scaffolds were reported by Yuan and Jin.[74] The hydrogels were formed after cooling hot p**EI** solutions to room temperature. X-ray diffraction confirmed that the hydrogels had formed due to dihydrate crystalline structures of p**EI**. Linear p**EI**s formed gels of branched bundles with widths of 5-7 nm. Fan-like bundles were formed by the six-armed system, and the four-armed system formed asterisk-like aggregates. The hydrogel formations were thermoreversible with gel-sol transition temperatures between 43 and 79 °C (upper critical solution temperature), depending on the structure. Glutaraldehyde was reported to improve the mechanical properties when utilized as an additional crosslinker. Formation of silica particles occurred within ten minutes at room temperature when p**EI** was added to an aqueous solution of tetramethoxysilane.[75] By varying the amount of the p**EI**s in the initial solutions, the shapes could be engineered, further suggesting that they formed from the aggregation of thinner nanofibres. It was apparent that the morphology of the particles was dependant on the shape of the polyamine involved in the initial growth of the particles. Temperature-formed hydrogels crosslinked by glutaraldehyde were used to form a silver network following immersion in various concentrations of aqueous silver nitrate solution and subsequent calcination.[76] Depending on the calcination temperatures, the shape of the monoliths as well as the pore sizes could be controlled.

Hasegawa et al. utilized mid and near IR in order to elucidate the mechanism of gel formation of linear p**EI**s.[77] Hydrogel formation was attributed to the presence of dihydrate crystallite structures. Thermal treatment resulted in the dissolution of the gel at 64 °C and both IR techniques showed disruption of the planar linear p**EI** chains to random coils when elevating the temperature above room temperature. Menzel and coworkers investigated linear p**EI**s with varied polymerization degrees.[78] Hydrogel formation resulted from the cooling of hot solutions of the polymers. It was found that the gelation concentration decreased as the polymerization degree increased, resultant of the fact that longer p**EI** chains are more effective regarding the quantity of water in gelation. XRD and IR analyses demonstrated water uptake by p**EI** and formation of various hydrates even under dry storage conditions, a result further proven by DSC measurements. Crosslinking of p**EI** with glutaraldehyde allowed preparation of slices for SEM imaging revealing fibrous bundles of a fan-like shape.

3.2.3.4. Hydrogels from Photogelation/Redox Trigger

Chujo et al. reported the synthesis of a poly(2-oxazoline) copolymer bearing anthracene and disulfide groups via the reaction of partially hydrolyzed p**MeOx** with (9-anthracenyl)methyl hydrogen 3,3'-dithiodipropanoate.[79,80] Hydrogel formation occurred in spincast films via the application of light (wavelengths of over 300 nm) in order to induce the photodimerization of the anthracene groups. Resulting from higher degrees of crosslinking, the swelling degrees of the hydrogels decreased upon prolonged exposure times. By reducing the amount of disulfide functionalization in the copolymers on the other hand, the swelling degrees of the hydrogels increased due to an increase of hydrophilicity. The gels possessed swelling degrees as high as 26 in water. Notably, the hydrogel could be cleaved by reduction of the disulfide bridges with $NaBH_4$ (Scheme 3-9).

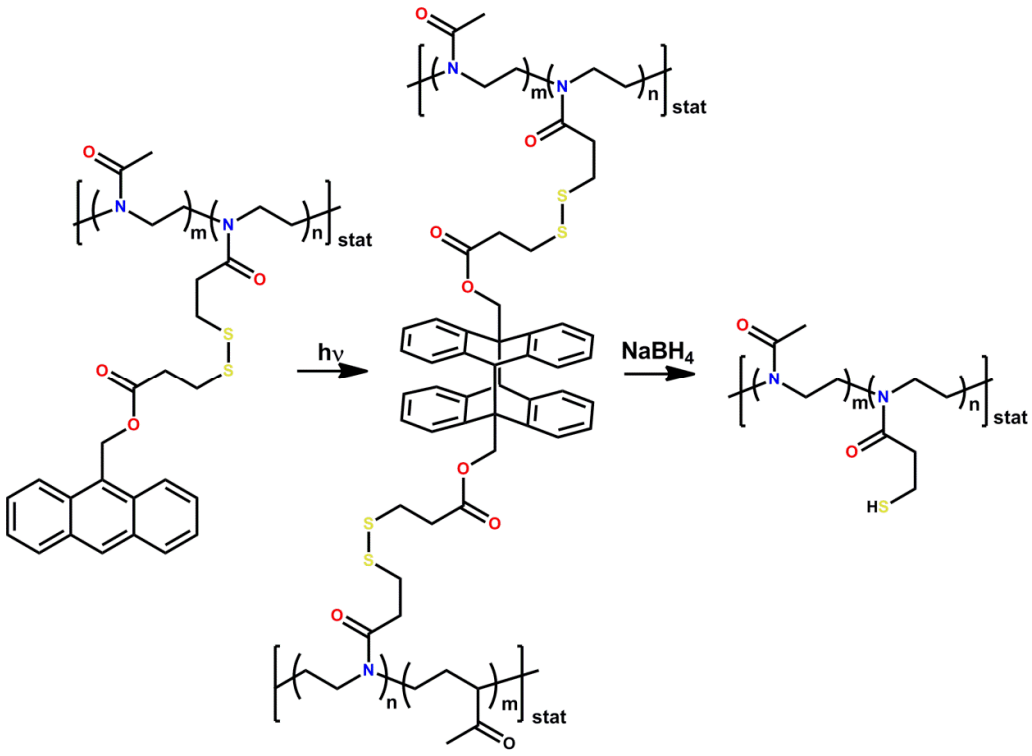

Scheme 3-9: Hydrogel formation by anthracene dimerization. The redox chemistry of thiols/disulphide bridges enables for reversible hydrogel formation.

The authors additionally described the reversible nature of the redox reaction by reoxidization of the thiols to yield disulfide bridges. Further studies showed that the copolymer p**MeOx**-p**EI** could be reacted with (7-coumaryloxy) acetic acid.[81] Subsequent irradiation with a high pressure 450 W mercury lamp (λ > 310 nm) for 7 h yielded hydrogels due to the photodimerization of pendant coumarin groups. Swelling degrees in water were shown to increase with decreasing coumarin content, which was representative of the crosslinking degree. The photogelation was shown to be reversible: A photocleavage reaction could be carried out with a low pressure mercury lamp (λ = 253 nm), rendering the hydrogel formation reversible upon application of the appropriate stimuli.

3.2.3.5. Redox-Induced Hydrogel Formation

Saegusa and coworkers reported another type of poly(2-oxazoline)-based hydrogels that were crosslinked via an intramolecular Diels-Alder reaction between a furan-bearing and a maleimide-modified statistical copoly(2-oxazoline) (Scheme 3-10).[82] The two polymers

were reacted in the film state at room temperature under light free conditions for one week. Swelling properties were dependent upon the number of substituent groups on the polymers, with a minimal amount of functionalization required for hydrogel formation from sufficient crosslinking. If the degree of functionalization increased beyond a certain value, however, swelling decreased. The retro Diels-Alder process could be induced by heating the gel above 80 °C and reversibly resulted in the reversal of the gel formation.

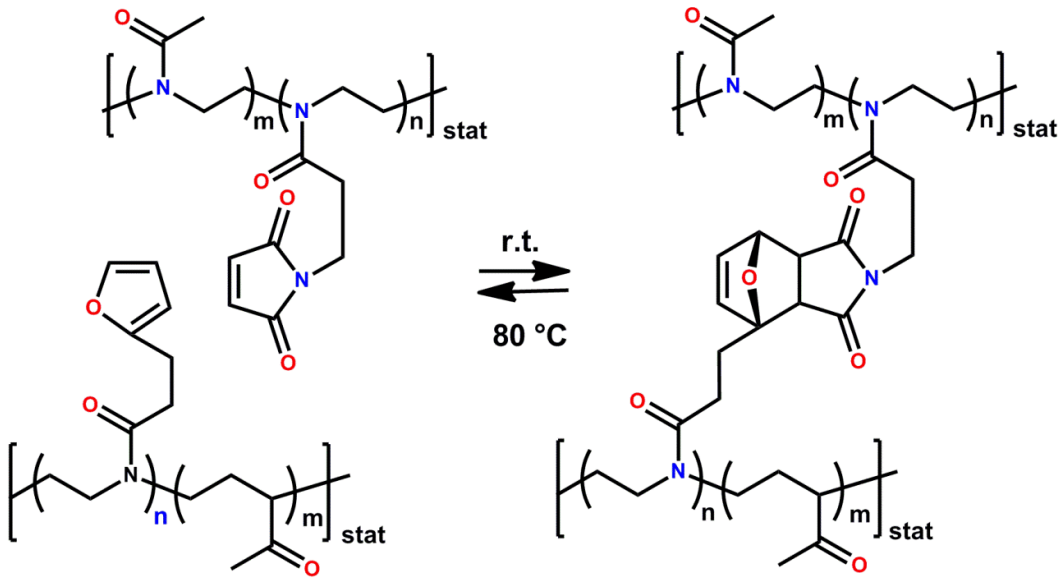

Scheme 3-10: Hydrogel formation by a (reversible) Diels-Alder reaction.

3.2.4 Crosslinking Strategies of (Co-)Poly(2-Oxazoline)s Involving ene-Functions

3.2.4.1. Poly(2-Oxazoline)s with Unsaturated End-Groups

Du Prez and co-workers prepared polymer networks from the (UV-induced) free-radical copolymerization of methyl methacrylate with α,ω-bisacrylate terminated p**MeOx** and p**EtOx** employing cationic ring-opening polymerizations initiated by 1,4-dibromo-2-butene.[83] An increased content of p**MeOx** from 20-70 weight-% (against methyl methacrylate) increased the amounts of water-soluble fractions from 5 to 22% and resulted in the lowering of the glass-transition temperatures from 43 to 36 °C. For p**EtOx**, similar trends were observed. Swelling studies revealed that, with increasing p**MeOx** or p**EtOx** content, swelling degrees were influenced by the varying hydrophilicity in each hydrogel and consequently increased in water whilst decreasing in acetone. In further

work, this group investigated networks of α,ω-bisacrylate terminated p**EtOx** with 2-hydroxyethyl methacrylate, 2-hydroxypropyl acrylate, and methyl methacrylate, prepared from a (UV-induced) free-radical polymerization.[84] 2-Hydroxyethyl methacrylate-blended networks possessed the highest swelling with degrees of 10 at 20 °C compared to degrees of 7 for blends with 2-hydroxypropyl acrylate and of 1.3 with methyl methacrylate. The swelling degrees were decreased at higher temperatures; for 2-hydroxypropyl acrylate-blended gels it could be shown that the hydrogels exhibited thermo-sensitive reversible swelling/deswelling in response to the applied temperature.

Meier and Nardin prepared networks based on the α,ω-bis(methacrylate) terminated block copolymer p**MeOx**-poly(dimethyl siloxane)-p**MeOx**.[85] Despite the networks being found to be thicker than lipid bilayers, they were considered good mimics of biological membranes. Proteins were found to remain active even following the crosslinking reactions when the gels were used as a matrix for membrane spanning proteins.

Rueda and co-workers used α,ω-bisvinyl terminated p**MeOx** as bis(macromonomers) in the synthesis of non-ionic hydrogels by radical homopolymerization or copolymerization with *N*-vinyl pyrrolidone.[86] The hydrogels were shown to possess increased swelling in water and other polar solvents with lowered amounts of *N*-vinyl pyrrolidone.

Rueda, Strumia and coworkers crosslinked *N*-acryloyl-tris(hydroxymethyl) aminomethane with an α,ω-bisvinyl terminated p**MeOx** bismacromonomer and compared the network to those crosslinked with methylenebisacrylamide and ethylene glycol dimethacrylate.[87] Studies of the gels and their swelling-degrees revealed that p**MeOx** crosslinked gels exhibited higher swelling degrees than either methylenebisacrylamide or ethylene glycol dimethacrylate crosslinked gels. The greater swelling of the p**MeOx**-based hydrogel could be attributed to the larger pore sizes of the hydrogel due to the greater length of the crosslinker. The hydrogels exhibited fluid characteristics and viscoelastic properties similar to those of (biogenic) soft body tissues, rendering them potential candidates for biomedic(in)al applications.

Kim and coworkers studied hydrogels synthesized from α,ω-bisacrylate terminated p**EtOx** and poly(vinyl alcohol) or chitosan by free-radical polymerizations.[88,89] Swelling of the poly(vinyl alcohol)-based hydrogels was dependent on variances in both temperature and pH. Regarding pH changes, maximum swelling degrees of 4.5 were observed at pH = 10 (ratio p**EtOx**:poly(vinyl alcohol) = 3:1). Swelling was found to increase with the p**EtOx** content in the hydrogel, which was attributed to the hydrophilicty of p**EtOx**.

Increase of the temperature reduced the swelling with reversible swelling behavior observed as a response to varying temperatures between 65 and 25 °C. In the case of chitosan-based hydrogels, however, an increase of the p**EtOx** content from 1:1 to 3:1 reduced the hydrogels' swelling degrees from 20 to 7. Swelling/deswelling was found to be stimuli-responsive towards changes of the pH, where lower pH values triggered increased swelling.

Kobayashi and coworkers prepared p***i*PrOx** with styryl end groups via cationic ring-opening polymerizations.[90] Hydrogels were prepared by copolymerization with ethylene glycol dimethacrylate. The hydrogels possessed thermal-dependent swelling properties: Swelling degrees decreased with increasing temperatures from 1 at room temperature to 0.2 for temperatures above 40 °C.

David and co-workers synthesized ternary hydrogels utilizing the radical copolymerization of *N*-isopropyl acrylamide), 2-hydroxyethyl methacrylate, and poly(2-alkyl-2-oxazoline)s with unsaturated end groups.[91] Yellowish, brittle hydrogels were formed and found to be thermally sensitive in the range of 28-38 °C giving faster response than homopoly(*N*-isopropyl acrylamide)s, which was referred to the greater prevalence of hydrophilic groups, the improved balance in hydrophobicity and hydrophilicity as well as the greater chain sensitivity of the ternary hydrogels. Wide channels were formed resulting in hydrogels with a highly porous structure.

3.2.4.2. Poly(2-Oxazoline)s with Unsaturated Groups in the Side-Chains

Gong et al. copolymerized ***i*Pr=Ox** with 2-(methacryloyloxy)-ethyltrimethyl ammonium chloride and *n*-butyl methacrylate.[92] The ternary copolymer was subsequently crosslinked with another ternary copolymer composed of acrylic acid, 2-(methacryloyloxy)ethyltrimethyl ammonium chloride, and n-butyl methacrylate via the reaction of the carboxylic acids of one copolymer with the 2-oxazoline pendant groups of the other copolymer. Changes in humidity were shown to have an effect on the electrical resistances of the gels: At 20% relative humidity, the resistance was 10^7 Ω compared to only 10^3 Ω at 95% humidity. The hydrogels responded within 90 seconds to changes in humidity as varied as from 33% to 94%.

Dargaville, Hoogenboom and coworkers synthesized a series of copoly(2-oxazoline)s from **NonOx** and either **MeOx** or **EtOx**.[93] These copolymers were crosslinked by thiol-ene reactions with dithiols such as 2,2'-(ethylenedioxy)diethanethiol or ethylene glycol

bis(3-mercaptopropionate), with in-situ photo-rheology allowing for observation of the reaction progress. Gels bearing **MeOx** as monomer with saturated side-chains exhibited higher swelling degrees than their homologues based on **EtOx** as monomer with saturated side-chains; swelling degrees in water of up to 14 were obtained. Degradation was observed for hydrogels crosslinked with ethylene glycol bis(3-mercaptopropionate).

3.2.4.3. Michael Additions

Kong et al. synthesized hydrogels from the Michael reaction between the amines of branched p**EI**s and poly(ethylene glycol) diacrylate.[94] By varying either the poly(ethylene glycol) diacrylate or p**EI** content, the compressive moduli of the hydrogels could be shifted from 1 to 8 MPa, which are one to two orders of magnitude higher than the elastic moduli of the pure poly(ethylene glycol) diacrylate hydrogels obtained from a radical crosslinking reaction. Cell mobilization over four days was possible when such a hydrogel was loaded with a cell growth stimulator and utilized in an intramuscular fashion. Hence, the hydrogel was shown to be a good candidate for biomedic(in)al applications.

3.2.4.4. Crosslinking of PEIs with Epoxides

Zheng and co-workers reacted p**EI** with polyhedral oligomeric silsesquioxane macromers in order to create inorganic-organic hybrid materials.[95] Networks were produced when monofunctional hepta(3,3,3-trifluoropropyl) glycidyletherpropyl or oligofunctional octaglycidyletherpropyl silsesquioxanes were used as initiators. The glass-transition temperatures and thermal stability of the hybrid compounds were higher than those of standard p**EI**s. All hybrid composites could be swollen in water. Hydrogels could be synthesized from the hybrids containing the octafunctional polyhedral oligomeric silsesquioxane, whereas the hybrids containing the monofunctional polyhedral oligomeric silsesquioxane were physical hydrogels, the formation of which was ascribed to the microphase-separated morphology in the hybrids.

Along with co-workers, Taubert examined the covalent crosslinking of linear p**EI** with poly(ethylene glycol) diglycidyl ether for subsequent use in mineralization.[96] In the form of a hydrogel, p**EI** served to promote hydroxyapatite and brushite nucleation and growth from the corresponding solutions. The morphologies were of spongelike nature,

independent of the crosslinking degree of the hydrogel. When tested against dictostelium discoideum, linear p**EI** however was found to be cytotoxic. The mineralized particles displayed no such properties and showed no disruption of cell structures.

Hedden and co-workers synthesized hydrogels using branched p**EI** that was crosslinked by bisphenol A diglycidyl ether.[97] Upon increasing molar ratios of epoxide to amine in the range from 0.02 to 0.07, the swelling degree increased, while those gels lacking additional lithium triflate showed a lower (maximum) swelling of 1.6 compared to that of 1.75 for those containing lithium triflate. However, when comparing the lithium ion conductivity before and after crosslinking, a drastic decrease of conductivity from 10^{-3} S cm^{-1} to 10^{-6} S cm^{-1} was observed. It was argued that the tethering of chain ends to the network in order to limit charge mobility concomitantly reduced the lithium ion conductivity. The crosslinking could be optimized and it was subsequently proposed that these hydrogels may prove useful in lithium ion battery applications.

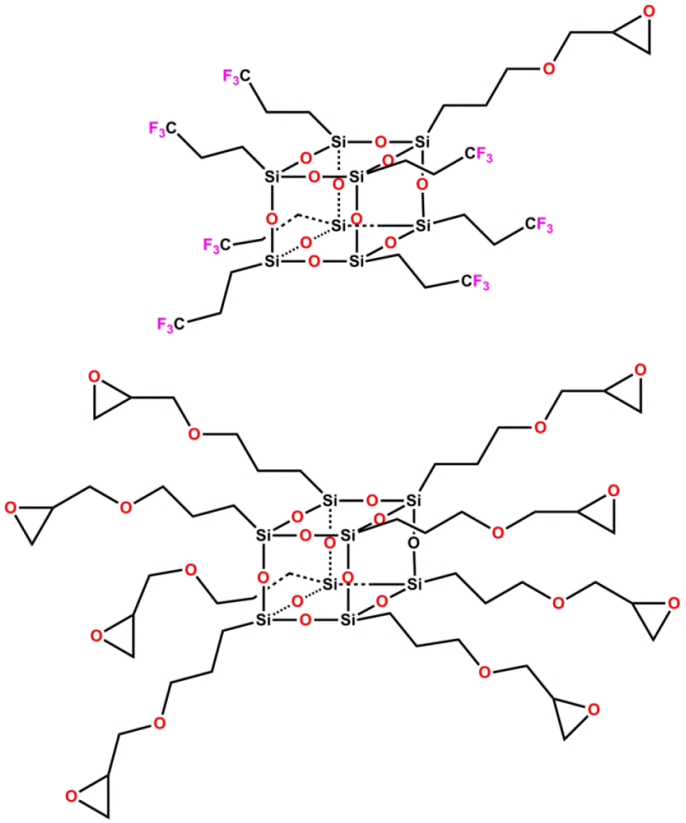

Figure 3-4: Structures of polyhedral oligomeric silsesquioxane macromers that allow for crosslinking with p**EI**s: Hepta(3,3,3-trifluoropropyl) glycidyletherpropyl polyhedral oligomeric silsesquioxane (top) and octaglycidylether polyhedral oligomeric silsesquioxane (bottom).

Further work by Hedden and Unal in the field of branched p**EI**s investigated the pH dependence of the swelling of gels formed by the reaction of epoxide-terminated poly(ethylene glycol) and p**EI**.[98] The hydrogels were swollen in hydrogen chloride and aminoethanol in order to correlate swelling degrees with the environmental pH values. For a p**EI**/poly(ethylene glycol) hydrogel with 56 wt.-% of p**EI** it was shown that the swelling ranged from 15 at low and high pH values (pH = 2, pH = 11) and exhibited a maximum of 35 at pH = 5. Theoretical modeling also predicted highest swelling for pH values in the range 4-5, however, its inability to consider the limited extensibility of the p**EI** chains led to the maximum swelling degrees being overestimated.

Ford and Yang examined the grafting of p**EI** onto UV-crosslinked hydrogel films of poly(2-hydroxyethyl methacrylate)-co-poly(acrylic acid) and tetrakis-(methoxymethyl)-glycouracil.[99] During the subsequent grafting of p**EI** onto these gels, bond formation occurred among the pendant hydroxyl groups of the hydroxyethyl methacrylate repeating units and amino groups of the p**EI**. These gels could be used as templates for the site specific growth of silica nanoparticles from sol-gel reactions at room temperature.

3.2.5 Crosslinking of PEIs with Isocyanates, Aldehydes, Acids and Their Derivatives

3.2.5.1. Isocyanates

Star-shaped poly(2-oxazoline)s were used to synthesize non-ionic hydrogels by Chujo and coworkers.[100] 1,3,5-tris(*p*-toluenesulfonyloxymethyl)benzene or 1,3,5-tris(iodo-methyl)benzene were utilized as initiators to yield poly(2-oxazoline)s with three living ends. The initiation of the polymerization was proven by NMR spectroscopy to occur stepwise at each functional group of the initiator. Crosslinking of the star-shaped oxazolines was caused by the reaction with bisfunctional isocyanates, and the gel fraction increased as the amount of trifunctional initiator increased. Swelling degrees of the hydrogels were shown to be similar in both, water and sodium chloride solution (5%), with a degree of 9 when the gel had a monomer:initiator ratio of 17:7 and gel yield of 38%.

Jordan et al. reported the first attachment of pendant amino groups to 2-oxazolines.[101] The BOC-protected monomer 2-[*N*-Boc-5-aminopentyl]-2-oxazoline **Boc-AmOx** was polymerized with *N*-methyl-2-methyl-2-oxazolinium triflate as initiator. Notably, the more

reactive methyl triflate failed to initiate the polymerization. By random copolymerization of **Boc-AmOx** with **EtOx** it was possible to vary the functional group density and solubility. Pendant accessibility of the amino group after deprotection could be shown by crosslinking of the polymer with bifunctional isothiocyanates, yielding hydrogels.

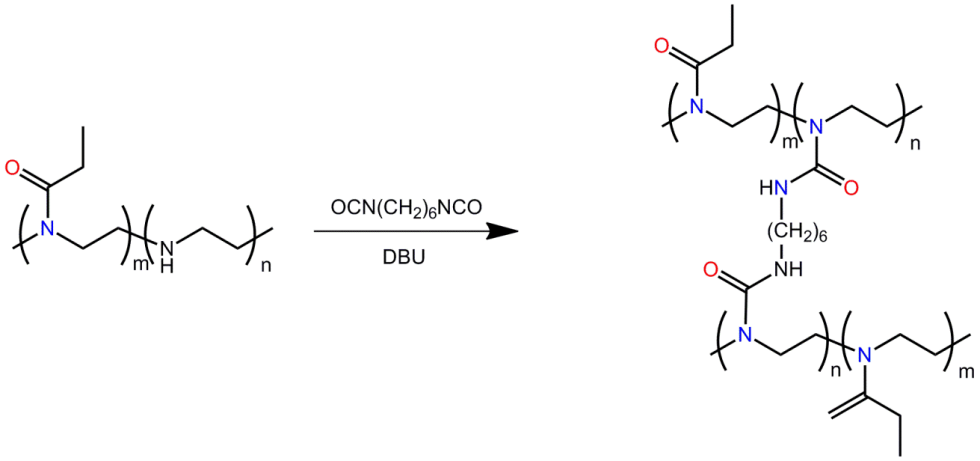

Scheme 3-11: Reactions of amines (p**EI** and copolymers) and bisfunctional isocyanates resulting in network formation.

Saegusa and co-workers prepared hydrogels from **MeOx** that was polymerized using the bisfunctional initiator *N,N'*-dimethyl-2,2'-tetramethylene-bis(2-oxazoline) bis(methyl-p-toluene sulfonate), synthesized from methyl tosylate and **TMBOx**.[102] Post-synthetic hydrolysis in sodium carbonate yielded α,ω-hydroxyl terminated polymers which were subsequently crosslinked with pluriisocyanates. Swelling was shown to be minimal in non-polar solvents such as toluene. In polar solvents on the other hand, swelling was shown to be much higher with maximum swelling degrees of up to 22 in DMF. Previous work of the group had given some of the first indications of **MeOx**-based hydrogels.[103] Partial hydrolysis of p**MeOx** (initiators for the polymerization: methyl tosylate or methyl triflate) was carried out in aqueous sodium hydroxide solution, and the resulting co-polymer p**MeOx**-co-p**EI** was crosslinked with hexamethylene diisocyanate (Scheme 3-11). Swelling of the gels in water varied from a minimum of 2 for high crosslinking degrees (hydrolysis degree: 18.2%, NCO:NH = 1.21) to a maximum of 72 for low crosslinking degrees (hydrolysis degree: 3.9%, NCO:NH = 0.59). Similar trends in swelling behavior were observed in 5% aqueous solution of sodium chloride.

3.2.5.2. Aldehydes

Glatzhofer and co-workers crosslinked p**EI** hydrochloride with malonaldehyde in aqueous solutions containing varying amounts of phosphoric acid.[104] The crosslinked materials were subjected to dehydration at 150 °C and used for four-probe a.c. conductivity measurements. The conductivity was shown to increase with phosphoric acid content; the polymer from reaction mixtures with a phosphoric acid content of 4.16 mol/polymer unit, for example, exhibited a conductivity of $8 \cdot 10^{-3}$ S cm^{-1} at 110 °C, whereas a conductivity of only $2 \cdot 10^{-7}$ S cm^{-1} was observed for polymers from mixtures containing phosphoric acid at a concentration of 0.35 mol/repeating units.

Crosslinking of p**EI** with aldehydes was also reported by Rempel and Chanda for uranium sorption applications.[105] Employing a copper-mediated process, p**EI** was first bound to partially hydrolyzed poly(acrylonitrile) fabrics and fibers bearing carboxylic acids at their surfaces and subsequently crosslinked by the reaction with bisfunctional glutaraldehyde. Sorption of uranium ions from aqueous solutions could be achieved with this material at a magnitude of 2 higher than currently available materials. Regeneration of the fiber could be carried out by rapid stripping with dilute acid whilst retaining the maximum sorption capabilities.

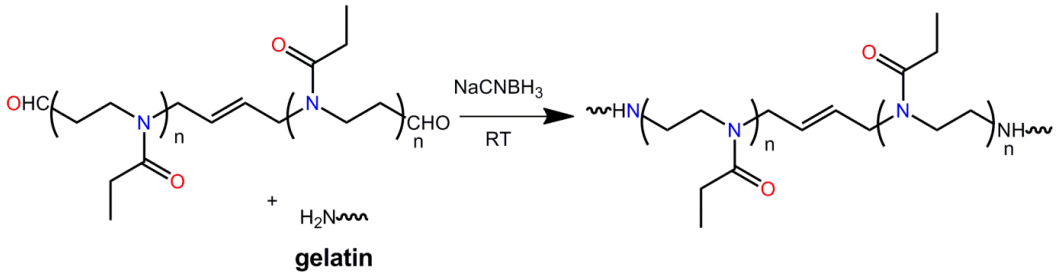

Scheme 3-12: Aldehyde based hydrogel formation utilising α,ω-CHO functionalized p**EtOx**.

Rathna reported work on gelatin hydrogels that were further crosslinked with linear p**EtOx** (bearing aldehyde groups at both ends) and discussed their potential as biomaterials and drug release matrices (Scheme 3-12).[106] When tested at 37 °C and pH = 4.5, gelatin-based hydrogels containing 25% p**EtOx** were shown to have comparable swelling degrees of 2 in water both in native form and loaded with drugs. At pH = 7.4, swelling degrees did not change, while at pH = 9.4, swelling degrees increased to over 4. Release studies of drug-loaded hydrogels revealed a more rapid release at pH = 4.5 than

at pH = 7.4; with complete release occurring within an hour. The hydrogels were additionally shown to possess good cell viability in in-vitro cytotoxicity tests.

3.2.5.3. Acids and Their Derivatives

Park et al. synthesized nanoparticles consisting of p**EI** and the polysaccharide heparin at room temperature within short reaction times of 30 minutes.[107] The nanoparticles were blended with poly(*N*-isopropylacrylamide)-co-poly(acrylic acid) yielding a thermo-responsive hydrogel. In comparison to poly(*N*-isopropylacrylamide)-co-poly(acrylic acid), the hydrogel exhibited higher contents of glycosaminoglycan when implanted in rats.

Swellable films were prepared by Appelhans and co-workers from maltose-substituted p**EI**.[108] Poly(ethylene-alt-maleic anhydride) was used to crosslink the maltose-functionalized p**EI** forming films which were shown to have excellent stability over 96 hours against a pH range of 4.0-7.4 but suffered almost immediate degradation at pH 10. Films coated on pre-treated silicon dioxide substrates exhibited significant swelling in water with an increase in film thickness of over 200 nm. Maximum swelling was observed to occur rapidly in less than 30 seconds. The films could be loaded with phosphate containing compounds as model pharmaceuticals, which were released over a two hour period.

Zewert and Harrington crosslinked p**EI** with a variety of crosslinkers, including adipoyl chloride, disuccinimidyl suberate and dithiobis(succinimidylpropionate).[109] When tested as potential candidates for applications in electrophoresis, the hydrogels were shown to possess greater tolerances to pH variances and general stability compared to poly(acryl amide), which loses mechanical strength at increased pH values due to its ease to hydrolysis.

Single-wall carbon nanotubes functionalized with acid chlorides and their reaction with p**EI** was described by Adronov et al. [110] Collagen was used to crosslink the p**EI** bearing single-wall carbon nanotubes as well as free p**EI** in order to investigate mechanical property variations (Scheme 3-13). Swelling degrees in water for both systems were of similar values around 40. The Young's modulus on the other hand was remarkably different for both systems: Gels formed of p**EI** bearing single-wall carbon nanotubes and collagen exhibited E Moduli that were approx. 5 times higher than their p**EI** / collagen analogues.

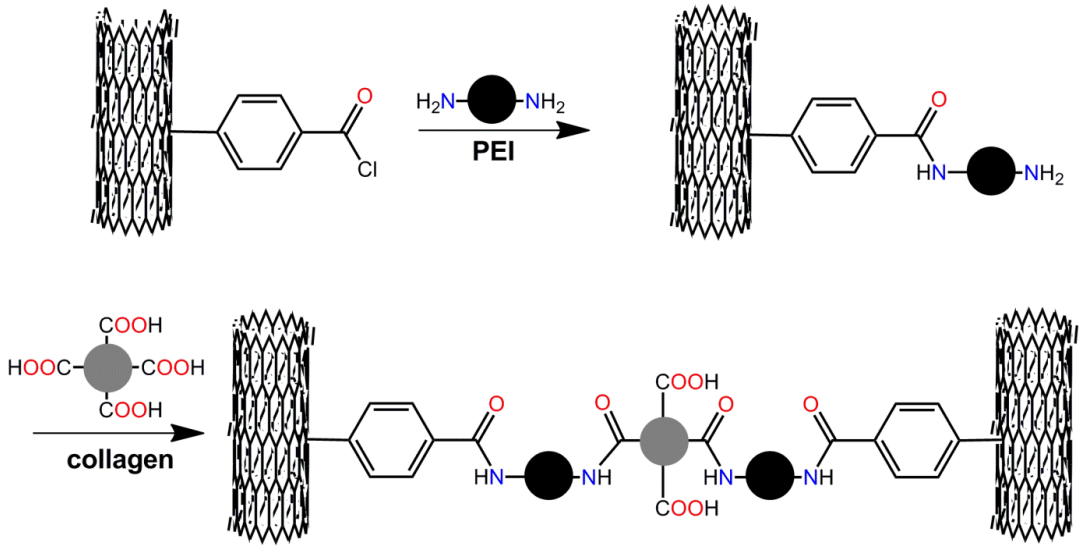

Scheme 3-13: Reactions of amines (p**EI**) with acid chlorides and carboxylic acids from single-wall carbon nanotube surfaces results in polymer network structures being formed.

3.2.6 Poly(2-Oxazoline)-co-Polyesters

3.2.6.1. Copolymers with Lactides

Wang and Hsiue reported on the copolymerization of p**EtOx** with three-armed poly(D,L-lactide).[111] Both polymers were initially converted to methacrylate bearing macromers, and hydrogels were prepared by UV-induced photopolymerization using 2,2-diethoxyacetophenone as initiator. Upon storage in acetone and ethanol for two days, pure products were obtained. SEM analysis revealed a positive correlation of poly(D,L-lactide) content and pore sizes in the networks. As the content of p**EtOx** increased, the swelling degree likewise increased with maximum swelling of 4 at 20 °C for the hydrogel containing 80% of p**EtOx**. The swelling degrees reversibly decreased for elevated temperatures of 40 °C as demonstrated by stepwise heating changes. Investigations in a range of pH = 4-10 showed enhanced swelling in more alkaline solutions: The swelling degree of the hydrogel containing 80% of p**EtOx**, for example, was increased from 4 to 8 in the range of pH = 4-10. In following studies, gelation of micelles of the triblock copolymer poly(L-lactic acid)-p**EtOx**- poly(L-lactic acid) was reported to occur at temperatures similar to physiological conditions,[112] while cytotoxicity tests revealed that pharmaceuticals incorporated into the micelles had lower cytotoxicity than the free pharmaceuticals.[113]

Liu and co-workers recently reported on p**EtOx**-poly(D,L-lactide)-p**EtOx** triblock copolymers prepared by coupling of monohydroxylated p**EtOx**-poly(D,L-lactide) diblock copolymers with bisfunctional adipoyl chloride.[114] The copolymers displayed temperature-dependent sol-gel transitions, while the gel range was found to positively correlate with the poly(D,L-lactide) content. The bulky hydrogels exhibited an interconnected system of pores allowing for the distribution fibroblasts encapsulated in the networks.

3.2.6.2. Copolymers with ε-Caprolactone

The copolymerization of α,ω-OH functionalized p**EtOx** and α,ω-COOH functionalized poly(ε-caprolactone) was carried out by Kim et al.[115] Films of the multiblock copolymers showed swelling degrees in the range of 0.2 at room temperature which reversibly rose to the range of 0.3 at 35 °C. Swelling degrees were also found to positively correlate with the p**EtOx** block lengths. Additional work focusing on di- and triblock copolymers of p**EtOx** and poly(ε-caprolactone) illustrated reversible sol-gel transitions, while the gel range could be increased by increasing the hydrophobic poly(ε-caprolactone) content.[116] Addition of salts such as sodium chloride lowered the phase change temperature, while the addition of sodium thiocyanate increased it.

Hwang, Hsiue et al. investigated triblock copolymers of the composition p**EtOx**-poly(ε-caprolactone)-p**EtOx**, obtained from OH-terminated p**EtOx** as initiator for the polymerization of ε-caprolactone and subsequent coupling with 1,6-hexamethylene diisocyanate.[117] The triblock copolymers displayed sol to hydrogel transition between room and body temperature. The gels were non-cytotoxic and could be used as an intraocular carrier for bevacizumab. Notably, Järvinen and her group characterized in an in-line matter the degradation products of poly(ε-caprolactone)s crosslinked with 2,2-bis(2-oxazoline)s.[118] Polymer films were immersed in a phosphate buffer of pH 7.5 and subjected to enzymatic degradation. Water soluble-polymers could be identified by HPLC and electrospray ionization tandem mass spectroscopy. Based upon the recovered oligomers, it was suggested that ester bonds were most susceptible to the enzymatic degradation, indicating pancreative lipase as the driving force behind the degradation of this polymer.

3.3 Contact Biocides

In everyday life, hygienic concerns grow daily as the world's population grows and bacteria become ever more resistant to traditional treatments. It is necessary to deal with new strategies to provide antimicrobial activity, particularly in applications such as water tanks and pipes, food processing and sanitary equipment. One key strategy, which has been suggested in recent years, is the equipment of surfaces with polymeric materials which exhibit permanent antimicrobial activity.[119,120] Much attention has been paid towards this strategy where the common features are the attachment of the antimicrobial polymer to a surface and the subsequent treatment of the bacteria by mere contact. In the last decade, numerous potential polymer and polyelectrolyte candidates for use in this field have been suggested and some prominent examples are given below.[121,122]

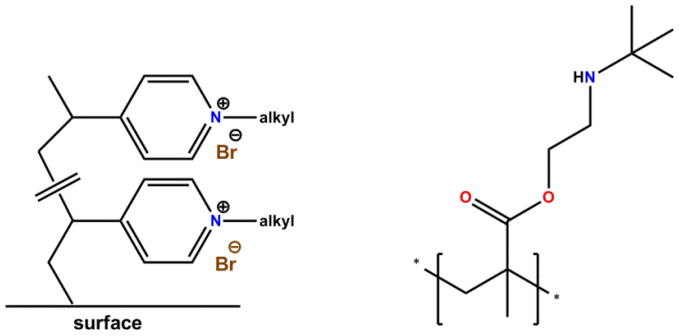

Figure 3-5: Two currently utilized polymer biocides: Poly(4-vinyl-*N*-alkylpyridinium bromide) attached to a glass substrate (left), poly(2-*tert*-butylaminoethyl) methacrylate compounded with LLDPE (right).

Klibanov et al. reported on glass slides which had been treated such that poly(4-vinyl-*N*-alkylpyridinium bromide) was covalently attached in order to provide antimicrobial activity against airborne bacteria.[123] By spraying a known content of bacterial cells on the surface, air drying and subsequently measuring the remaining bacterial cells, the antimicrobial activity could be determined. Dependent on the amount of alkyl chains present, various degrees of antimicrobial activity were observed. For a hexyl chain, the material was shown to kill up to 94 ± 4% of *S. aureus*. Additionally tests of this material against *S. epidermidis* and the gram negative bacteria *P. aeruginosa* and *E. coli* showed a reduction in activity by a factor of 100.

The group of Kern reported work on the modification of PE compounds to provide antimicrobial surface activities.[124] LLDPE was compounded with the biocide poly(2-*tert*-butylaminoethyl) methacrylate and tested for antimicrobial properties and compared

against unmodified LLDPE (Figure 3-5). Against the test species *E. coli* and *S. aureus*, significant reduction in the quantity of colony forming units CFU on the surface was noted with an average decrease of 10^4 CFU mL^{-1}. Additionally over a period of 16 weeks, biofilm tests revealed that adhesion of the film was reduced significantly upon increasing amounts of the biocidal additive.

Current disadvantages of sterile surfaces can subsequently be overcome utilizing these methods. As of today, such surfaces commonly involve small molecule release. Mammalian bodies will often suffer cytotoxic effects from small molecule accumulation, particularly from metals. This strategy eliminates this drawback. Additionally to maintenance-free surfaces, they may have no release at all, and the biocidally active materials may be accessible to continued usage.[125]

3.3.1 Mechanism and Requirements

The precise mechanism for the antimicrobial activities displayed by various polymers has not yet been fully determined on the molecular level and is the subject of much debate. Three models dominate current thinking on the matter: the barrel-stave, toroid and carpet mechanisms.[126-129] In all three mechanisms, the presence of cationic functionalities (usually peptides) at the surface of membranes is considered one of the initial phases of activity as they are attracted to the negative charge of the membrane phospholipids.

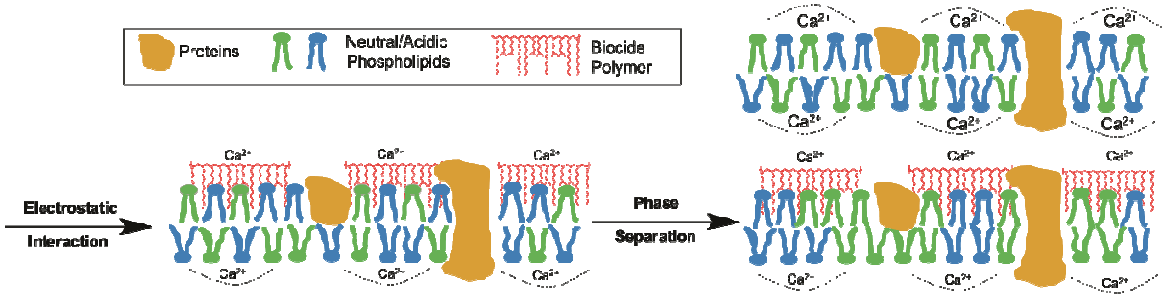

Scheme 3-14: Proposed method of interaction between antimicrobial polymers and bacterial membranes.[130]

Another common feature is the repulsion of the calcium layer of the bacterial membrane, which acts to stabilize the membrane structure. Adhesion to the bacteria is similarly universal prior to the various methods of phase separation. In each case, the charged and neutral lipids in the membrane are disturbed leading to degradation of the entire membrane and subsequent cell death (Scheme 3-14). Numerous sources of

experimental data have verified the necessity of the cationic charge in polymers for antimicrobial activity. Nonetheless, further details have not been confirmed, though recent work suggests that the presence of hydrophobic side chains in the polymer can further aid the induction of the phase separation. Such synergistic effects in cell-wall perturbation, however, require further research.

3.3.1.1. Barrel-Stave Model

This mechanism relies upon the self-association of peptides leading to the formation of pores which transverse the membrane. Due to disruption of cell potentials and ion gradients, internal portions of the cell are released through the pore and, lacking all the necessary components to survive, cell lysis occurs. The hydrophobic peptide parts orientate themselves towards the phospholipid chains, whilst the hydrophilic parts face inwards forming a channel through which water can flow. In such way the name of the mechanism is clear; the hydrophobic parts act as the exterior of a barrel, whilst the water channels formed by the hydrophobic part mimic the interior staves of the same barrel. Sufficiently long peptides are required that can fully penetrate the membrane layer and the peptides must be able to be in contact with one another. Circular dichroism measurements of the insertion of the fungal peptide alamethicin into a membrane showed a reversible and continuous pore formation (Figure 3-6).[131]

3.3.1.2. Toroid Model

In essence, the toroid model bears many similarities to the barrel-stave method; both are indeed concerned with pore formation through the cell membrane leading to cell lysis (Figure 3-7). However, the method of pore formation and indeed the pore size are different. Peptides form along the surface of the membrane in a similar manner to the other models but then cause the bilayer of the membrane to “bend back” on itself. This bending of the phospholipids in particular results in toroidal pores being formed.[132] Such a type of pore answers one of the main drawbacks of the barrel-stave method. In the toroidal model, the peptides do not need to be very long as the pore formation is often a subsequent process to a thinning of the membrane by peptide induction.[133,134] Additionally, as the pore not only comprises of the peptide as in the barrel stave method, but additionally of the cell’s own lipids, they can be shorter and still achieve sufficient penetration for cell lysis.

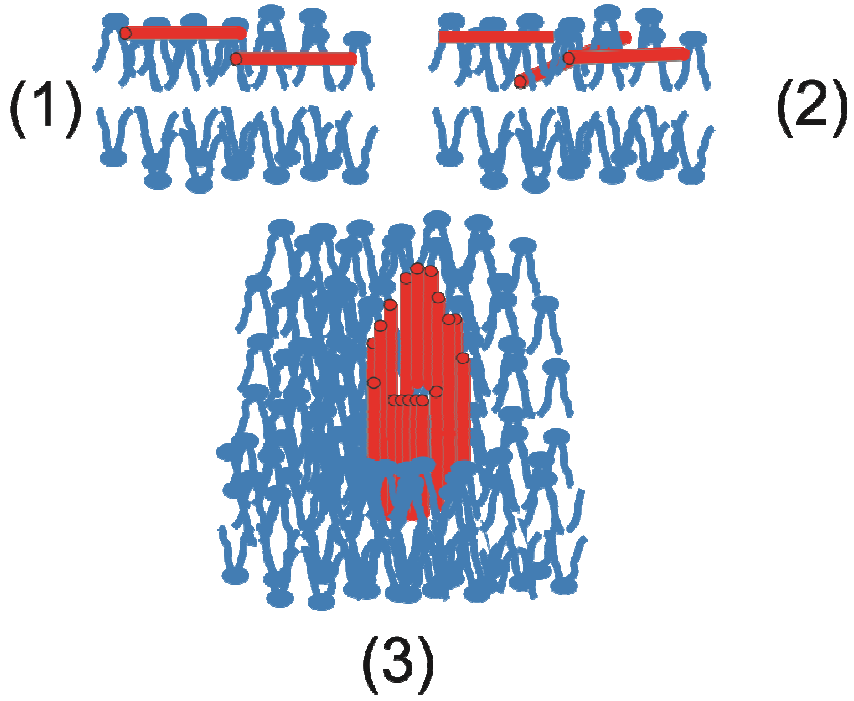

Figure 3-6: Barrel-stave model: Peptides (cylinders) attach in parallel manner to membrane surfaces either on the surface (1) or with slight embedding (2). Once sufficient surface concentration is reached, the peptides fully penetrate the membrane forming pores (3).

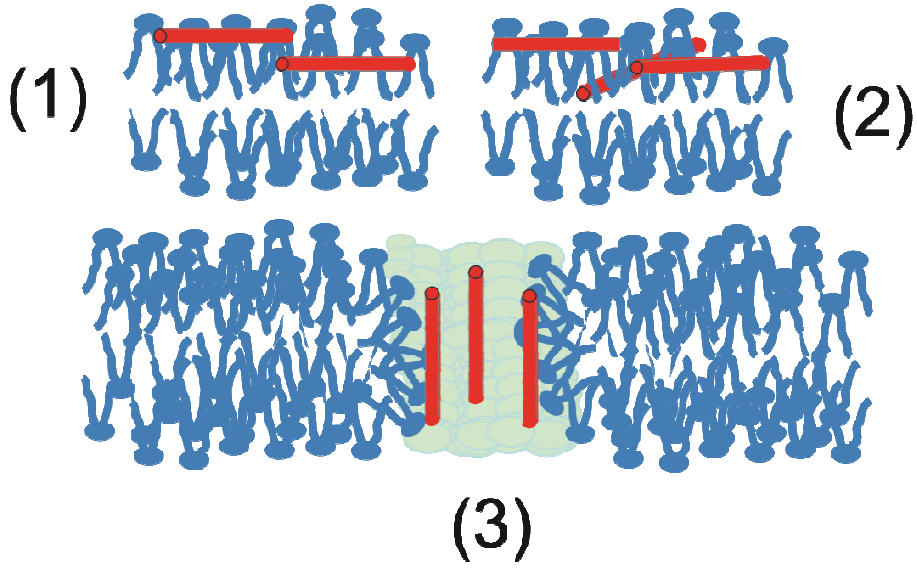

Figure 3-7: Toroidal pore model: Peptides (cylinders) attach in parallel manner to membrane surfaces either surfacially (1) or with slight embedding (2). Once sufficient surface concentration is reached, the peptides induce localized pore formation (3).

3.3.1.3. Carpet Mechanism

According to the carpet mechanism, peptides congregate close to the surface of the bilayer surface of a cell membrane (Figure 3-8). This model envisages the process as being like a carpet being laid down to cover a floor, namely that the peptides form a flat "layer" over the membrane. Once there is a sufficiently high concentration of peptides present, permeation of the membrane initiates. The membrane is subsequently destroyed forming detergent like structures, leading to cell lysis. Notably, this varies from the toroid model in that no discrete channels are formed during the permeation phase. Steiner first proposed this mechanism when observing that the amount of cecropin A required to kill 50% of bacterial cells was sufficient to entirely cover the surface of the bacterial cell.[135] Additional work by Shai et al. utilised ATR-FTIR spectroscopy to show that cecropin P1 was incorporated onto a membrane in a parallel fashion and was not absorbed into the core.[136] Despite the lack of observed pores, some similarities to the toroidal model do exist; the peptides remain associated to the membrane head groups throughout the process.[137]

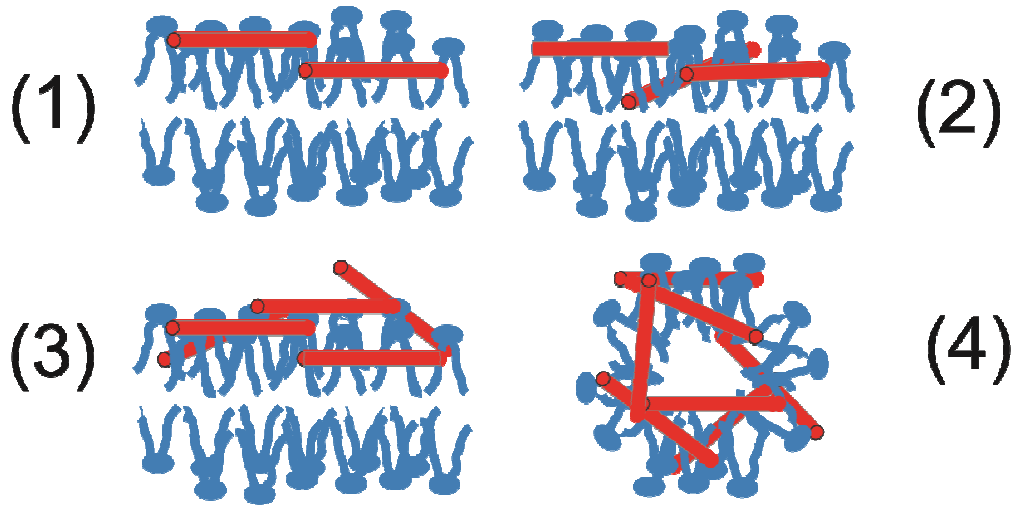

Figure 3-8: Membrane disruption according to the carpet model: Cylinders represent peptides that initially (1) bind and (2) accumulate parallel to the surface before covering the bilayer and (3) penetrating it, leading to (4) detergent like disintegration.

3.3.1.4. Requirements

In order to provide benefits over traditional antimicrobial materials, numerous factors need to be taken into consideration when synthesizing biocidal polymers. As the goal of

such materials is not only to possess the biocidal material but to be used maintenance-free, this increases the complexity of designing the materials.[11]

Firstly, as with all such materials, they must not only possess sufficiently high activity to kill bacteria, but must do so against a wide variety of species due to the range of applications required. The materials require long-term stability if they are to be referred to as permanent biocides. Additionally, they must possess stability against reactions such as hydrolysis given the potential nature of their usage environment. In order to be of use under aqueous conditions, the polymers must either be insoluble in water on their own or be anchorable in a water-proof way to the target surface. In order to provide significant advantages over existing methods involving small molecule release, the polymer must either release no compounds of a similar nature or have very high levels of release suppression. Finally, as with most cases, a cheap and easy synthesis of the polymer must be possible, particularly when considering factors such as scale-up and also the purification procedure as high purity is required to ensure no unwanted compound release or molecular interactions.

3.3.2 Prominent Examples

The group of Tew investigated the use of “Synthetic Mimics of Antimicrobial Peptides” SMAMPs in antimicrobial applications.[138] SMAMPs mimic the peptides found in the body’s immune system and can be prepared easily from facially amphiphilic oxanorbornene based monomers. Variance of amphiphilicity, monomer ratio and molecular weight was employed and polymers prepared via ROMP. It was found that by tuning the molecular weight from 750-1100 g/mol to 3000 g/mol, the selectivity can be changed from *S. aureus* to *E. coli*. By combining a non-active polymer with such an active polymer, it was shown that the selectivity against *S. aureus* could be increased to over 533 against red blood cells. The ability to tune both the properties against different bacteria and the activity against blood cells make these interesting candidates for use as biocidal materials.

Subsequently, Tew et al. reported on the preparation of amphiphilic poly(norbornene)s for antimicrobial applications via the addition of hydrophilic groups to the polymer Poly3 (Figure 3-9).[139] The species used were sugar, zwitterionic and pEG based and could be incorporated either during the copolymerization involving protection groups or post-synthetically, where acrylate functionalized pEG could be reacted with an amine

functionalized poly(norbornene) via a Michael addition. The copolymers were of narrow PDI values in the region of 1.1. It was shown that, as the hydrophilicity of the additive decreased, the antimicrobial effect was increased. The co-polymers containing pEG groups showed the highest antimicrobial activity with 30% lower MIC values than the standard poly(norbornene). Due to the greater biocompatibility of the sugar incorporating polymers the biocidal effects can be more selective.

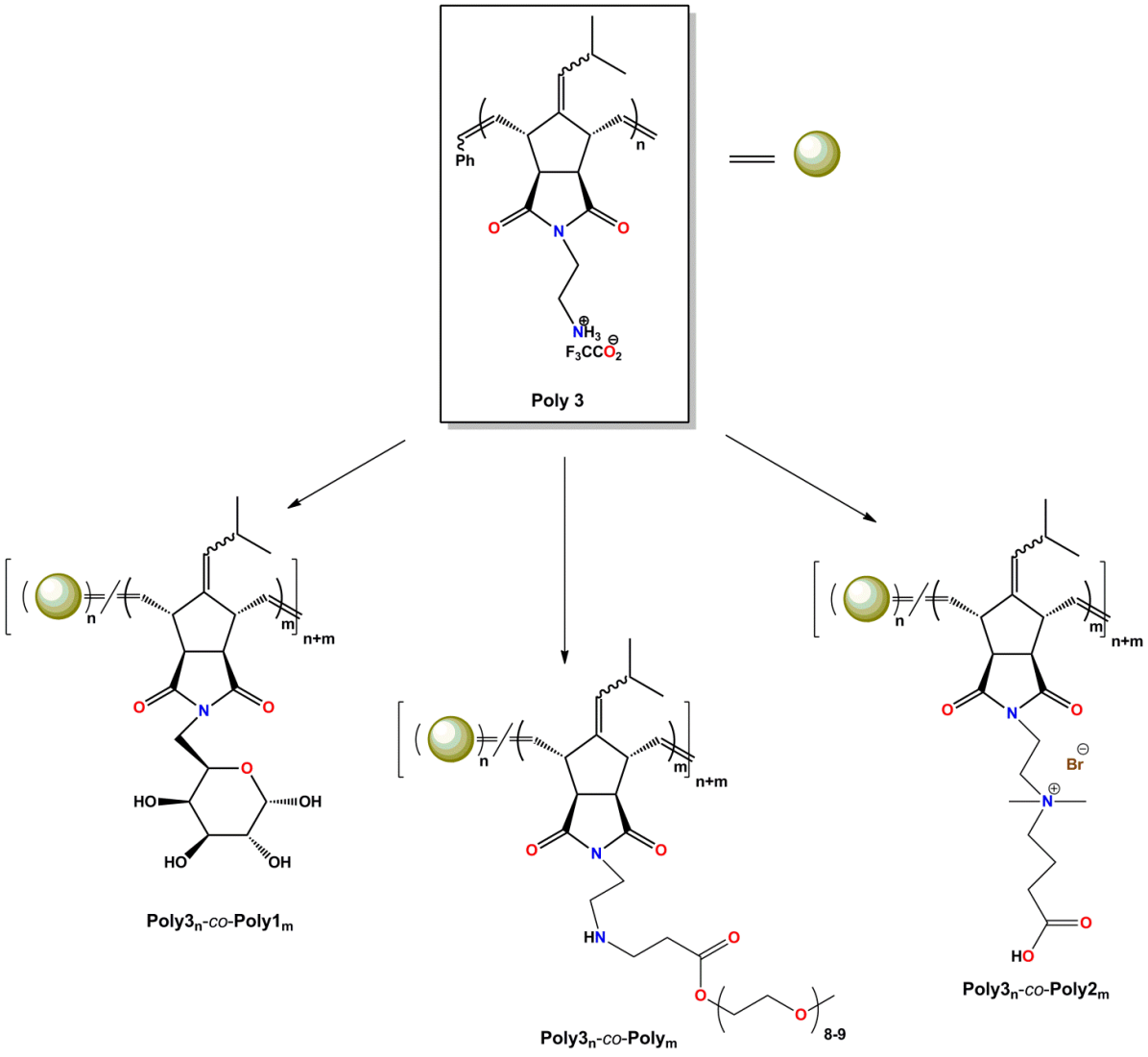

Figure 3-9: Poly3 modification utilizing hydrophilic groups. N = mol fraction of M3 and m = mol fraction of M1 in the copolymer.

Further work by the group compared the copolymerization of poly(oxanorbornenes) via traditional methods to a method employing “facially amphiphilc” FA monomers in order to increase both the activity and selectivity of the polymers.[140] Polymers obtained under normal synthetic means possessed separated cationic and non-polar moieties. By engineering the monomers to be “facially amphiphilic”, the charged and non-polar species could be balanced in local positions as opposed to across the entire polymer chain. Fluorescence microscopy reveled that when *E coli* was incubated with samples of each polymer, the activity of the FA polymers showed clearly the cell adhesion, whereas the traditionally produced polymers did not interact as well. It was suggested that similar strategies may be employed with other polymer backbones such as poly(acrylate)s and poly(styrene)s.

3.3.3 Poly(2-oxazoline) Based Contact Biocides

Despite many applications in other fields of polymer chemistry, as previously shown, the development of contact biocides utilizing poly(2-oxazoline) based materials has been relatively minimal. Nonetheless, research has begun in this field and, due to the many benefits of 2-oxazolines, promises to continue to grow.

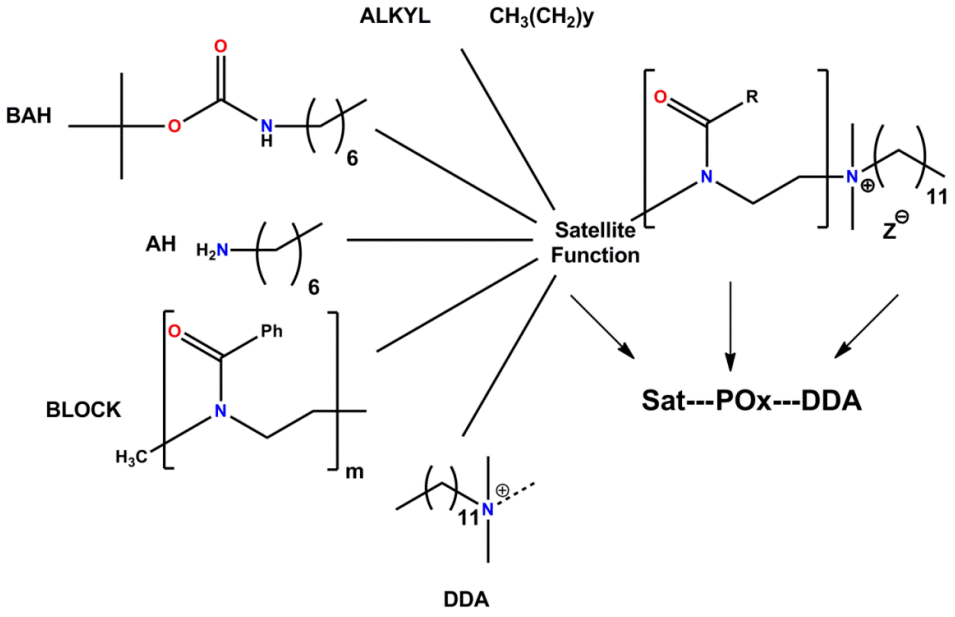

Figure 3-10: Telechelic poly(2-oxazoline)s bearing the antimicrobial DDA group in addition to a satellite function.

Tiller and his group reported on poly(alkyloxazoline) telechelics utilizing one quaternary *N*,*N*-dimethyldodecylammonium (DDA) end group (Figure 3-10).[141] The non-bioactive section was referred to as the satellite group and the effects of this group on the overall antimicrobial activity were investigated. Various materials with alkyl, aminoalkyl and poly(phenyl oxazoline) satellite groups were produced with low PDI values in the range of 1.06-1.20. When tested against *E. coli* and *S. aureus*, the antimicrobial activity increased by a factor of 2-3 against the known biocide dodecyltrimethylammonium chloride when the alkyl satellite groups contained 4-10 carbon atoms. Above this number, the CMC was found to decrease rapidly and reduce activity. The increase of antimicrobial activity was attributed to disruption of cell membranes caused by the satellite groups.

Further work by this group utilized p**MeOx** as a polymer spacer with one end functionalized by the known biocide DDA and at the other end with a polymerizable methacrylate group.[142] Biocide tests were carried out against gram-positive bacteria and showed 10 times longer activity than with DDA in its normal form as well as requiring 87 times less quantity of material. The modification allows for methacrylate networks to contain a biocidal function without release of any small molecules.

Work by Aguiar-Ricardo et al. described the amine quaternization of 2-oxazoline based oligomers which had been prepared utilizing super critical carbon dioxide.[143] Polymerization of 2-oxazolines (methyl, ethyl and phenyl) could be carried out in solvent-free manner in CO_2 and allowed for the formation of biocompatible oligomers. Additionally, oligo(ethylene imine) hydrochlorides and oligo(2-bisoxazoline)s could be prepared either through a similar method or via hydrolysis. It was shown, following quaternization with DDA, that quaternized oligo-**MeOx** and oligo-**TMBOx** were the most effective biocides against *S. aureus* and *E. coli*. Linear oligo(ethylene imine) hydrochloride showed higher activity against the same bacteria, but the time for cell lysis was significantly longer.

4 Results and Discussion

4.1 Poly(2-oxazoline) Based Gels

4.1.1 Synthesis of Gels

Crosslinked polymer networks were synthesized from the two mono-functional monomers 2-ethyl-2-oxazoline **EtOx** and 2-phenyl-2-oxazoline **PhOx** and the bis-functional crosslinker phenylene-1,3-bis-(2-oxazoline) **PBO** (Scheme 4-1). Due to the improved reaction rates possible, microwave-assisted means were employed in the gel synthesis. Samples of each monomer were added to sealable microwave vials along with the initiator methyl tosylate MeTsO. Reactions were carried out under (single-mode) microwave irradiation at a temperature of 140 °C for one hour, ensuring maximum conversion.

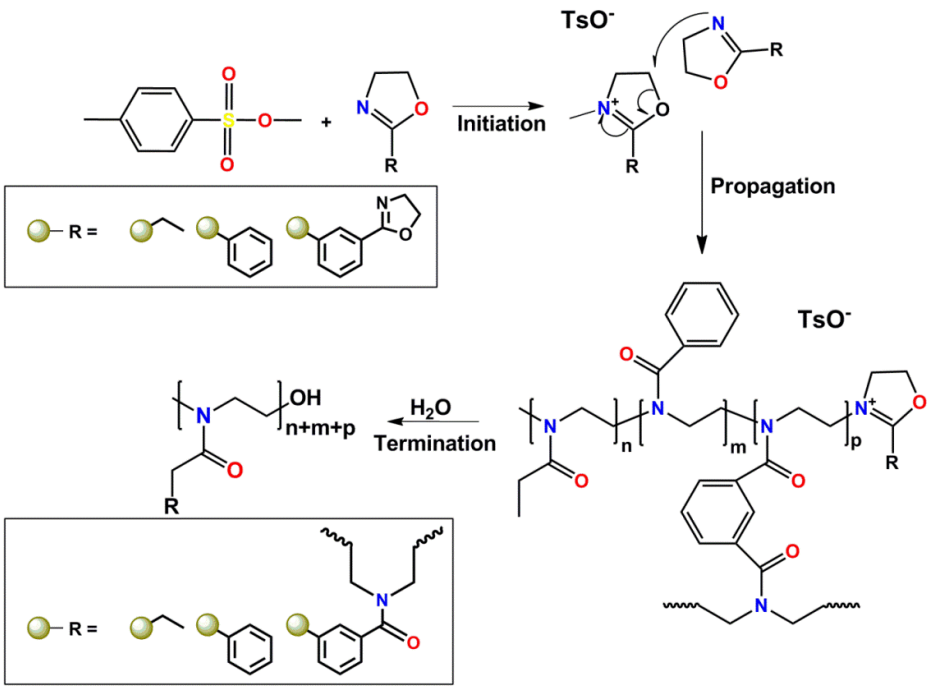

Scheme 4-1: Cationic ring opening copolymerization of the three monomers **EtOx**, **PhOx** and **PBO** using MeTsO as initiator, resulting in the formation of gels of the form p**EtOx**$_m$-p**PhOx**$_n$-p**PBO**$_q$.

For all syntheses, a constant monomer:initiator ratio of 150:1 was maintained with respect to the total of the mono-functional oxazolines **MonOx** (namely the sum of **EtOx** and **PhOx**). In order to investigate the effect of monomer composition, four varying ratios

of **EtOx**:**PhOx** were selected for the syntheses: 150:0, 100:50, 50:100 and 0:150. Additionally, the effect of varied crosslinking degrees was investigated: The amount of bisfunctional oxazoline **BisOx** (for all cases **PBO**) was varied. For each series of monomer ratios, relative amounts of **PBO** were added to achieve molar ratios of **MonOx**:**BisOx** = 150:30, 150:15, 150:10, 150:7.5 150:6, 150:3, 150:2, 150:1.5. These values correspond to crosslinking ratios of 5:1, 10:1, 15:1, 20:1, 25:1, 50:1, 75:1 and 100:1 and allow for a wide range of gels to be synthesized. Slightly yellowish gels were obtained with brittle nature in their un-swollen state.

4.1.1.1. Kinetics

In order to ensure optimized reaction conditions for the gel syntheses, three important factors were considered. Firstly, by utilizing existing polymerization methods, the maximum monomer conversion was determined. Secondly, it was important to optimize the reaction time of the polymerizations by looking at the relative reactivity of the three monomers **EtOx**, **PhOx** and **PBO**. Finally, it was necessary to verify that **PBO** was indeed capable of crosslinking (see section 4.1.1.2).

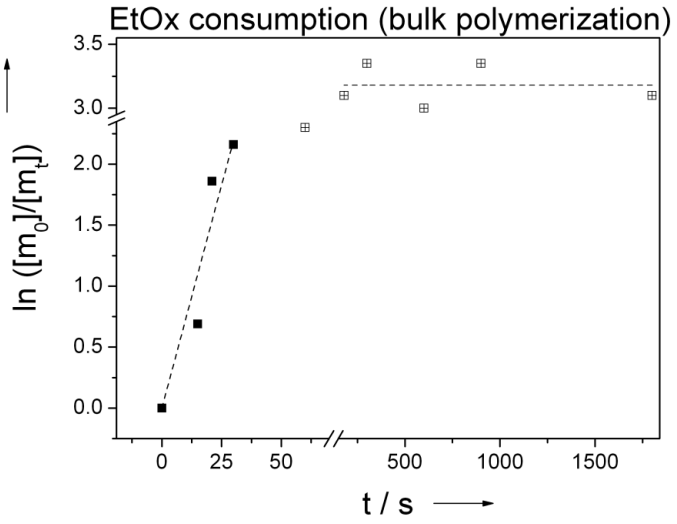

Figure 4-1: Consumption of **EtOx** monomers during the polymerization under microwave irradiation.

The solvent-free polymerization of **EtOx** was investigated using MeTsO as initiator in order to answer the first abovementioned concern. The polymerization was shown to

initially follow first order kinetics up to a value of $\ln([m_0]/[m_t])$ of 2.2. This value corresponds to a maximum conversion of around 90%. Above this point however, the kinetic profile was shown to deviate significantly from the first order (Figure 4-1). The maximum conversion was achieved after 5 minutes of reaction time with a $\ln([m_0]/[m_t])$ value of 3.2, representing a conversion of 96%. These results could be reproduced in good order even utilizing prolonged reaction times. Owing to the comparably high monomer conversion from solvent-free mixtures, it was not required to employ solvents during gel syntheses. Additionally, solvent-free syntheses of gels are desirable due to minimization of dilution effects and low levels of insufficient crosslinking.

The second concern was investigated by determining the relative reactivity of each monomer when the polymerization was carried out using microwave assisted heating protocols under solvent-free conditions. Such methods allowed for homopolymerizations to be carried out achieving monomer conversions of 95% and higher.[30,32] Previous research had reported on the significant difference of the reactivity of **EtOx** and **PhOx**, which was attributed to the resonance stability of the positively charged **PhOx** which inherently results in a lower reactivity (Scheme 4-2).[32,33]

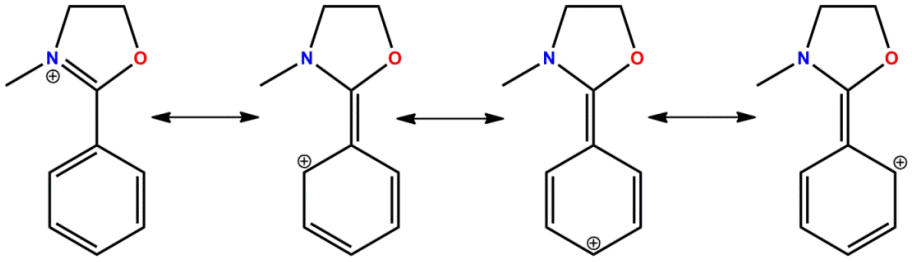

Scheme 4-2: Resonance structures of **PhOx.** Due to its aromatic nature, a reduction in reaction rates occurs compared to the aliphatic monomer **EtOx**.

During the copolymerization of **EtOx**, **PhOx** and **PBO** with molar ratios of 100:50:15, similar observations could be made. The reaction was examined until the first drops of gel were precipitated from the reaction mixture (Figure 4-2). During the first 15 seconds of the reaction at 140 °C, a plateau was observed for all monomers with **EtOx** having undergone conversion of around 20% and **PhOx** and **PBO** having either minimal or no conversion at all. Following this period, the conversion proceeded for all species. However, the conversion rate of **EtOx** compared to **PhOx** and **PBO** was significantly

more rapid. Such results were reproducible and it was assumed that they result from the combination of the various resonance effects of **PhOx** and **PBO** (Schemes 4-2 and 4-3). Additionally, polymer formation results in increasing viscosity of the reaction mixture and affects the conversion in a similar manner when the reaction was preheated from room temperature to 140 °C within 45 seconds. Once the target temperature had been reached, the polymerization proceeded involving all three species. As before, the **EtOx** consumption remained significantly higher than the consumption of either aromatic monomer. It is worth noting that excess monomer is able to diffuse out of gels of a sufficient swelling degree (see section 4.3), yielding enhanced purity than those of low swelling degrees.

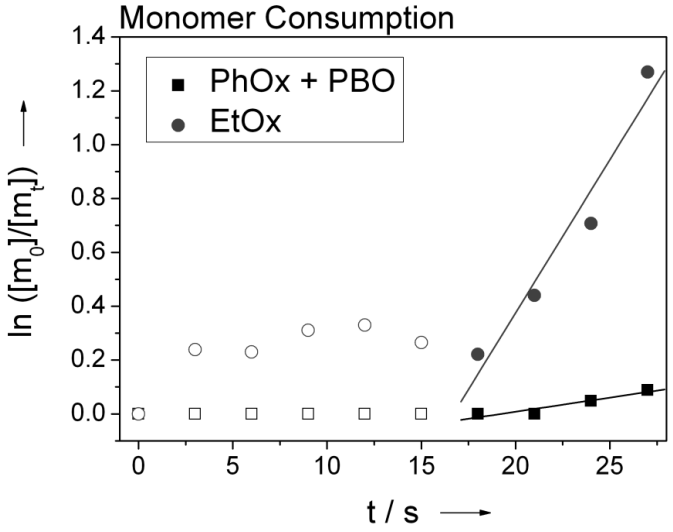

Figure 4-2: Initial monomer consumption of the three monomers **EtOx**, **PhOx** and **PBO** under solvent-free conditions.

4.1.1.2. Crosslinker Considerations

Initially, two isomers of **PBO** were considered as potential crosslinkers in the gel syntheses. Both 1,3-**PBO** and 1,4-**PBO** upon initial inspection seemed to offer valid choices in network formation. However, when tested, only the 1,3-**PBO** allowed for successful polymerization of **EtOx** and **PhOx**. The 1,4-isomer indeed failed to result in gel yields at greatly extended reaction times of 8 hours. It can be suggested that resonance stabilization of the positively charged 1,4-isomer resulted in a lower reactivity of the crosslinker. Additionally, resonance of the 1,4-isomer results in α-elimination of a proton (Scheme 4-3, bottom row). Subsequently, an olefinic species is generated in addition to a proton that has a relatively low reactivity towards re-initiation of the

polymerization and effectively terminates the novel polymer chain. Hence, 1,3-**PBO** was used as the exclusive crosslinker for the gel syntheses carried out.

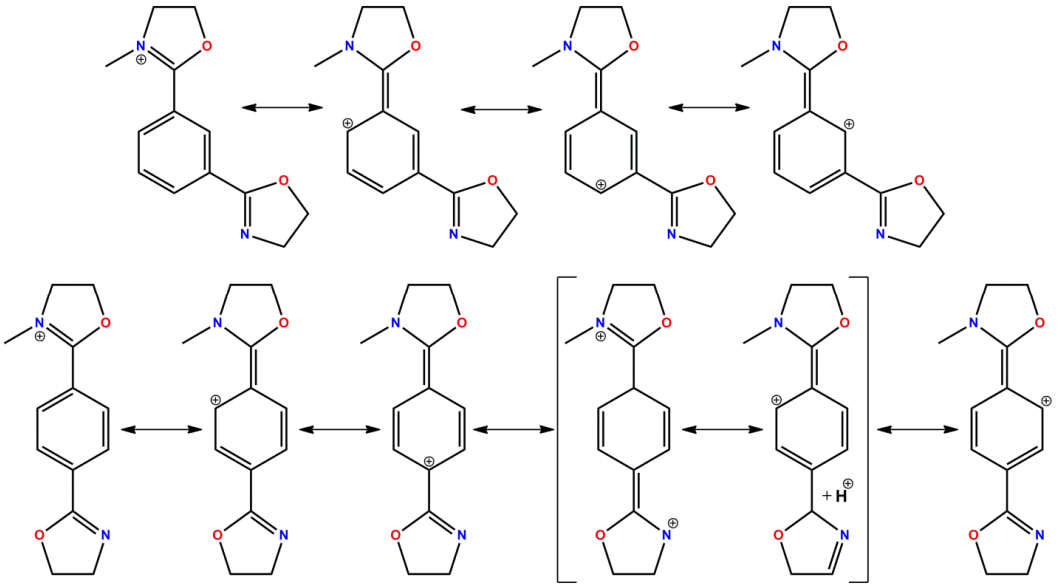

Scheme 4-3: Resonance structures of 1,3-**PBO** showing similarities to those of **PhOx** (top), resonance structures of 1,4-**PBO** highlighting the α-elimination of a proton resulting in the termination of the polymerization (bottom).

4.1.2 Gel Purification

Each of the 32 synthesized gels underwent the same purification process. The gels were swollen repeatedly in dichloromethane, recovered and subsequently dried resulting in a yield of purified gels of over 95%. Purified gels were slightly yellow colored but mostly colorless. The gel p**EtOx**$_{150}$-p**PBO**$_{1.5}$ could not be recovered due to its solubility in dichloromethane.

Gels with a crosslinking degree of 2% or lower swelled sufficiently in chloroform to allow for ^{1}H-NMR measurements to be carried out (Figures 4-3 to 4-6). Analysis of hydrogels is often difficult; GPC for instance fails due to the insoluble nature of gels. The NMR analyses therefore, allowed for the best investigation of the actual composition of the gels compared with the targeted compositions (Table 4-1).

Table 4-1: ^{1}H-NMR data for gels with high swelling degrees, illustrating good agreement with calculated integral values (calculated values / experimental values).

δ (ppm) =	1.0-1.3	1.8-2.6	3.0-4.0	6.9-7.1
p**EtOx**$_{150}$- p**PBO**$_2$	450 / 458	300 / 307	616 / 616	0 / 0
p**EtOx**$_{100}$-p**PhOx**$_{50}$-p**PBO**$_2$	300 / 301	200 / 202	616 / 616	100 / 95
p**EtOx**$_{50}$-p**PhOx**$_{100}$-p**PBO**$_2$	150 / 154	100 / 98	616 / 616	200 / 201
p**PhOx**$_{150}$-p**PBO**$_2$	0 / 0	0 / 0	616 / 616	300 / 301

Based upon the integral values obtained and the peak positions, it was shown that the targeted compositions were achieved with good accuracy. This indicates that chain flexibility is additionally averaged throughout the gel. In the region of 4.0 to 5.0 ppm, signals representing the methylene units of a 2-oxazoline ring are present when the gels were purely composed of aromatic moieties: p**PhOx**$_{150}$-p**PBO**$_q$ ($q \leq 3$). This corresponds to residual monomer, which apparently does not diffuse out of the system during purification.

The other series p**EtOx**$_m$-p**PhOx**$_n$-p**PBO**$_q$ ($m \geq 50$; $n \leq 100$) showed no such signals and were said to be monomer free. The diffusional differences were attributed to sterical reasons. The high bulk of the aromatic groups in the gels containing only aromatic moieties as well as the monomers results in hindrance and an overall reduction in diffusivity, and monomer retention is significantly lowered in the p**PhOx**$_{150}$-p**PBO**$_q$ series because of sterical reasons due to the high abundance of comparatively bulky aromatic groups in the monomer as well as in the gels.

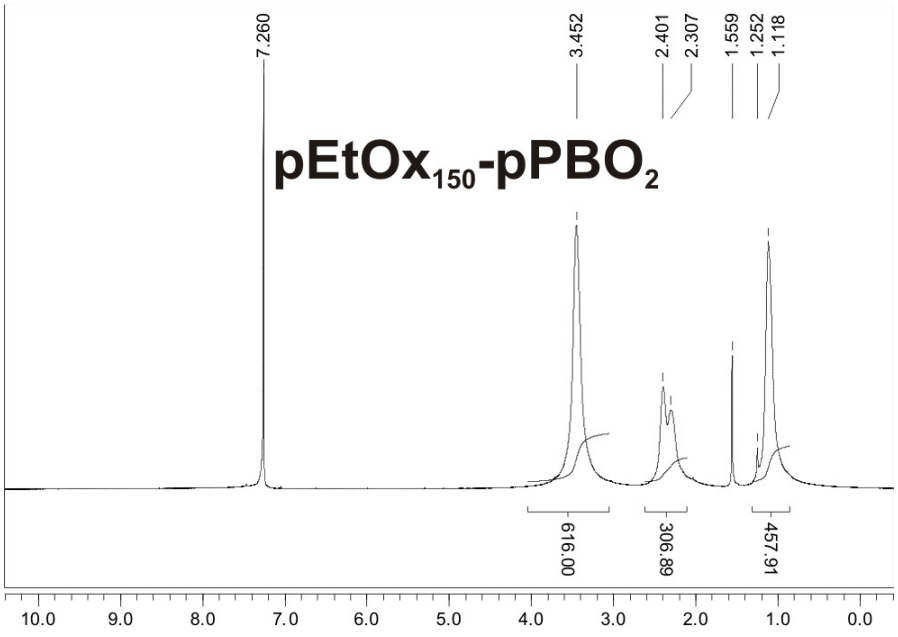

Figure 4-3: ^{1}H-NMR spectrum of p**EtOx$_{150}$**-p**PBO$_2$**.

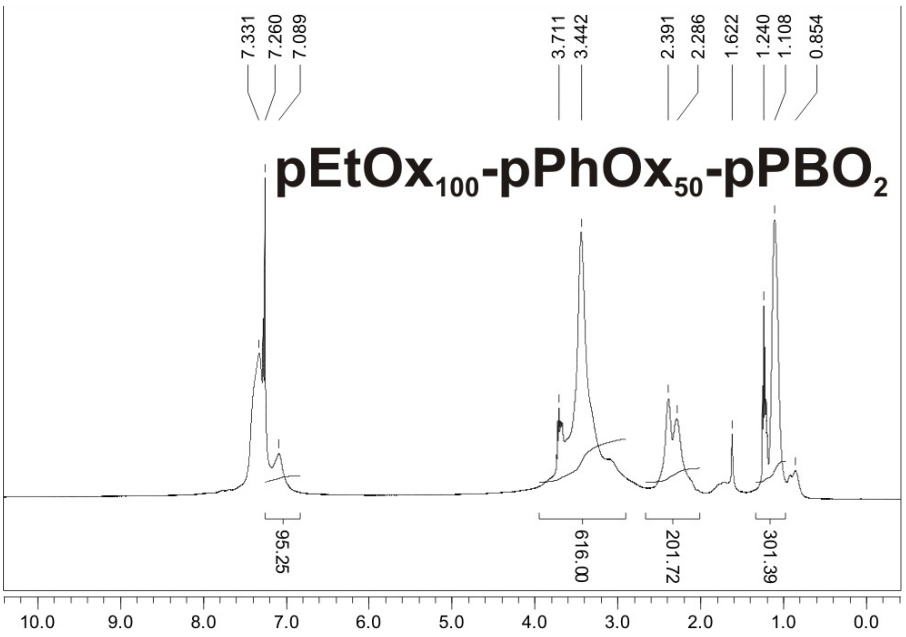

Figure 4-4: ^{1}H-NMR spectrum of p**EtOx$_{100}$**-p**PhOx$_{50}$**-p**PBO$_2$**.

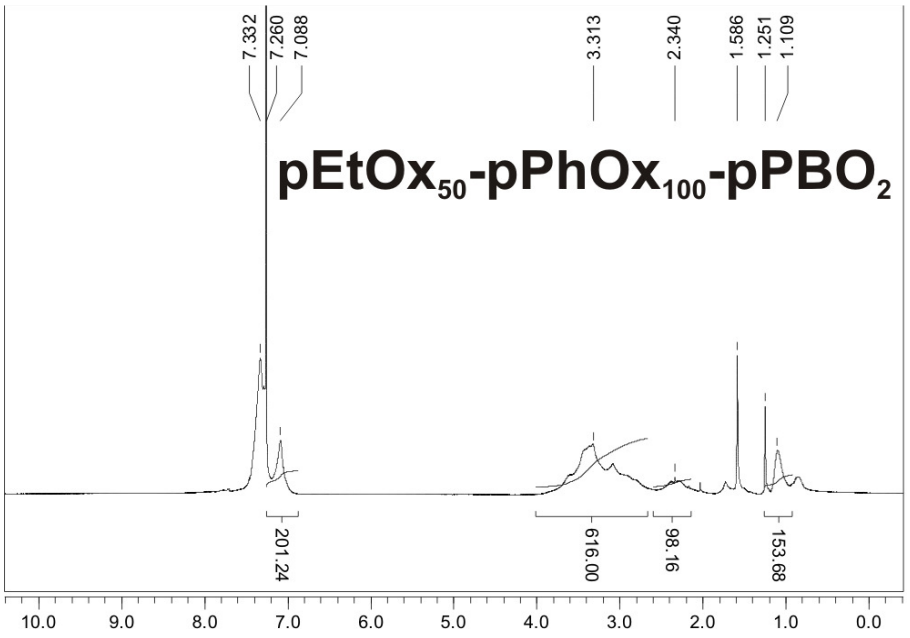

Figure 4-5: ^{1}H-NMR spectrum of p**EtOx$_{50}$**-p**PhOx$_{100}$**-p**PBO$_2$**.

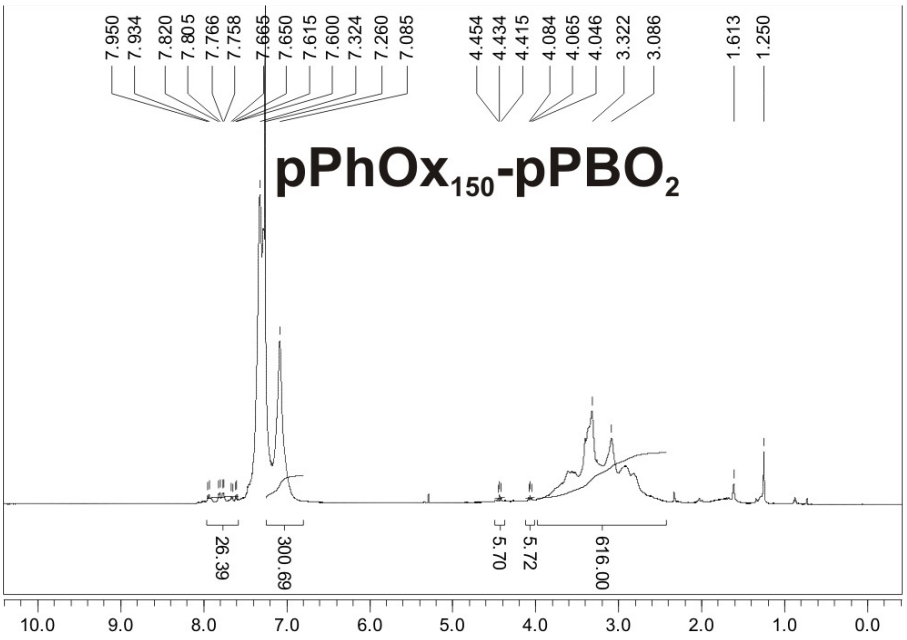

Figure 4-6: ^{1}H-NMR spectrum of p**PhOx$_{150}$**-p**PBO$_2$**.

4.1.3 Swelling Degree Experiments

Characterization of the gels in terms of their swelling degrees is essential in order to develop their further usage towards compound uptake and release. Swelling degrees are a measure of the amount of liquid of specific polarities and molecular sizes which the tested gel can adsorb into the network structure. For possible applications as drug delivery matrices, the swelling degrees are therefore a key characteristic of each gel.

Gels of the composition p**EtOx**$_m$-p**PhOx**$_n$-p**PBO**$_q$ were swollen in test liquids under atmospheric conditions with maximum swelling degrees being obtained after a maximum of 48 hours. By forming a mass balance between the mass of the purified un-swollen gels and the gels swollen for 48 hours the swelling degree of each gel was calculated according to:

$$\text{swelling degree} = \frac{m_{swollen} - m_{gel}}{m_{gel}} \qquad \textbf{Equation 4-1}$$

where $m_{swollen}$ is the mass of the gels after swelling in the test liquids and m_{gel} is the mass of the dry gels.

For each of the 32 synthesized gels of the compostion p**EtOx**$_m$-p**PhOx**$_n$-p**PBO**$_q$, swelling was carried out in the three test liquids water, ethanol and dichloromethane. These liquids were chosen for their varying hydrophobicity/hydrophilicity as well as the differing size of the solvent molecules. Notably, in all three liquids the hydrogel p**EtOx**$_{150}$- p**PBO**$_{1.5}$ was soluble.

4.1.3.1. Swelling Degrees in Water

When stored in water for 48 hours, minimal swelling was observed for gels with the compositions p**PhOx**$_{150}$-p**PBO**$_q$ and p**EtOx**$_{50}$-p**PhOx**$_{100}$-p**PBO**$_q$. Beginning with the gel series of the composition p**EtOx**$_{100}$-p**PhOx**$_{50}$-p**PBO**$_q$, the reduced phenyl content within the gels resulted in evidence of swelling. As the crosslinking degree decreased, the swelling was shown to increase to a maximum of 2.7 for p**EtOx**$_{100}$-p**PhOx**$_{50}$-p**PBO**$_{1.5}$. The gels of the series p**EtOx**$_{150}$-p**PBO**$_q$ had no aromatic mono-functionalities and experienced a vast increase in swelling degrees. With lower degrees of crosslinking the swelling increased, most noticeably after the ratio of mono-functional moiety to crosslinker reached 50:1. The swelling degrees reached a maximum of 14 for p**EtOx**$_{150}$-p**PBO**$_2$. This dependence upon **PBO** content in determining the swelling degree is

attributed to the pore sizes between the crosslinking sites. With higher crosslinking degrees, the network structure is more rigid lessening its ability to uptake fluids. Likewise, as less crosslinker is present, pore sizes and network flexibility increase to allow for more liquid to be adsorbed (Figure 4-7).

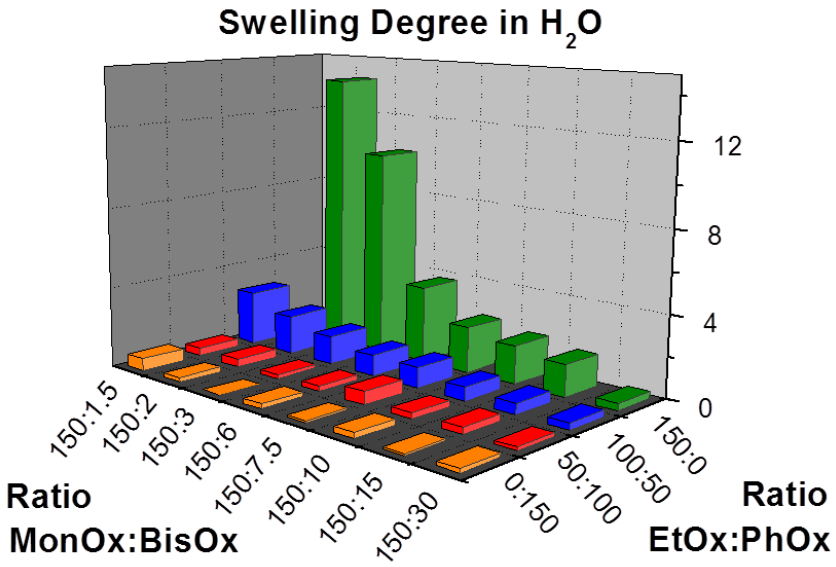

Figure 4-7: Maximum swelling degrees of the 32 p**EtOx**$_m$-p**PhOx**$_n$-p**PBO**$_q$ based gels constituting the small compound library in water.

4.1.3.2. Swelling Degrees in Ethanol

Differing from the series of gels tested in water, the series tested in ethanol showed a greater range of swelling degrees, allowing for a more differentiated correlation between the swelling degree and the gel composition. There was again negligible swelling for the series p**PhOx**$_{150}$-p**PBO**$_q$; however, with crosslinking ratios higher than **MonOx:BisOx** = 50:1, small degrees of swelling could be observed. As with the test solvent water, the crosslinking degree was found to influence the swelling degree: As it decreased, the swelling degree increased for all series. With a decrease in **PhOx** content, the gels were shown to have an increase in swelling degrees (Figure 4-8). Due to the solubility of p**EtOx**$_{150}$-p**PBO**$_{1.5}$, the maximum swelling degree observed was 11.7 for the gel p**EtOx**$_{100}$-p**PhOx**$_{50}$-p**PBO**$_{1.5}$.

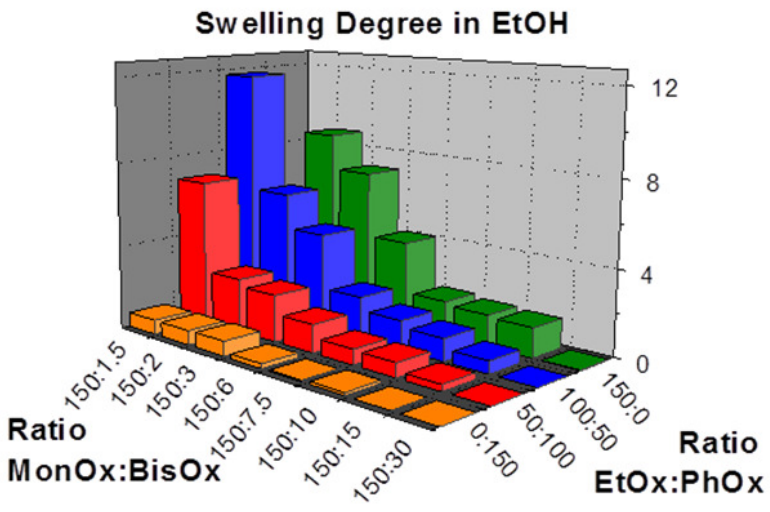

Figure 4-8: Swelling degrees in ethanol of the 32 p**EtOx**$_m$-p**PhOx**$_n$-p**PBO**$_q$ based gels are shown to vary with both ethyl versus phenyl content and crosslinking degree.

4.1.3.3. Swelling Degrees in Dichloromethane

Gels swollen in dichloromethane showed the highest overall swelling of all the series tested (Figure 4-9). Swelling degrees up to a maximum of 20 were observed when the crosslinking degrees were at their lowest. These measurements occurred for gels of the composition p**EtOx**$_m$-p**PhOx**$_n$-p**PBO**$_{1.5}$ ($m \leq 100$; $n \geq 50$). However, unlike with ethanol, the variances in swelling degrees were only noticeable when the crosslinking degrees differed. The ratio **EtOx**:**PhOx** in the gels is not a significant factor determining swelling in dichloromethane. Resultantly, two conclusions can be drawn. Firstly, the accessible pore size arising from the different size and shapes of the ethyl and phenyl side chains has no effect on the swelling degree of the gels. Secondly, regardless of the varying reactivity of **EtOx** and **PhOx**, the pore size distribution is not influential in determining the swelling degrees. It can be shown therefore that only the differences in gel composition brought about by varying crosslinking degrees are a factor in overall swelling characterization in dichloromethane.

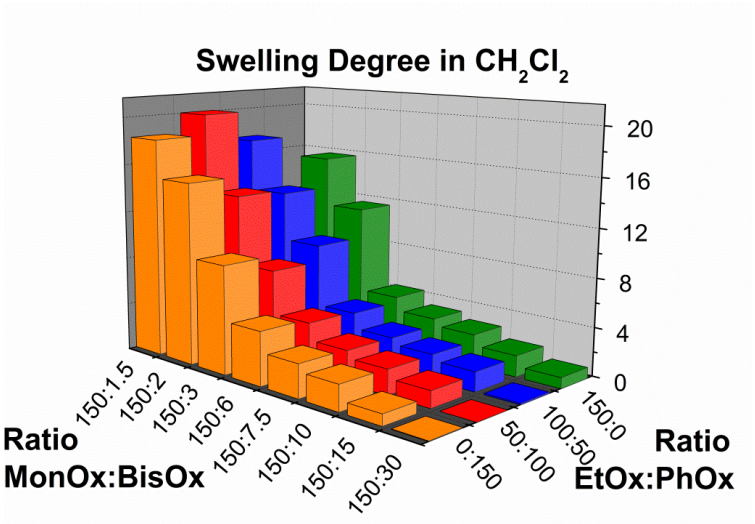

Figure 4-9: When swollen in dichloromethane, the 32 p**EtOx**$_m$-p**PhOx**$_n$-p**PBO**$_q$ based gels attain their maximum swelling degrees that are dependent only upon crosslinking degree.

4.1.4 Compound Inclusion

The swelling degrees of the 32 members of the gel library showed a wide range of values dependent upon composition. In order to determine the potential of the gels as drug delivery matrices, it was necessary to study the ability of the gels to include model compounds in order to simulate their uptake behavior. Two main methods of inclusion were considered: uptake of the compounds through diffusion and in-situ inclusion during polymerization. Whilst the gels with high swelling degrees could be expected to take up the compounds through diffusive properties, the alternate strategy of synthetic inclusion was preferable in the case of gels with limited swelling degrees. Two model compounds, the dye Eosin Y and the drug Ibuprofen, were selected to examine the uptake parameters for the gels.

4.1.4.1. Dye Inclusion

Eosin Y, a dye, was selected as a model compound to show that organic molecules can be easily incorporated within gels during the polymerization. The two negative functional groups within Eosin Y (Figure 4-10), the phenolate and benzoate, made it an ideal candidate for in-situ inclusion. Due to the negative functionalities, the Eosin Y molecule could expectantly bind covalently to the propagating polymer chains. Additionally, due to the functionalities, the chain growth could be terminated.

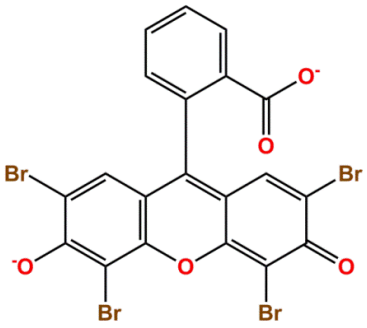

Figure 4-10: Structure of Eosin Y. The negative functionalities of the benzoate and phenolate can bind with and terminate the growing polymer chain making it an ideal candidate for in-situ inclusion.

The series of gels p**EtOx**$_m$-p**PhOx**$_n$-p$_q$**PBO**$_q$·[Eosin Y]$_{0.04}$ was prepared synthesizing the gels as previously described but additionally including 0.2 wt.-% of Eosin Y (m/n = 150/0, 100/50, 50/100, 0/150, q = 3; 7.5). The syntheses preceded quantitatively producing 2 g of each gel. When fully swollen in any of the test liquids, no Eosin Y was released from the gels where it had been synthetically included (Figure 4-11). Indeed, in order to cause release of the dye, degradation was required under lowered pH and increased temperatures.

Whilst for gels with comparatively low swelling degrees synthetic inclusion was necessary, those with high swelling degrees could be post-synthetically impregnated with Eosin Y. Swelling of gels such as p**EtOx**$_{150}$-p**PBO**$_3$ in dichloromethane allowed for dissolved molecules to migrate in a diffusion-mediated manner into the hydrogels where they were subsequently trapped. Gels could be loaded with Eosin Y, which had been added to a dichloromethane/ethanol mixture in 0.5 wt.-% amount. Gels were swollen for 24 hours to achieve their maximum swelling degree. The concentration of Eosin Y within the solution was assumed to have negligible variability throughout the swelling process as a result of the high swelling degrees leading to little diffusive resistance in the gels. Based upon previous swelling degree determination and the amount of Eosin Y dissolved in the solution, the amount of dye within the recovered gel could be calculated. In the case of the aforementioned gel, the gel produced when swollen in the Eosin Y solution was p**EtOx**$_{150}$-p**PBO**$_3$·[Eosin Y]$_{1.25.}$ Whilst such a gel had a high swelling degree in dichloromethane, in water its swelling degree was minimal. Hence, when the dried gel was swollen in water, the diffusion which would allow for the transport of Eosin Y out of the gel was not prevalent and the dye was trapped with the gel. This factor also allows for the washing of Eosin Y which has adhered to the gel surface with water without the

risk of reducing the internal content of the compound. To test the long term validity of these results, gels which had been impregnated with Eosin Y both synthetically and post-synthetically were stored in water for four weeks. During this time, negligible release of the dye from the gel to the liquid could be observed.

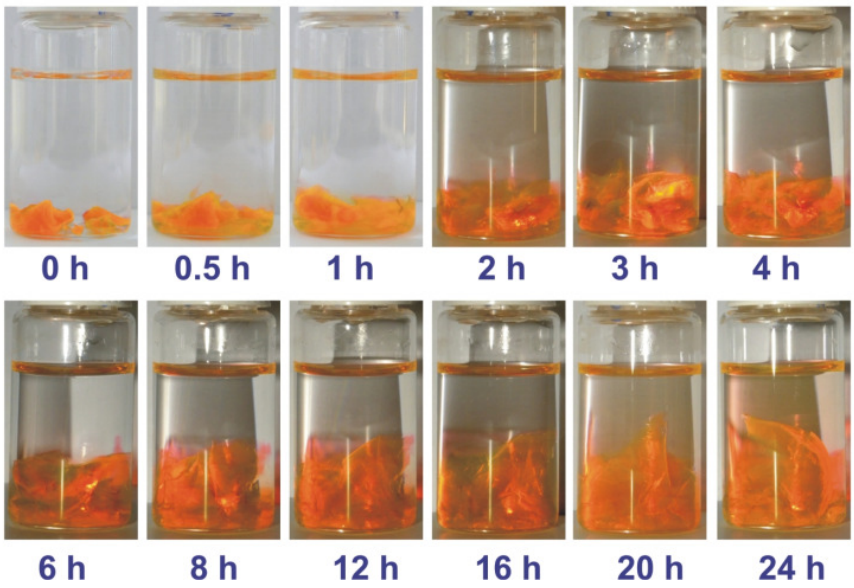

Figure 4-11: Sample of Eosin Y-impregnated p**EtOx**$_m$-p**PhOx**$_n$-p$_q$**PBO**$_q$·[Eosin Y]$_{0.04}$ gel swollen over 24 hours in water, showing no release of the dye.

4.1.5 Stimuli-Triggered Compound Release

4.1.5.1. Solvent Change

Due to differences in both the hydrophobic and hydrophilic character of both solvent and the gels it was possible to employ solvent change as a method for compound release. Gels which had been post-synthetically loaded with Eosin Y via typical swelling protocols allowed for this to be illustrated. It was particularly noticeable for gels with pronounced hydrophobic character and subsequent low swelling in water. When swollen in a solution of Eosin Y, the compound was taken up by gels such as p**PhOx**$_{150}$p**PBO**$_3$. Upon drying of the gel the liquid was removed but the dye remained within the gel network. Subsequent addition to water resulted in no release of the compound. However, addition of the gel to DCM (or chloroform) or a water/DCM (or water/chloroform) biphasic system resulted in the rapid release of the compound. This was attributed to not only the varied

hydrophobic/hydrophilic nature of the gel but also to the higher swelling in this solvent system allowing for greater diffusion (Figure 4-12).

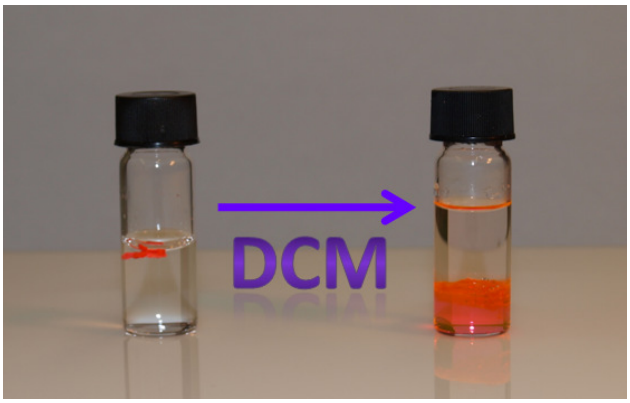

Figure 4-12: Release of Eosin Y from gels upon change of solvent from water to DCM.

4.1.5.2. Degradation

An alternate strategy for compound release under consideration was the acid mediated degradation of the gel network through hydrolysis of the amide bonds present in poly(2-oxazoline)s (Scheme 4-4). When considering the potential of the materials for drug delivery applications, the environment in which such drug release may occur must be taken into account. In the body, numerous processes can result in chemical degradation including among others acid mediated hydrolysis and enzymatic degradation. Acid mediated hydrolysis is of particular interest for anti-cancer drug delivery materials due to the lowered pH of cancer cells (pH= 5.3) compared to the pH within the body (7.4).[144] Such mechanisms were thus investigated to give an idea of the model of degradation which could be expected for these materials.

Release of compounds via complete degradation was expected to take somewhere in the range of several weeks to months in lowered pH aqueous environments. It was shown that not only were the expected hydrolysis products produced but also that included molecules were released. Two tests were carried out, firstly, a verification of the method, namely a quantitative hydrolysis of the gel at elevated temperature, and secondly, a set of tests across a series of gels with the same crosslinking degree but varying ethyl/phenyl content in order to establish a kinetic relationship between degradation rate and gel composition.

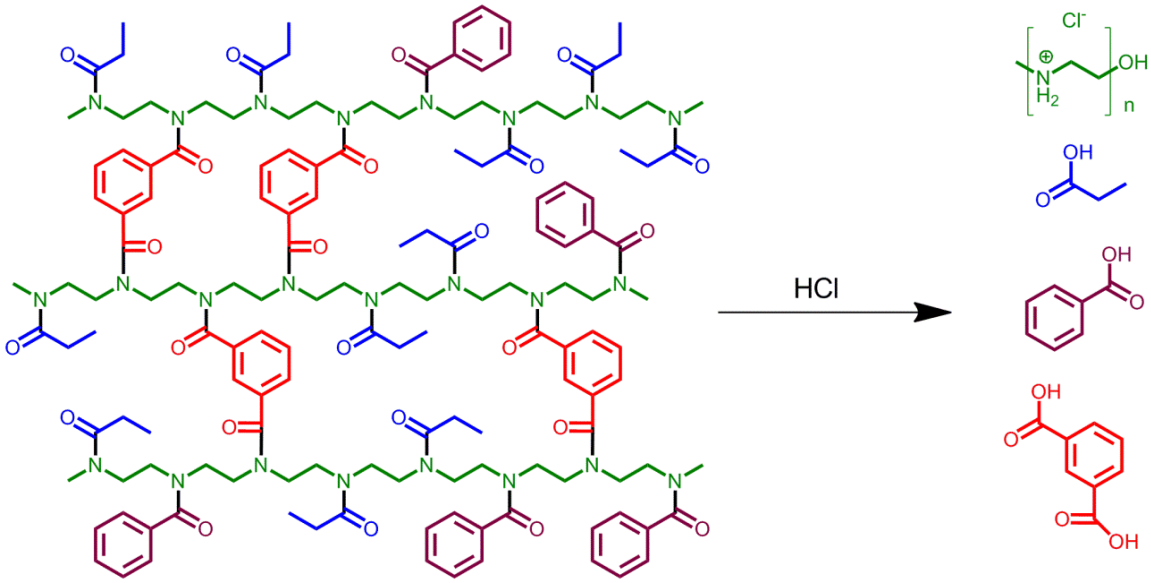

Scheme 4-4: Acid mediated hydrolysis of gels p**EtOx**$_m$-p**PhOx**$_n$-p**PBO**$_q$ yielding the products poly(aziridinium chloride), propionic acid, benzoic acid and phthalic acid.

The quantitative hydrolysis was carried out over four hours at the elevated temperature of 160 °C in a microwave reactor. The test was not designed to simulate conditions occurring naturally, but merely to determine the species present in the degradation mixture. By performing the reaction not in normal hydrochloric acid but a 1 M deuterated analogue, the reaction mixture could immediately be sampled for NMR analysis. Degradation under these conditions indeed yielded the expected degradation products and any incorporated organic molecules such as Eosin Y.

In order to determine the differences in hydrolysis rate dependent upon ethyl/phenyl content, gels of the composition p**EtOx**$_m$-p**PhOx**$_n$-p**PBO**$_2$ (m/n = 150/0, 100/50, 50/100, 0/150) were reacted at the same temperature for 30 minutes in DCl that also contained acetone as an internal standard for comparison (20:1 v/v). By comparing the ratio of the internal standard to the degradation product poly(aziridinium chloride), the relative degradation ratios could be determined. A decrease in the phenyl content of the gel was shown to accelerate the rate of hydrolysis. Going from p**PhOx**$_{150}$-p**PBO**$_2$ to p**EtOx**$_{150}$-p**PBO**$_2$, the amount of poly(aziridinium chloride) present in the degradation mixture increased according to 1:9:34:84 indicative of an increase in reaction rates. Such results are expected when considering the swelling degrees. With increasing ethyl content, the swelling degrees in aqueous environments were shown to increase. As more of the lowered pH aqueous media could enter the network, the accessibility of the acid to the

amide bond was increased allowing for hydrolysis to occur more rapidly. It does however, not explain fully the effect of the stability of aliphatic and aromatic amides on the degradation rate. Nonetheless, a sufficient kinetic model to predict the rates of degradation can be easily established for this class of gels.

4.1.6 Cytotoxicity

In order to determine the potential of the gels for usage within mammalian bodies, it was necessary to determine their cytotoxicity. Cytotoxicity is the ability of a compound to inhibit the normal growth of healthy tissue. For the cytotoxicity test, p**EtOx**$_{50}$-p**PhOx**$_{100}$-p**PBO**$_6$ was chosen as a representative candidate of the library of gels, as it was composed of all monomers investigated in this study and exhibited a medium degree of crosslinking. Tests were carried out by BSL Bioservice Scientific Laboratories GmbH in Planegg, Germany; study number 103716. Over a 24 hour period, extraction of the test gel was carried out in compliance with ISO 10993-5, -12. Several controls were set up in addition to the test material in order to prove the validity of the results. A non-cytotoxic poly(ethylene) extract was used as negative control, a cytotoxic positive control of DMSO and a sample of the extraction vehicle, DMEM 10% FCS, with no test material present was utilized as solvent control. The test was carried out with L929 cells (ATCC No. CCL1, NCTC clone 929 (connective tissue mouse), clone of strain L (DSMZ)).

Each set of cultures was incubated for 68 to 72 hours at 37±1 °C under an atmosphere of 5% CO_2 to 95% air. Coloumetrically (at 550 nm), the individual culture protein contents were measured and used to calculate the growth inhibition, where %growth inhibition **%GI** can be calculated from:

$$\%GI = 100 - 100.\frac{(A_{550nm}sample) - (A_{550nm}blank)}{(A_{550nm}control) - (A_{550nm}blank)} \qquad \textbf{Equation 4-2}$$

where A_{550nm}sample/blank/control corresponds to the absorption of the test extract / blank cultures without cells / solvent control.

According to ISO 10993-5(3), cytotoxic effects can be related to the protein content of test cultures, which can be used as a measure for cell growth. Clear cytotoxicity is defined by a threshold inhibition of cell growth of more than 30% compared to cultures

within the solvent control. Proving the validity of the study, the negative control had a **%GI** of 5% and the positive control had a **%GI** of 93%. Dilutions of both the test item and the solvent control in DMEM 10% FCS were carried out in order to evaluate the variance of cytotoxicity with content volume. For the dilutions 1, 0.667, 0.444, 0.296, 0.198 and 0.132 v/v, the gel extract displayed **%GI** values of 4/3/0/2/0/0, respectively. Given that these values are all considerably lower than the 30% threshold for cytotoxic activity, it is shown that no leachable substances were released from the test gel in cytotoxic concentrations. It was therefore concluded that the gel p**EtOx**$_{50}$-p**PhOx**$_{100}$-p**PBO**$_{6}$ can be classified as non-cytotoxic.

4.2 Poly(2-oxazoline) Based Contact Biocides

4.2.1 Polymer Synthesis

In order to investigate as wide as possible a range of contact biocides, the two monomers 2-ethyl-2-oxazoline and 2-nonyl-2-oxazoline were selected. These allow for syntheses of polymers of different natures: p**EtOx** possesses a hydrophilic side group and is water-soluble, and p**NonOx** is insoluble in water due to the hydrophobic nonyl side-chain. The two polymers nonetheless can be easily synthesized under microwave irradiation. Due to solubility issues, p**EtOx** was synthesized in acetonitrile and p**NonOx** in chloroform. The polymerization times varied from 15 minutes at 140 °C for **EtOx** and 1 hour at the same temperature for **NonOx**.[32]

In this work, both polymers were synthesized with the same polymerization degree (100) in order to ensure that mass considerations when investigating biocidal activity could be minimized as well as providing quick reaction and recovery times. The polymers p**EtOx** and p**NonOx** will be referred to as $\mathbf{E_{100}}$ and $\mathbf{N_{100}}$ (and lower numbers when in hydrolyzed form) throughout this chapter.

4.2.2 Hydrolysis

As with the synthesis of the polymers, their modification via acid-mediated cleavage of the amide bond was carried out within a microwave reactor. This allowed for rapid synthesis of the copolymers in an environment where concentrated acids would be relatively safe to use even under elevated temperatures. In order to best understand the effect on antimicrobial activity over the full range of hydrolysis degrees, reaction times were varied to produce a library of potential antimicrobial materials (Figure 4-13). For the nonyl series hydrolysis, co-polymers with hydrolysis degrees of 25% $\mathbf{N_{75}A_{25}}$, 50% $\mathbf{N_{50}A_{50}}$ and 75% $\mathbf{N_{25}A_{75}}$ as well as the pure polymer $\mathbf{N_{100}}$ were prepared. For the ethyl series, the copolymers had hydrolysis degrees of 25% $\mathbf{E_{75}A_{25}}$, 50% $\mathbf{E_{50}A_{50}}$, 75% $\mathbf{E_{25}A_{75}}$ and 100% $\mathbf{A_{100}}$. The fully hydrolyzed polymer poly(azirdinium chloride) $\mathbf{A_{100}}$ was prepared exclusively via hydrolysis of $\mathbf{E_{100}}$ due to the commercial availability of the 2-ethyl-2-oxazoline monomer as opposed to 2-nonyl-2-oxazoline.

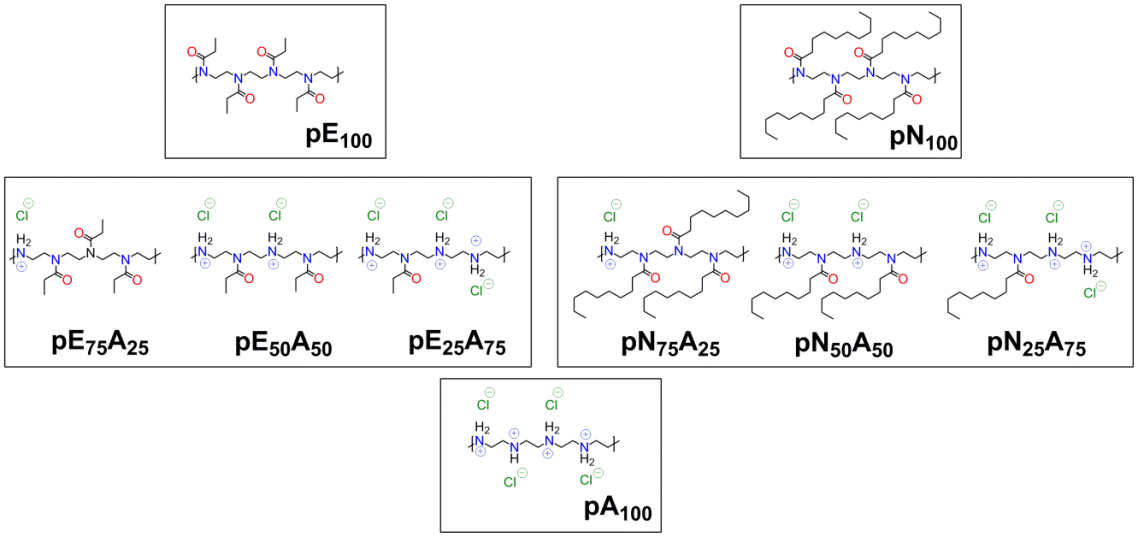

Figure 4-13: Library of the nine copolymers (native and partially or fully hydrolyzed polymers) of chain length 100 investigated for their antimicrobial activity.

4.2.2.1. Kinetics

Under the conditions employed, first-order kinetics was observed for the hydrolysis of both, p**E**$_{100}$ and p**N**$_{100}$ (Figure 4-14). The rates of hydrolysis varied greatly between p**E**$_{100}$ and p**N**$_{100}$: While 75% of hydrolysis was achieved within less than five minutes for p**E**$_{100}$, the same degree of hydrolysis required 30 min in the case of p**N**$_{100}$.

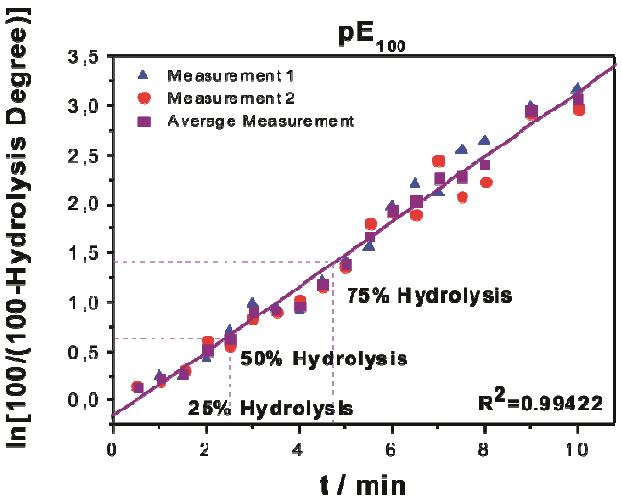

Figure 4-14: Hydrolysis of the p**E** series showing fast reaction times and first-order kinetics.

It was very tempting to refer this observation to the insolubility of p**N**$_{100}$; however, no deviations from initial reaction rates during continued hydrolysis (concomitant with increased solubility) were observed, and the lower rates for the hydrolysis of p**N**$_{100}$ seemingly originated from the steric shielding of the reaction center by the nonyl chains that collapsed around the amide bond in aqueous environments. Nonetheless, fast hydrolysis could be performed for both poly(2-oxazoline)s; fully hydrolyzed p**A**$_{100}$ was prepared from p**E**$_{100}$ due to the faster hydrolysis rates.

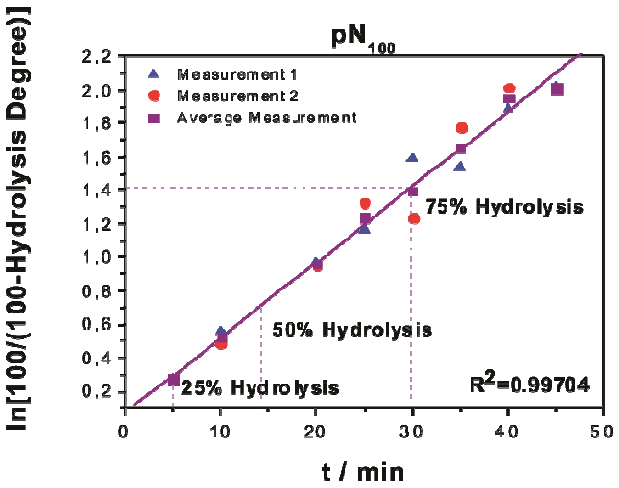

Figure 4-15: Hydrolysis of p**N** series showing first-order kinetics. Notably, the reaction rates are significantly slower than with the ethyl series.

4.2.2.2. Purification

Following many attempts at establishing an effective work-up technique that balances ease with product yield, an optimized protocol was developed (for full details see Experimental section). For ethyl based materials, this comprised evaporation of the acid, washing with THF and filtration to yield the hydrolyzed product which was subsequently vacuum dried overnight. The nonyl series proved to be more challenging. Low degrees of hydrolysis required dissolution of insoluble parts which were stuck in the reaction vessel, followed by evaporation of the acid, re-dissolution in DCM and freeze drying, washing with acetone and filtration as before. For high degrees of hydrolysis, the residues could be simply washed with acetone and filtered.

Table 4-2: ^{1}H-NMR data for the poly(2-oxazoline) based biocidal materials showing both calculated and measured integral values from which the degrees of hydrolysis were determined (experimental values with calculated values in brackets).

	0.8-1.2^{A1}	**1.2-1.4^{A2}**	**1.4-1.8^{A3}**	**2.0-2.8^{A4}**	**2.8-4.8^{A5}**
pE_{100}	297 (300)			201 (200)	400
$pE_{75}A_{25}$	221 (225)			150 (150)	400
$pE_{50}A_{50}$	157 (150)			105 (100)	400
$pE_{25}A_{75}$	72 (75)			50 (50)	400
pA_{100}					400
pN100	306 (300)	1196 (1200)	201 (200)	201 (200)	400
$pN_{75}A_{25}$	227 (225)	903 (900)	152 (150)	150 (150)	400
$pN_{50}A_{50}$	157 (150)	604 (600)	100 (100)	99 (100)	400
$pN_{25}A_{75}$	76 (75)	354 (350)		49 (50)	400

These optimized work-up conditions allowed for the preparation of high-purity partially hydrolyzed polymers (Table 4-2). ^{1}H-NMR data revealed that all integral values are in good agreement with predicted values. Notably for the nonyl series, there is no trace of TsOH which forms when the initiator counter ion is worked-up.

4.2.2.3. Scale up

Due to safety concerns regarding the large scale usage of concentrated acids at high temperatures, it was decided to lower the reaction temperature to 125 °C, resulting in a reduced operational pressure maximum of 12 bar. Despite the still relatively harsh conditions, PDI values indicated that there was no degradation of the partially hydrolyzed polymers (Table 4-3).

Table 4-3: Reaction times for the targeted degrees of hydrolysis at 125 °C and PDI values for polymer soluble in the eluent $CHCl_3/Et_3N/^{iso}PrOH$ (94/4/2).

	Hydrolysis(min)	**PDI**
pE_{100}		1.26
$pE_{75}A_{25}$	5	
$pE_{50}A_{50}$	15	
$pE_{25}A_{75}$	30	
pA_{100}	300	
pN_{100}		1.82
$pN_{75}A_{25}$	30	1.71
$pN_{50}A_{50}$	80	1.76
$pN_{25}A_{75}$	95	1.43

Full kinetic studies were not carried out at this lower temperature. However, based upon the limited data set collected (only four points), there was no obvious deviation from first-order kinetics observed for the hydrolysis. The lowered temperatures resulted in longer reaction times as would be expected. Additionally, it was necessary to slightly lower the reaction times due to longer cooling periods for the larger reaction volume if the targeted degrees of hydrolysis were to be achieved. Each material was tested via elemental analysis providing results in close agreement with the calculated values.

Table 4-4: Calculated and experimental values for the elemental analysis of the library of poly(2-oxazoline) based polymers and co-polymers.

	Carbon%		**Nitrogen%**		**Oxygen%**	
	Calc.	**Actual**	**Calc.**	**Actual**	**Calc.**	**Actual**
pE_{100}	60.60	58.77	14.10	13.69	9.10	8.97
$pE_{75}A_{25}$	51.71	58.77	14.20	13.45	8.87	8.83
$pE_{50}A_{50}$	42.75	41.58	14.25	14.09	8.11	8.65
$pE_{25}A_{75}$	33.72	34.43	14.30	14.65	8.43	8.13
pN_{100}	73.47	71.06	7.14	6.92	11.22	11.31
$pN_{75}A_{25}$	66.23	64.08	8.13	7.63	11.18	11.08
$pN_{50}A_{50}$	57.05	59.57	9.50	9.57	10.53	10.34
$pN_{25}A_{75}$	49.71	53.56	12.89	9.82	9.21	10.27

4.2.3 Sample Preparation

The statistical copolymers were obtained in their protonated form, and, due to their high thermal stability, not deprotonated prior to compound plate preparation (see below). According to previous reports, the apparent pK_a values of the ammonium groups decrease linearly with lowered environmental pH,[145] which, in final consequence, results in protonation equilibria in aqueous environments. Due to the fact that every third atom in poly(ethylene imine)s is a nitrogen atom, they have been referred to as a "proton sponge at virtually any pH",[146] which enables for reversible protonation-deprotonation cycles in the course of antimicrobial activity in the presence of water.

In order to produce plates suitable for biocide tests, the unhydrolyzed polymers as well as the hydrolyzed species were compounded with **PP** due to its common usage in surfaces and other applications where sanitary considerations are prevalent. Samples of

p**E**$_{100-25n}$**A**$_{25n}$ and p**N**$_{100-25n}$**A**$_{25n}$ (n = 0-4) were thoroughly ground by hand until a fine powder was obtained. The powders were then mixed with **PP** (5/95, 3/97, 1/99 w-%) ensuring that the distribution of the biocide test material was as uniform as possible. Likewise, when pouring the mixture into the moulds (150x150x2 mm), care was taken to spread the powder as evenly as possible. Platen pressing was carried out in a preheated oven in order to ensure constant initial conditions for each series of plates. Between the series, the only difference in plate appearance was a slight yellowing of the p**N** series due to the slightly colored nature of the polymers themselves.

4.2.4 Sample Characterization

4.2.4.1. Surface Energy Determination

Prior to the compound PP plates undergoing antimicrobial tests they were subjected to contact angle measurements in order to determine the surface energies. For the ethyl series of plates (including the fully hydrolyzed species p**A**$_{100}$) the test solvents water and diiodomethane were used as test liquids. Diiodomethane was again used along with ethylene glycol for the nonyl series (Figure 4-16; for full data see Appendix).

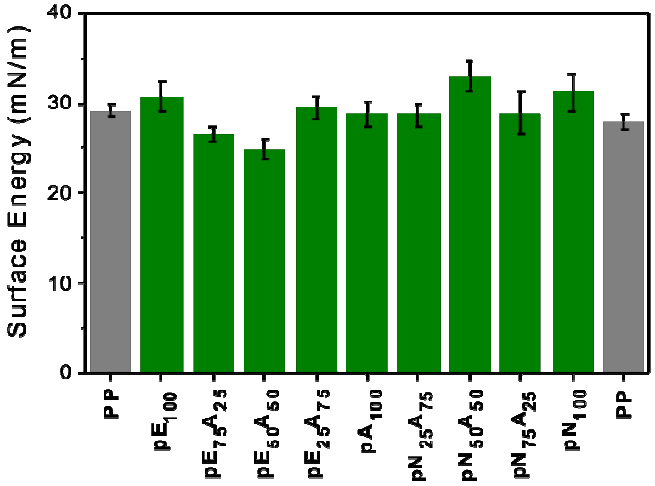

Figure 4-16: Surface energy values of p**E**$_{100-25n}$**A**$_{25n}$ (n = 0-4) and p**N**$_{100-25n}$**A**$_{25n}$ (n = 0-3) compound plates, calculated from contact angle measurements.

As a reference, the pure PP plate was shown to have a surface energy of 28.5 mNm^{-1} in good agreement with literature data.[147] The surface energies of all other test plates were of similar values with a range of 25-33 mNm^{-1}. Due to the relative similarity of the values, the plates are shown to possess neither overly hydrophobic or hydrophilic character. The

wettability of all compound plates was additionally deemed suitable for application of the compound materials as potential replacements for existing PP based products. However, the test cannot determine anti-fouling properties of the plates and their fouling character can subsequently not be concluded.

4.2.4.2. ATR-IR

In order to verify the presence of the antimicrobial polymers in the surface-near region of the specimen plates, attenuated total reflectance infra-red spectroscopy ATR-IR was employed. ATR-IR works based on principles of refractive indexes and allows for samples such as the plates used for biocide determination to be analyzed. Species which are present in the surface or near surface area of the plates can be identified via this technique. Plates prepared of pure PP as well as those containing the ethyl- and nonyl- based contact biocides were analyzed via this technique. The full spectra of each series showed the peaks expected at wavenumbers: 1170, 1300, 1370, 1450, 1600-1700, 1740, and 2800-3000 cm^{-1}. For all plates, the signal at 1370 cm^{-1} corresponding to the symmetrical alkane CH_3 deformation was present and used as reference peak by which the relative presence of the biocidal additives could be determined at the surface and near surface regions.

Analysis of the $\mathbf{pE_{100-25n}A_{25n}}$ series revealed a decrease in the signal corresponding to the combined asymmetrical CH_3 and CH_2 deformation at 1470 cm^{-1} as the degree of hydrolysis increases. This can be attributed to the reduction of the number of aliphatic side chains present in the polymer due to hydrolysis of the amide bond. The asymmetrical CH_3 bond becomes stronger relative to the CH_2 scissor deformation in this series. More noticeably, the signal from 1600-1700 cm^{-1} is shown to decrease as the degree of hydrolysis increases. This signal is a result of the strong absorbance of the tertiary amide deformation and the weaker absorbance of the secondary ammonium deformation. As hydrolysis increases and the number of amide bonds decreases, the amide signal correspondingly decreases.

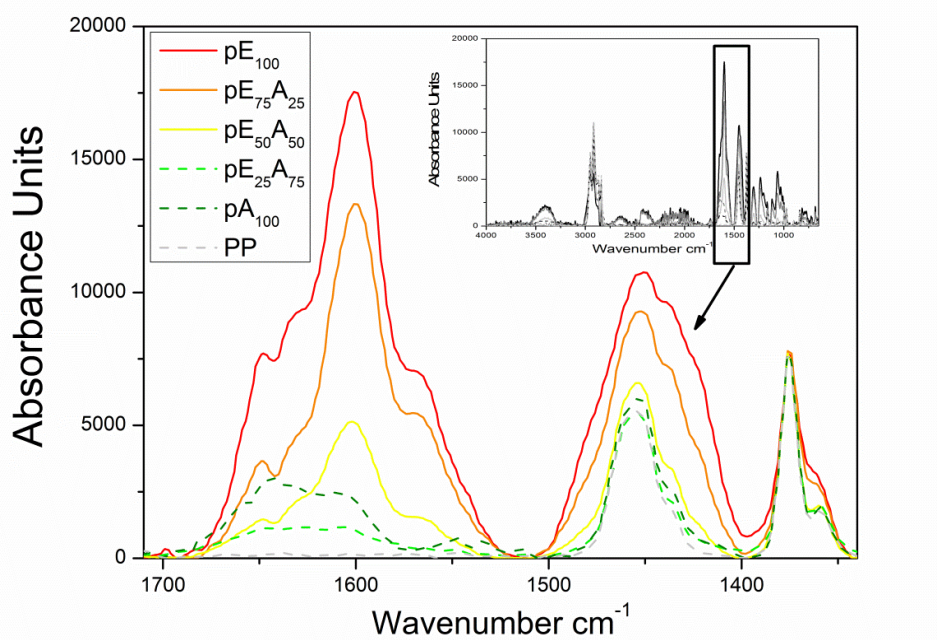

Figure 4-17: ATR-IR spectra of the p$\mathbf{E}_{100\text{-}25n}\mathbf{A}_{25n}$ (n = 0-4) compound plates and 100% PP. The full spectrum is shown as an insert into a detailed zoom in the region from 1700 to 1300 cm^{-1}.

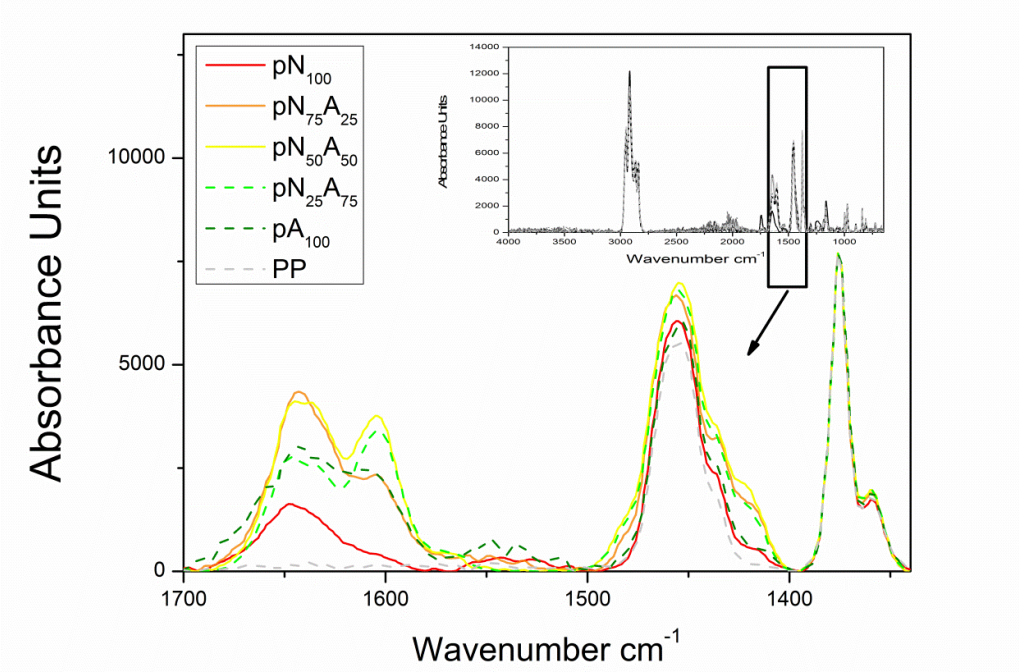

Figure 4-18: ATR-IR spectra of the p$\mathbf{N}_{100\text{-}25n}\mathbf{A}_{25n}$ (n = 0-4) compound plates and 100% PP. The full spectrum is shown as an insert into a detailed zoom in the region from 1700 to 1300 cm^{-1}.

Due to the lower abundance of methyl groups relative to other groups in the nonyl side chain as opposed to an ethyl side chain, the same trends of the signal at 1470 cm^{-1} could not be observed throughout the series p$\mathbf{N_{100-25n}A_{25n}}$. The signals corresponding to both the amide and ammonium groups in the range of 1600-1700 cm^{-1} were substantially different in their relationship for the nonyl series as in the ethyl series. Plates containing hydrolyzed species showed reduced absorbance with increased hydrolysis degree as with the ethyl series, but the plate with the native polymer p$\mathbf{N_{100}}$ had the lowest absorbance of all the plates. Given the hydrophobic nature of p$\mathbf{N_{100}}$ this result can be referred to the preferential mixing of the polymer into PP as opposed to being directed towards the surface where it would come in contact with moisture from air. As the polymer is hydrolyzed, the hydrophilic ammonium groups change the position within the PP matrix and direct the biocidal polymers towards the plate surface, resulting in the increase of the absorbance. Regardless of signal strength, the signal at 1600-1700 cm^{-1} is present for all plates with additives whereas it is not present at all for the pure PP plates, indicative of surface or near surface presence of the antimicrobial compounds.

4.2.4.3. Zeta Potential

Given the interesting nature of the ATR-IR spectra of the p$\mathbf{N_{100-25n}A_{25n}}$ series, it was decided to gain further understanding of the plate surfaces of these compounds. Hence, zeta potential measurements were recorded in order to determine the isoelectric points IEPs. Unlike other testing methods where factors such as morphology may affect the result, this method gives measurements affected by only the surface charge (as a result of pH) of the compound plates. Pure PP was shown to possess an IEP of pH = 5. The next lowest pH value was the one for the unhydrolyzed polymer with a pH value between 8 and 9. The value higher than that of pure PP was attributed to the surficial presence of the amide group of p$\mathbf{N_{100}}$. As the degree of hydrolysis increased the amount of amide groups present decreased and the number of amine groups increased. This was correspondingly shown in the IEP which increased also, indicative of the varied pK_b values of amide and amine groups. The plates containing p$\mathbf{N_{50}A_{50}}$ and p$\mathbf{N_{25}A_{75}}$ had the highest IEP at around 13.5. Such results show that protonable groups are present on the plate surfaces and also confirm that the ammonium groups are surface accessible.

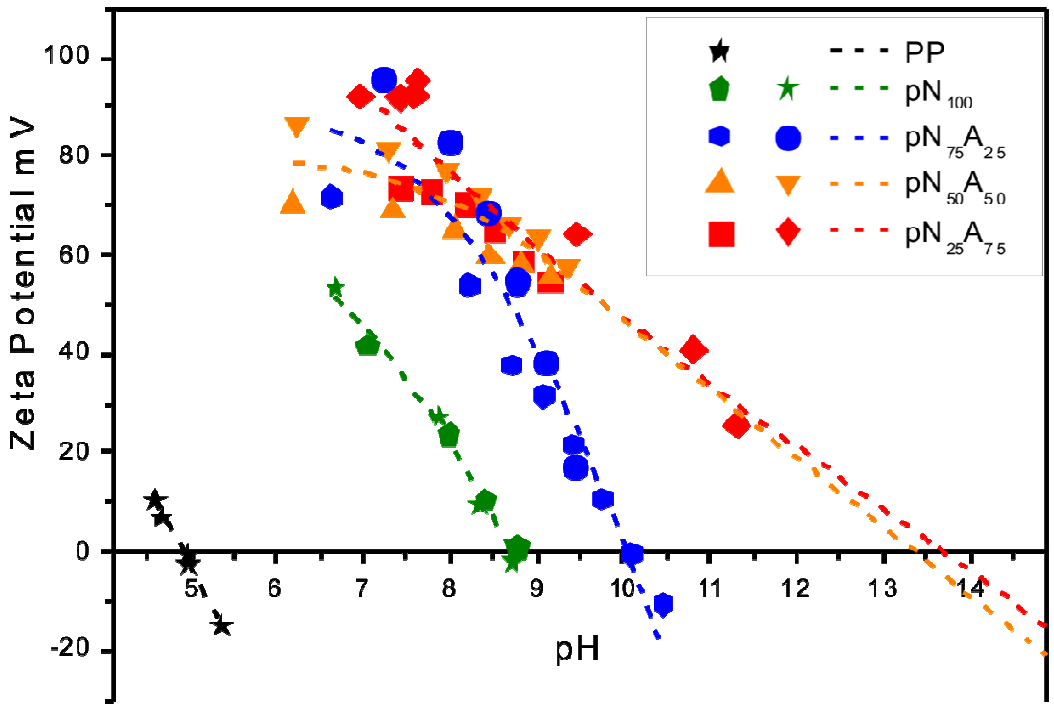

Figure 4-19: Zeta potential measurement of the nonyl series of compound plates as well as a pure PP plate. As hydrolysis increases, the isoelectric point shifts towards higher pH.

4.2.4.4. SEM-EDX

The previous measurements provided important information regarding the presence of both the antimicrobial copolymers themselves and the ammonium groups required for antimicrobial activity in the surface and surface near region. However, it was required to additionally utilize SEM-EDX measurements in order to determine the distribution of the biocial materials both on the surface of the compound plates and within the PP matrix itself. A compound plate containing p$\mathbf{N_{25}A_{75}}$ was chosen to represent the series which demonstrated the best biocidal activity (see below). A plate which had been stored for many months was selected additionally to ensure that the ionic nature of the surfaces was maintained. EDX measurements of the chloride counter ion were taken.

The compound plate was compared with a pure PP plate as blank sample. When examining the surfaces it was clear that the morphologies of both plates were similar. The plates share in common few monolithic structures and near homogeneity. This is in good correlation with previous tests; changes in morphology would likely affect other surface measurements.

The chloride counterion was used as an indicator for the poly(2-oxazoline)-based (co-)polymers. Pure PP plates were used as blank samples (not containing any chloride anions) and exhibited morphologies at the surface as well as at the cross-section similar to those of the compound plates containing poly(2-oxazoline)-based (co-)polymers. Elemental mapping of the chloride counter ion in the compound plate showed a wide abundance of the ion. Since the counter ion will be in the vicinity of the positively charged ammonium group, this suggests an almost uniform biocidal activity across the plate surface (Figure 4-20).

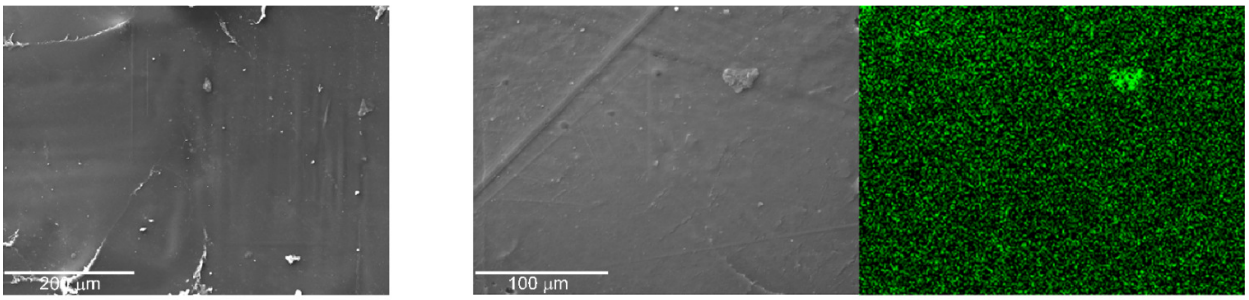

Figure 4-20: SEM image of a PP surface (left) and SEM-EDX images of a compound plate surface (right) showing the presence of chloride counterions in green.

A cross-section of both a pure PP plate and a biocide containing compound plate was also measured. Again morphologies were similar and showed comparable results of the cutting process. More important nonetheless was the elemental mapping. The chloride counterion was shown to be deposited throughout the plate matrix. This phenomenon reduces problems associated with scratching of the plate and similar damage. Should a scratch appear on the antimicrobial surface, the presence of the material throughout the entire matrix would result in the activity being retained (Figure 4-21).

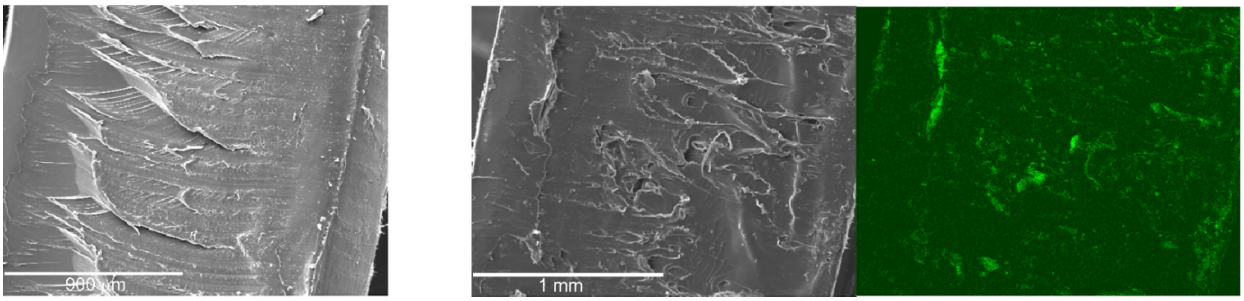

Figure 4-21: SEM image of a PP cross-section (left) and SEM-EDX images of a compound plate cross-section (right), showing the presence of chloride counterions in green.

4.2.5 Antimicrobial Activity

In order to test the antimicrobial activity of both the complete ethyl and nonyl series and narrow down the investigation of applicability to a preferred candidate, antimicrobial tests were carried out in accordance with ISO 22196:2007. Plates containing 5 wt.-% of each test material in **PP** were prepared and cut to appropriate size. In order to meet the standards required, each test was carried out in triplicate. To ensure that future investigations would be carried out on the best possible candidate, a wide variety of microbes were chosen for the study: two gram-negative bacteria, *E coli* ($1.40\pm0.10\ 10^6$ colony forming units CFUs) and *P. aeruginosa* ($1.50\pm0.27\ 10^5$ CFUs), gram-positive *S. aureus* ($3.27\pm0.40\ 10^4$ CFUs) and the fungus *C. albicans* ($6.83\pm0.23\ 10^4$ CFUs).

Each plate was sterilized using ethanol before testing. Each test organism was spread onto the plate surfaces in a suspension of known activity after which it was incubated for 24 hours at a temperature of 35 °C. Utilizing a sterilized saline solution, the microbial suspensions were rinsed from the plate surfaces once this time had passed. Subsequently, the CFUs remaining in the suspension could be determined.

By calculating a logarithmic value of the reduction factor based on the number of colony forming units present on the plates against those present in the suspension, the antimicrobial activity of the compound plates could be quantified. The tests were referenced against a PP plate to which no antimicrobial polymers had been added. In this test positive values indicate a decrease in the number of CFUs, whilst an increase is shown by a negative value. A negative value suggests that as opposed to killing bacteria a surface actually promotes their growth. Reduction factors between 0 and 2 belong to a surface which is microbially static, and values above 2 to a surface where microbes are killed that can be described as antimicrobially active surfaces.[148]

4.2.5.1. Candidate Screening

As previously mentioned for a polymeric material to possess antimicrobial properties there is a necessity for a cationic character. The non-hydrolyzed poly(2-oxazoline)s p$\mathbf{E_{100}}$ and p$\mathbf{N_{100}}$, due to their neutral state, showed no antimicrobial activity against any of the microbes tested.

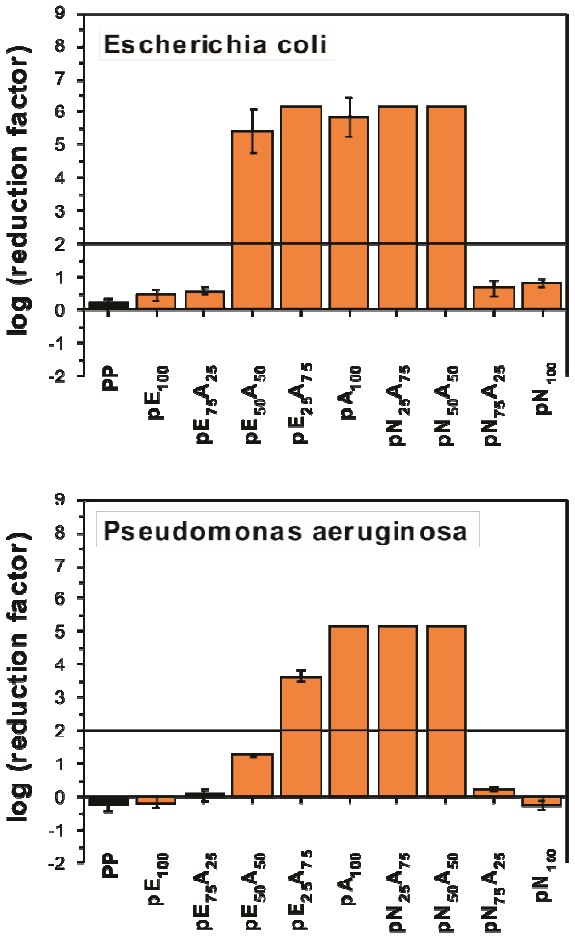

Figure 4-22: Log reduction factors of gram-negative *E. coli* and *P. aeruginosa* against all test plates. Antimicrobial activity depends on the number of cationic charges present in the polymer additive.

Across all tested microbes, the antimicrobial activity increased as the degree of hydrolysis and subsequently the number of available cationic charges increased. Gram negative bacteria clearly demonstrated this trend (Figure 4-22). For both the ethyl and nonyl series, strong antimicrobial activity was observed once a threshold hydrolysis degree had been reached. In *E. coli* biocidal activity was initially observed at 50% hydrolysis for the series p$\mathbf{E_{100-25n}A_{25n}}$ and p$\mathbf{N_{100-25n}A_{25n}}$ (n = 2-4). In the case of *C. albicans*, similar levels of antimicrobial activity were observed for the same specimens with the exception of p$\mathbf{E_{50}A_{50}}$ that exhibited only microbially static behavior.

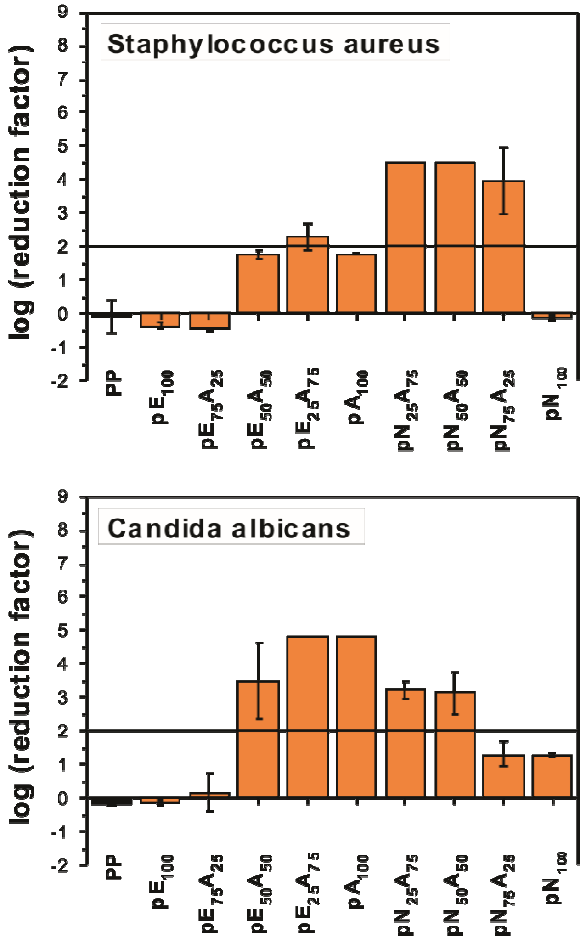

Figure 4-23: Log reduction factors of gram-positive *S. aureus* and the fungus *C. albicans* against all test plates. Whilst for the fungus cationic charge is the determinant for antimicrobial activity, *S. aureus* requires additional aliphatic side chains to experience antimicrobial activity.

These trends were also observed when the plates of the same series, p$\mathbf{E_{100-25n}A_{25n}}$ and p$\mathbf{N_{100-25n}A_{25n}}$ (n = 2-4), were tested against the fungus *C. albicans* (Figure 4-23). The fully hydrolyzed polymer p$\mathbf{A_{100}}$ possessed higher antimicrobial activity than all of those of the nonyl series. When tested against the gram positive bacteria *S. aureus* however, this trend was not valid. Possessing cationic charges alone was not sufficient to induce antimicrobial activity, evidenced by the fully hydrolyzed polymer $\mathbf{pA_{100}}$ having a log reduction factor less than 2 and therefore being merely microbially static. The nonyl series of polymers p$\mathbf{N_{100-25n}A_{25n}}$ (n = 1-3) possessed log reduction factors greater than 2. Of the ethyl series, the plate containing p$\mathbf{E_{25}A_{75}}$ was only slightly in excess of the threshold log reduction factor. Based upon these results it is suggested that cationic

charge is not the only factor responsible for antimicrobial activity against *S. aureus* in polymer contact biocides. The long hydrophobic side chains in the nonyl series influence the antimicrobial effects against certain bacteria. This was limited to test polymers of the form p$\mathbf{N_{100-25n}A_{25n}}$ (n = 1-3). Additionally, the threshold of log $\geq$ 2 was only slightly exceeded by p$\mathbf{E_{25}A_{75}}$. The interaction of cationic charges and long hydrophobic side-chains indicated that the proposed synergism between these factors was indeed present for gram-positive *S. aureus*.

Two of the nine polymers, namely p$\mathbf{N_{50}A_{50}}$ and p$\mathbf{N_{25}A_{75}}$, showed antimicrobial activity against all microbes tested. It should be pointed out that concerns of residual TsOH from the polymerization process contributing to the biocidal effect were not an issue due to its complete absence from these two materials.

Further elaborating on the idea of synergism between cationic charge and hydrophobic side-chain, it is worth looking at the structure of a gram positive bacteria's cell wall that abundantly contains lipoteichoic acids. This characteristic structure of bacteria such as *S. aureus* provides some idea of the reason for the cationic charge/ hydrophobic part synergism. The cationic charges are attracted to a polyanionic rod within the cell wall. The presence of hydrophobic side chains allows for interaction with the hydrophobic anchor of this anionic part to the cell and causes the structure to be disturbed. Such disruption of the outer part of the cell eventually results in cell lysis.

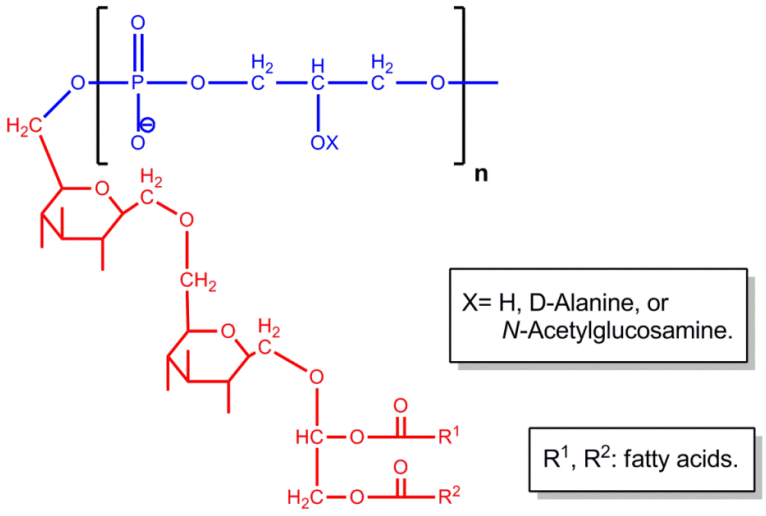

Scheme 4-5: Chemical structure of lipoteichoic acids found in *S. aureus*, which consist of a hydrophobic anchor (red bonds) and a polyanionic moiety (blue bonds; X = D-alanine in *S. aureus*).[149]

4.2.5.2. Validation of the Selected Candidate

Based on the precedent studies, the statistical copolymer of the composition p$\mathbf{N_{20}A_{80}}$ was chosen for expanded investigations of the biocidal activity as it was expected to retain activity against gram positive bacteria whilst potentially increasing activity against species where higher amounts of cationic charges were required. The tests against *E. coli* were performed twice using the same 95% PP compound plate for both runs (Figure 4-24). Upon completion of the first incubation, the plate was thoroughly rinsed to remove any colonies remaining from the test and incubated again. Both tests were carried out using a 100% pure PP plate as a reference in compliance with ISO 22196:2007.

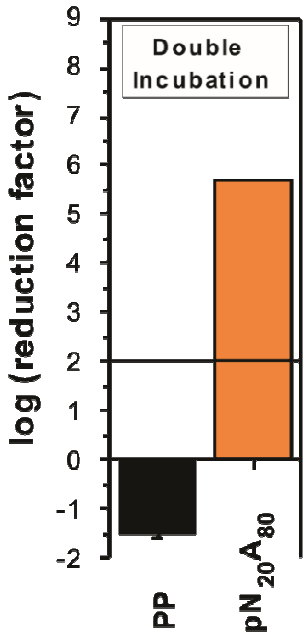

Figure 4-24: Log reduction factors of the gram-negative bacteria *E. coli* against p$\mathbf{N_{20}A_{80}}$ after double incubation illustrating maintenance of biocidal activity.

On this occasion, the PP reference plate was shown to promote bacterial growth upon second incubation, possessing negative "reduction" factor of −1.5. On the plate containing the biocide, however, the bacteria were destroyed completely with a log reduction factor of 5.5. Shown by the double incubation, there is maintenance of the antimicrobial properties according to this test.

4.2.5.3. Quantification of Activity

When considering the scale-up and potential industrial application of the materials, it makes sense to possibly lower the amount of biocidal material required for retention of the antimicrobial effect, thus reducing the material costs. For this purpose, a series of compound plates again containing p$\mathbf{N_{20}A_{80}}$ were produced with contents of 5%, 3% and 1% in PP. PP was used as the reference plate, and all plates were tested against *E. coli* (Figure 4-25).

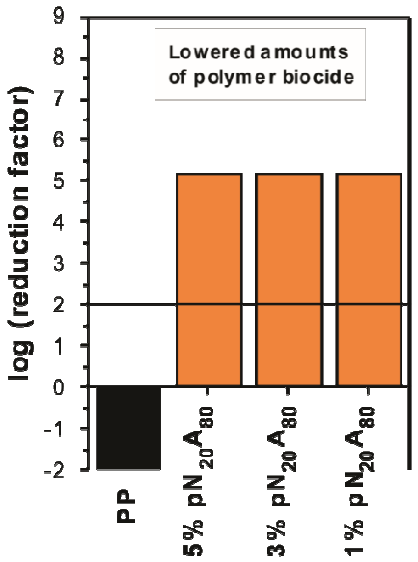

Figure 4-25: Log reduction factors of the gram-negative bacteria *E. coli* against p$\mathbf{N_{20}A_{80}}$ compound pltes with reduced weight contents.

Again **PP** notably promoted bacterial growth, indicated by a logarithmic "reduction" factor. For the plates containing the test materials, biocidal activity was observed in all cases. Each plate regardless of the biocide content showed a significantly high log reduction factor of 5 against *E. coli*. It is shown, hence, that for contents of the biocide as low as 1% in PP no loss of antimicrobial effect could be observed. It is perhaps worthwhile to investigate even lower quantities of the material being used.

4.2.5.4. Test Against Legionella

Legionnaires' disease is a major problem particularly in hospitals and industrial locations.[150] Due to its waterborne nature and the difficulty by which it is killed,

developing a contact biocide which displays activity against *Legionella* would prove immensely beneficial. Currently measures to kill *Legionella* involve the use of non-permanent means involving both oxidizing and non-oxidizing species. Oxidizing species provide a significantly greater effect against *Legionella*.

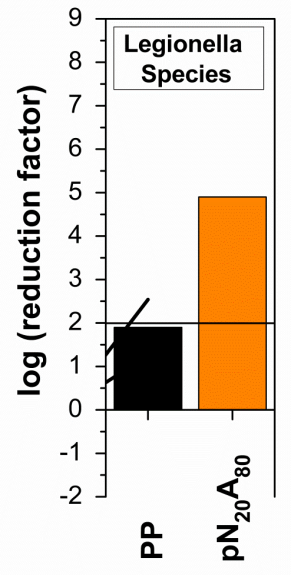

Figure 4-26: Log reduction factor of p$\mathbf{N_{20}A_{80}}$ against *Legionella* demonstrating excellent antimicrobial capabilities.

Utilizing once more the tests described in ISO 22196:2007, biocide tests were carried out against *L. species*. PP was again used as reference and p$\mathbf{N_{20}A_{80}}$ as the biocidal test material (Figure 4-26). After 24 hours, the log reduction factor of the colony forming units on the plate surface was around 5 indicating extremely high biocidal activity. Notably, the PP reference plate could be shown to be microbially static. Such biocidal activity suggests that the test material may provide an attractive alternative over such currently preferred materials for *Legionella* disinfection such as chlorine.

4.2.6 Scale-Up

In order to investigate the potential of the materials in biocide applications to the fullest extent possible, it was necessary to establish the viability of the reactions on a much larger scale than previously carried out. Utilizing the Anton Paar Masterwave reactor, which allows for microwave assisted chemistry to be carried out up to the kilogram scale,

two tests were carried out to investigate firstly whether each reaction is possible on such a scale and secondly whether the reactor stability is sufficient that the reactions can be carried out on this scale reproducibly.

4.2.6.1. Polymerization

Due to the longer reaction time of **NonOx** against **EtOx** it was decided that the polymerization of **NonOx** would give a good indication of the reactor stability during the polymerization process over an extended time period on the hundred gram scale. Reaction temperature and time were not varied from the small scale and work-up protocols were unchanged. The resultant product was analyzed via both NMR and GPC measurements. The NMR data obtained were in good agreement with previous results (Figure 4-27). Data obtained following GPC measurements indicated a polydispersity index of 1.7, slightly higher than on the small scale but within acceptable ranges.

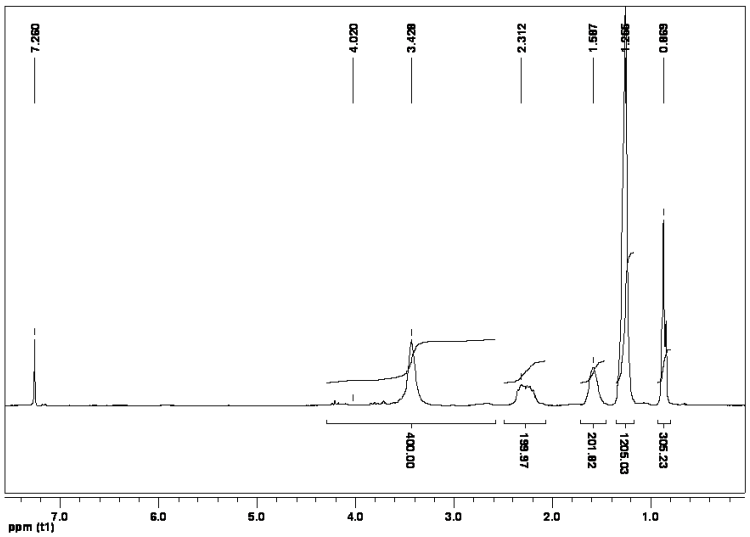

Figure 4-27: ^{1}H-NMR (δ, 20 °C, $CDCl_3$, 300 MHz) spectrum of poly(2-nonyl-2-oxazoline).

Notably, the microwave output indicates excellent stability in the reaction vessel throughout the reaction. Overshoot of the target temperature is minimal limiting possible degradation of the polymer and the power fluctuated only slightly once it had reached its optimal operating output (Figure 4-28). Due to the larger size of the reaction vessel and the polymerization mixture the cooling time was longer in the range of 15 minutes as opposed to on the small scale where it is in the range of 5 minutes.

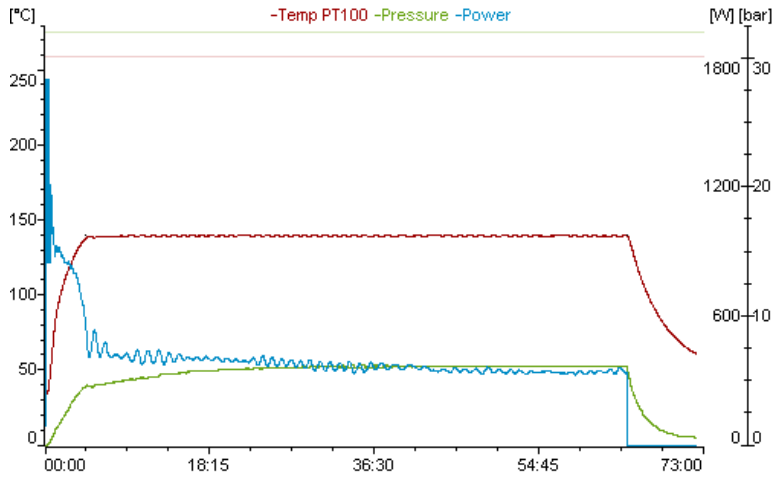

Figure 4-28: Masterwave output run data for the large-scale synthesis of poly(2-nonyl-2-oxazoline).

4.2.6.2. Hydrolysis

Utilizing p**E**$_{100}$, again due to the monomer availability and faster polymerization time, quantitative hydrolysis was carried out to produce p**A**$_{100}$ on the almost kilogram scale using the same reaction conditions as for the hydrolyses carried out using only 2.5 g of polymer. Despite the relatively harsh conditions in the reaction vessel and the ionic character of the reaction medium, the reaction occurred successfully with NMR data corresponding with the small scale reaction (see Appendix). The microwave reactor exhibited good stability and, even on such a large scale, was not damaged by high temperature and high molarity hydrochloric acid. These results indicate the possible scale-up of both, the polymerization and hydrolysis of 2-oxazoline based materials, for applications in the antimicrobial field. As such work was preliminary and intended to show only if such scale-up was feasible, there is scope for further optimization of reaction conditions on the larger scale.

5 Summary

The aim of the presented work was to develop materials capable of contributing to the biomaterials field either through enabling for drug delivery or through provision of antimicrobial surfaces for hygienic applications. Due in part to the living nature of their polymerization, the wide variety of monomers available, and the ease of rapid synthesis utilizing microwave reactor systems, poly(2-oxazoline)s were selected as candidates suitable for both fields.

Current methods of drug delivery either rely on the patient taking the medication themselves or being administered to regularly by healthcare professionals. Both represent challenges in terms of availability of doctors for instance, or mistakes in self prescription. Drug delivery matrices, where an implant releases drugs into the blood stream on a regular basis suffer from many problems such as mechanical rigidity and degradation into non-preferential products. Hydrogels, with their ability to absorb fluids and release them in a designed manner whilst being less mechanically rigid and thus more body-friendly are considered as potential materials for this purpose.

In this work, 32 gels of the composition p**EtOx**$_m$-p**PhOx**$_n$-p**PBO**$_q$ (m/n = 150/0, 100/50, 50/100, 0/150; q = 1.5-30) were prepared as potential candidates for this kind of drug delivery (Scheme 5-1). Using a microwave reactor, the gels were prepared rapidly under solvent-free conditions and in high yields. For medical applications, high throughput is a much desired property and these materials have been shown to comply. Furthermore, being able to tailor-make a gel to a patient's needs is essential. The living CROP of 2-oxazoline monomers allowed for highly defined gels to be synthesized. By varying both the monomer composition and amount of crosslinker, the gels can therefore easily be tailor-made to purpose.

The gels were swollen in the three test liquids water, ethanol and dichloromethane revealing that the major factors in determining maximum swelling were the ratio of **EtOx** vs. **PhOx** in their composition and the crosslinking degree. As the crosslinking degree decreased, the swelling degree increased. The maximum swelling degrees were exhibited for the gel p**EtOx**$_{150}$-p**PBO**$_{1.5}$ and were of the values 11.7/13.8/20.0 in water/-

ethanol/dichloromethane, respectively. Swelling could be carried out repeatedly with maximum swelling occurring within the first 24 hours. Additionally, the repeated swelling/deswelling of the gels allowed for an effective purification method, resulting in removal of monomers eventually remaining in the gel matrices. Varying the **EtOx**/**PhOx** ratio enabled for the preparation of hydro-, lipo-, and amphigels.

Compound inclusion within the gels, mimicking the inclusion of pharmaceuticals, could be achieved either during synthesis or post-synthetically for gels with sufficiently high swelling degrees. The organic dye Eosin Y was selected to illustrate this as its ability to attach to and terminate the growing polymer chain made it ideal for in-situ attachment. The dye was shown to be retained by the gels synthesized by both methods even when stored in water for over 4 weeks.

In order to release the test compounds, stimuli were required. Variance of the solvent from water to dichloromethane allowed for the diffusion-mediated release of Eosin Y from the gels. For the gels with synthetically attached dye this was insufficient, and pH-mediated degradation was required. Degradation studies of the gels were carried out quantitatively at elevated temperatures over a short time. The degradation products poly(aziridinium chloride), propionic acid, phthalic acid and benzoic acid were identified. Additionally, the relative degradation rates were determined for a gel series. The series p**EtOx**$_m$-p**PhOx**$_n$-p**PBO**$_2$ (m/n = 150/0, 100/50, 50/100, 0/150) showed that as crosslinking decreased the rate of degradation was increased with a ratio of 1:9:34:84.

The ability to tailor the degradation of the gels is essential for drug delivery applications and these results prompt further investigation into degradation particularly by other methods such as via an enzymatic scheme. Long term release studies of compounds from within the gels are necessary in order to investigate the full potential of material applicability. Such steps would allow for the further development over an extended period of time of more highly tailored materials for a large selection of treatments. Finally, cytotoxicity tests were carried out on the gel p**EtOx**$_{50}$-p**PhOx**$_{100}$-p**PBO**$_6$, representative of the library. The gel was shown to be non-cytotoxic, suggesting that this series of gels are excellent candidates for further research towards the overall goal of drug delivery matrices.

The second section of the work concerned the development of polymer based contact biocides. As bacteria become ever more resistant to traditional antibiotics it is imperative that new ways to kill harmful cells are developed. Hygienic applications such as water pipes, cooking surfaces and surfaces in medical establishments in particular are of growing importance. Existing methods involve the release of small molecule biocides to disinfect surfaces. Such means are not desirable as they require maintenance and the released small molecules can be harmful to mammalian bodies. Contact biocides, and polymer based varieties in particular, are of great interest currently as the mere act of contact on the surface will kill the bacteria, which requires little to no maintenance.

Such polymers require cationic charges in the backbone to initiate antimicrobial effects. It is additionally suggested that the presence of aliphatic side chains can enhance this effect. Due to the ability to control molecular weight easily, and due to the wide monomer availability conveying many possible side group variation, poly(2-oxazoline)s represent an excellent choice as biocide materials. Starting with the monomers **EtOx** and **NonOx**, a library of nine test materials was prepared (Scheme 5-2). Polymers were initially synthesized and subsequently subjected to acid-mediated hydrolysis in a microwave reactor.

Hydrolysis of the polymers was shown to follow first-order kinetics, with the hydrolysis of **pNonOx** taking longer due to the nonyl side chains folding back on the main chain and limiting availability to the amide bond for hydrolysis. For each polymer, hydrolysis products corresponding to 25/50/75 % of hydrolysis were obtained, and from p**EtOx** a 100% hydrolyzed species in addition was synthesized. Following scale-up of the hydrolysis and characterization (via NMR, GPC and elemental analysis), the test materials were compounded with PP in a 5/95 wt.-% manner to create test plates.

The test plates were characterized using surface energy, ATR-IR, zeta-potential and SEM-EDX measurements. The characterization made it clear that whilst the plates were of similar wettability to standard PP and as such could be used for likewise applications, the biocidal materials were present in all plates. The biocides could be shown to be

present in the surface and near surface region. SEM-EDX revealed that there was distribution throughout the entire PP matrix of the biocides.

Notably, other processing techniques for the test polymers are potentially available, particularly injection molding. These techniques exist on the large scale in industry and allow for a great number of shaped materials to be produced. However, in the scope of this thesis such methods were not investigated. The ISO test for contact polymer biocides requires plates of a specific shape and dimension best prepared utilizing a platen press and so injection molding was deemed unsuitable for investigation at this stage. It may be worth considering though for potential upscaling of this process.

Biocide tests of the plates revealed that whilst gram-negative and fungal species were killed by all polymers of sufficiently high hydrolysis degree (and consequently high cationic charge presence), the gram positive bacteria *S. aureus* was only killed by the nonyl-based polymers with a hydrolysis degree of 50% or higher (Figure 5-1). This suggested that the proposed additional effect of hydrophobic side chains was applicable. Based upon this a new set of plates of the composition $\mathbf{pN_{20}A_{80}}$ were prepared and additional tests run.

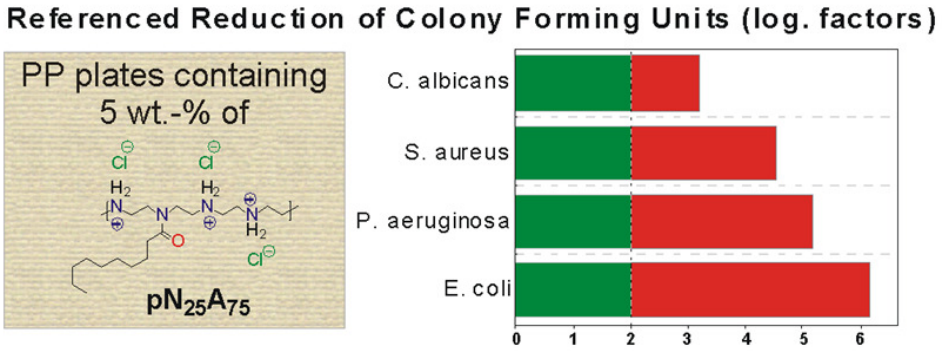

Figure 5-1: Biocidal activity against all bacteria was best illustrated for the plate containing 5 wt% $\mathbf{pN_{25}A_{75}}$.

Firstly, retention of the biocidal effect against *E. coli* was determined by repetition of the test on the same plate after 24 hours. Such a test revealed no change in the biocidal effect suggesting that the materials possess long-term biocidal properties. A second test reduced the amount of biocidal material present in each test plate to as low as 1% by weight, whilst still retaining activity against *E. coli*. The final test measured the effectiveness of the plates against *Legionella* which is notoriously difficult to kill. For even this species, the test plates demonstrated excellent biocidal activity. Such a wide spread activity against so many species in a repeatable manner even with low biocide content suggests that this group of materials are an excellent candidate for use in hygienic applications. Additionally, tests of the synthesis on the 100 g plus scale revealed that the reactions can be successfully scaled-up indicating that the method is of high relevance to industrial purposes. Further optimization of the scale-up considering areas such as continuous processing are perhaps considerable should industrial production be a possibility.

5.1 Perspectives

Based upon the substantial results obtained during the course of the work presented in this thesis, a number of suggestions for future work stemming from the research can be suggested.

Research into poly(2-oxazoline)-based crosslinked polymer networks yielded a series of gels with tuneable swelling degrees in numerous liquids as well as allowing for the inclusion and release of organic compounds. In order to determine the potential of these gels for drug delivery applications within the human body, it is necessary to further evaluate the release properties particularly with respect to the degradation of the gels. Preliminary tests indicate that the hydrolysis of the gels will be in the medium to long term time range, indicative of a material with potential in delivering medications for chronic diseases. Notably, the gels were obtained in sizes unsuitable for excretion from the body, in particular by renal excretion. In order to determine ideal suitability for use in the body, additionally, tests under normal physiological conditions could be carried out. Additionally the possibilities of enzymatic degradation can be looked at potentially allowing for a plethora of further applications of the gels.

Work of poly(2-oxazoline)-based contact biocides resulted in the generation of materials, which exhibited excellent activity against a wide range of microbes. In order to further develop the materials, both, reaction and processing parameters, may be optimized. Further optimization of the hydrolysis degrees may be desirable in order to specifically design the materials such that they destroy the targeted bacteria. Additionally, varying the reaction temperatures may be considered to reduce the severity of the conditions. Scale-up of the reactions, whilst preliminarily investigated within this thesis, should be expanded upon once a dedicated contact biocide should be available on the industrial level. Existing research has verified the success of both, the polymer synthesis and quantitative hydrolysis, on the kilogram scale – the investigation of targeted hydrolysis degrees requires study with a larger scope.

Once produced, it is necessary to consider the amount of polymeric material used to generate the biocidal effect. In this study, weight percentages as low as 1% in PP were shown to retain biocidal activity. However, in order to enhance the viability of the materials for industrial purposes an investigation of even lowered amounts retaining this activity should be considered. Additionally, alternative methods of compounded material preparation should be considered. Within the aims of this thesis and the corresponding biocide tests, plates of dedicated shape and size needed to be produced using a platen

press. For other specimen geometries and sizes, it would be worth studying the possibilities of other processing methods such as injection moulding. Such work could allow for a number of different applications of the materials to be evaluated.

5.2 Abstract

Poly(2-oxazoline)-based materials currently receive great interest due to their versatile properties such that can be tailor-made by easily incorporated modifications. The living nature of their cationic ring-opening polymerization allows for low polydispersity indices of the polymers making their usage in the biomaterials field desirable. Coupled with their rapid syntheses in microwave reactors this makes them excellent candidates in applications such as drug delivery and the hygienic equipment of surfaces.

Crosslinked gels of the composition p**EtOx**$_m$-p**PhOx**$_n$-p**PBO**$_q$ (m/n = 150/0, 100/50, 50/100, 0/150; q = 1.5-30) were prepared from 2-ethyl- **EtOx**, 2-phenyl-2-oxazoline **PhOx**, and phenylene-1,3-bis-(2-oxazoline) **PBO.** In total, a 32-membered library was created. Polymerizations could be carried out under solvent-free conditions under microwave irradiation at 140 °C with short reaction times of up to an hour. Upon purification, not only were residual monomers removed, but the yields were as high as 95% or greater. Depending on the crosslinking degree and the ethyl/phenyl balance, the gels properties such as swelling degree and acid-mediated hydrolysis rates could be varied over a wide range. In water/ethanol/dichloromethane, the swelling degrees varied from 0 to 11.7/13.8/20.0. The gels were able to incorporate test organic molecules such as the dye Eosin Y via either synthetic or post-synthetic methods. Post-synthetic incorporations allowed for gels where the dye would be released via stimuli changes such as solvent or pH variation. Notably, both quantitative hydrolysis (to determine the degradation products) and partial hydrolysis (to determine relative hydrolysis rates) of the gels under acidic conditions were possible.

Poly(2-oxazoline) derived biocides were synthesized via the acid-mediated hydrolysis of 2-ethyl- and 2-nonyl-2-oxazoline. Species with hydrolysis degrees of 0/25/50/75/100% were synthesized and characterized via NMR, GPC and elemental analysis. The materials were compounded with 95% PP to produce test plates. The plates were surface characterized to prove that the test materials were present not only within the **PP** matrix but indeed on the surface. Antimicrobial activity was shown to be high against *E. coli*, *P. aeruginosa* and *C. albicans* with high amounts of cationic charges in the polymer. However, against *S. aureus* only the nonyl series showed activity indicative of a synergistic effect from the hydrophobic side-chains. Additional tests showed the retention of the biocidal activity over time, retention of activity with reduced amount of biocide in the plates and excellent activity against *Legionella*.

5.3 Kurzfassung

Poly(2-oxazolin)-basierte Materialien gewinnen dank ihrer variablen Eigenschaften zunehmend an Interesse. Durch einfach durchzuführende Modifikationen können sie an unterschiedliche Bedingungen und Bedürfnisse angepasst werden. Die kationische ringöffnende Polymerisation liefert Polymere mit niedrigen Polydispersitätsindices. Die schnellen mikrowellenunterstützen Synthesen machen poly(2-oxazolin)-basierte Materialien zu exzellenten Kandidaten für Anwendungen im Bereich der Medikamentenverabreichung und zur Herstellung von antimikrobiellen Oberflächen.

Gele mit den Zusammensetzungen p**EtOx**$_m$-p**PhOx**$_n$-p**PBO**$_q$ (m/n = 150/0, 100/50, 50/100, 0/150; q = 1.5-30) wurden ausgehend von 2-Ethyl- **EtOx**, 2-Phenyl-2-oxazolin **PhOx** und Phenylen-1,3-bis-(2-oxazolin) **PBO** hergestellt. Insgesamt wurde eine Bibliothek bestehend aus 32 Gelen erhalten. Die Polymerisationen konnten lösemittelfrei im Mikrowellenreaktor bei 140 °C mit kurzen Reaktionszeiten (1 h) durchgeführt werden. In Abhängigkeit des Vernetzungsgrades sowie des **EtOx**/**PhOx** Verhältnisses konnten die Eigenschaften der Gele wie Quellgrad und säurekatalysierte Hydrolyserate verändert werden. In Wasser/Ethanol/Dichlormethan lagen die Quellgrade zwischen 0 und 11,7/13,8/20,0. In den Gelen konnten Moleküle wie Eosin Y durch synthetische oder post-synthetische Methoden eingelagert werden. Durch post-synthetische Einlagerungen wurden Hydrogele hergestellt, die den Farbstoff nur bei Lösemittel- oder pH-Änderungen abgaben. Die Gele wurden quantitativ (Abbauprodukte) als auch partiell hydrolysiert.

Weiters wurden poly(2-oxazolin)-basierte Biozide mittels säurekatalysierter Hydrolyse von **EtOx** und **NonOx** hergestellt. Polymere mit Hydrolysegraden von 0/25/50/75/100% wurden synthetisiert und anschließend mittels NMR-, GPC-Messungen und Elementaranalysen charakterisiert. Die Materialien wurden mit 95% PP compoundiert um Testplatten herzustellen. Die Analyse der Platten zeigte, dass sich das Testmaterial innerhalb der PP-Matrix und an der Oberfläche befand. Die polymeren Additive mit hoher positiver Ladung wiesen eine hohe antimikrobielle Aktivität gegenüber *E. coli*, *P. aeruginosa* und *C. albicans* auf. Gegenüber *S. aureus* besaß hingegen nur die Nonylserie antimikrobielle Aktivität, was auf einen synergistischen Effekt der hydrophoben Seitenkette schliessen lässt. Weitere Tests zeigten die Erhaltung der bioziden Aktivität über einen längeren Zeitraum, auch bei Verwendung von Platten mit geringeren Anteilen an Bioziden. Diese Platten wiesen außerdem exzellente Aktivität gegenüber *Legionella* auf.

6 Experimental

6.1 Materials

Chemical	Supplier	Purity
Acetonitrile (dry)	Sigma-Aldrich, Austria	99,8%
Benzonitrile	Sigma-Aldrich, Austria	≥ 98%
Cadmiumacetate Dihydrate	Sigma-Aldrich, Austria	≥ 98%
Chloroform (dry)	Sigma-Aldrich, Austria	≥ 99%
Decanoic Acid	Sigma-Aldrich, Austria	
Dichlormethane (dry)	Sigma-Aldrich, Austria	≥ 99,8%
Eosin Y	Sigma-Aldrich, Austria	
Ethanol-2-amine	Sigma-Aldrich, Austria	≥ 99%
2-Ethyl-2-oxazoline	Sigma-Aldrich, Austria	≥ 99%
Methyl p-toluenesulfonate (Methyltosylate)	Sigma-Aldrich, Austria	98%
Molecular Sieves (4 Å)	Sigma-Aldrich, Austria	
Tetrahydrofuran	Sigma-Aldrich, Austria	≥ 99%
Titanium(IV) *n*-butoxide	Sigma-Aldrich, Austria	≥ 97%,

1,3-**PBO** and 1,4-**PBO** were kindly provided by Evonik (Hannau, Germany). PP was provided in powder form by Heraeus (Borealis, Austria).

6.2 Methods

6.2.1 Gel Synthesis

Gels were prepared utilizing **EtOx**, **PhOx**, and **PBO** under solvent-free conditions employing **MeOTs** as initiator. **MonOx** ratios were selected from [**EtOx**]:[**PhOx**] = 150:0, 100:50, 50:100, or 0:150 (4 ratios), the ratio [**MeOTs**]:[**MonOx**] was constant at 1:150, and the ratio [**MonOx**]:[**PBO**] was varied according to 150:30, 150:15, 150:10, 150:7.5, 150:6, 150:3, 150:2, or 150:1.5 (8 ratios), yielding a 32-membered library. Following a typical procedure, a ratio of [**EtOx**]:[**PhOx**] of 100:50, a ratio of [**MonOx**]:[**PBO**] of 150:7.5, and a ratio of [**MonOx**] :[**MeOTs**] of 150:1 was mixed from 1.34 g (13.5 mmol,

100 eq) **EtOx**, 0.99 g (6.7 mmol, 50 eq) **PhOx**, 0.22 g (1 mmol, 7.5 eq) **PB** , and 0.0242 g (0.13 mmol, 1 eq) **MeOTs**. Under inert conditions, the mixture was added to a microwave vial, which was sealed with a septum. Microwave irradiation was applied at 140 °C for 1 h. The solid colorless to slight yellowish products were recovered and subjected to swelling/drying cycles in dichloromethane until a constant weight had been achieved. The yields of the purified gels were equal to or higher than 95%.

6.2.2 Swelling Degree Determination

Subsequent to purification, samples of 0.3 g for each of the 32 hydro- and amphigels were swollen in excess amount of deionized water, ethanol, or dichloromethane. After 24 hours, each gel was dried over cellulose based paper until all liquid had been removed from the vial and as much as possible from the gel surface. The sample was then weighed and the swelling degree determined. Each gel was re-swollen in the same test liquid for a further 24 hour period and the same procedure applied the next day to determine if the swelling degree had changed. This was to be repeated until constant mass had been achieved; however, all gels showed maximal swelling within 24 hours.

6.2.3 Dye Inclusion

Gels of the composition p**EtOx**$_m$-**PhOx**$_n$-p**PBO**$_3$ (*m*/*n* = 150/0, 100/50, 50/100, and 0/150) were swollen in a 0.5 wt.-% solution of Eosin Y in dichloromethane/ethanol (4.5:0.5 mL) for a period of 24 h. The swollen gels were recovered in the same manner as detailed above. The gels were dried and washed multiple times with water to remove remaining dye from the gel surface. Following purification, the presence of the dye within the gel could be observed via the color change from almost colorless to a dark orange.

6.2.4 Gel Degradation

Samples of gels of the composition p**EtOx**$_m$-p**PhOx**$_n$-p**PBO**$_2$ (m/n = 150/0, 100/50, 50/100, 0/150) were weighed (100 mg) and heated in 2 mL of D_2O/DCl at 160 °C for 30 min to determine the relative hydrolysis rates of each gel under microwave irradiation. Using the same method quantitative hydrolysis was achieved upon 4 hours of irradiation. For ^{1}H-NMR measurements, acetone was used as an internal standard in 20:1 v/v quantity.

6.2.5 Cytotoxicity Tests

The test item p**EtOx**$_{50}$-p**PhOx**$_{100}$-p**PBO**$_6$ was analyzed by BSL Bioservice Scientific Laboratories GmbH in Planegg, Germany; study number 103716. The extraction of the gel was carried out in compliance with ISO 10993-5, -12 over 24±2 h. Parallel controls were set up against the test item cultures, namely a negative control of polyethylene extract, a positive control of DMSO, and a solvent control of the extraction vehicle DMEM 10% FCS only. The extract of the test gel and the solvent control were diluted five times with DMEM 10% CFS at a ratio of 2:3. The test was carried out utilizing L929 cells (ATCC No. CCL1, NCTC clone 929 (connective tissue mouse), clone of strain L (DSMZ)). Log phase L929 cultures were subsequently washed and trypsinized employing Trypsin EDTA; a single cell suspension at a density of 1.0·105 cells/mL was made and added in 50 µL quantities to samples of 100 µL. The cell cultures with the test extracts were incubated for 68-72 h at 37±1 °C, 5% CO_2 / 95% air. Protein contents of the individual cultures were measured colorimetrically at 550 nm. The percentage of growth inhibition %GI was calculated according to

$$\%GI = 100 - 100.\frac{(A_{550nm}sample) - (A_{550nm}blank)}{(A_{550nm}control) - (A_{550nm}blank)} \qquad \textbf{Equation 6-1}$$

with A_{550nm}sample/blank/control as the absorption of the test extract / blank cultures without cells / solvent control.

6.2.6 Polymer Synthesis

6.2.6.1 Poly(2-ethyl-2-oxazoline)

2-Ethyl-2-oxazoline (8.00 g, 81 mmol, 100 eq.) was added to a 20 ml microwave vial containing a stirring bar along with methyl tosylate (150 mg, 0.81 mmol, 1 eq.) and acetonitrile (9.3 g). The reaction mixture was heated under microwave irradiation for 15 minutes. Upon completion, the solvent was removed under reduced pressure and the polymer dried in a vacuum oven overnight.

Elemental analysis calcd. for p**E$_{100}$**: C 60.60, H 9.10, N 14.10%. Found: C 58.77, H 8.97, N 13.69%.

^{1}H-NMR (δ, 20 °C, $CDCl_3$, 300 MHz): 0.8-1.2 (m, C(O)CH_2CH_3), 2.2-2.6 (m, C(O)CH_2CH_3), 2.8-4.0 (m, NCH_2CH_2N), 7.1-7.2 (d, 2 ϕ*H* TsOH), 7.6-7.7 (m, 2 ϕ*H* TsOH).

6.2.6.2 Poly(2-nonyl-2-oxazoline)

2-Nonyl-2-oxazoline (6.8 g, 34 mmol, 100 eq.) was added to a 20 ml microwave vial containing a stirring bar along with methyl tosylate (65 mg, 0.34 mmol, 1 eq.) and chloroform (17 g). The reaction mixture was heated under microwave irradiation for 60 minutes. Upon completion, the solvent was removed under reduced pressure and the polymer dried in a vacuum oven overnight.

Elemental analysis calcd. for p**N**$_{100}$: C 73.47, H 11.22, N 7.14%. Found: C 71.06, H 11.31, N 6.92%.

^{1}H-NMR (δ, 20 ℃, $CDCl_3$, 300 MHz): 0.8-1.0 (m, $C(O)C_8H_{16}CH_3$), 1.2-1.4 (m, $C(O)CH_4C_6H_{12}CH_3$), 1.4-1.8 (m, $C(O)CH_2CH_2C_7H_{15}$), 2.2-2.4 (m, $C(O)CH_2C_8H_{17}$), 2.8-4.0 (m, NCH_2CH_2N), 7.1-7.3 (d, 2 ϕ*H* TsOH), 7.6-7.8 (d, 2 ϕ*H* TsOH).

6.2.7 Polymer Hydrolysis

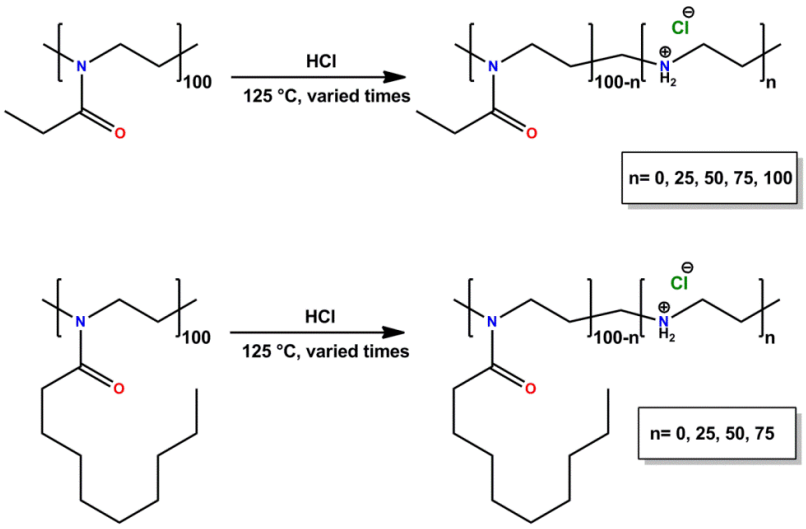

Scheme 6-1: General hydrolysis schemes for the two examined series.

6.2.7.1. Poly(2-ethyl-2-oxazoline)$_{75}$-stat-poly(aziridinium chloride)$_{25}$

2.5 g p**E**$_{100}$ (25.2 mmol) were added to a 20 mL microwave vial containing a stirring bar and dissolved in 10 mL of 6 M HCl before being heated at 125 ºC under microwave irradiation for 5 min. Upon completion, the reaction mixture was transferred to a round bottomed flask. HCl was removed under reduced pressure, and the residue was

ultrasonicated in THF. p$\mathbf{E_{75}A_{25}}$ was recovered by filtration and dried in a vacuum oven overnight at 70 ºC. Yield : 77%.

Elemental analysis calcd. for p$\mathbf{E_{75}A_{25}}$: C 51.71, H 8.87, N 14.20%. Found: C 49.09, H 8.83, N 13.45%.

^{1}H-NMR (δ, 20 ℃, D_2O, 300 MHz): 0.8-1.2 (m, C(O)CH_2CH_3), 2.2-2.6 (m, C(O)CH_2CH_3), 3.0-4.0 (m, NCH_2CH_2N).

6.2.7.2. co-Poly(2-ethyl-2-oxazoline)$_{50}$-stat-poly(aziridinium chloride)$_{50}$

2.5 g p$\mathbf{E_{100}}$ (25.2 mmol) were added to a 20 mL microwave vial containing a stirring bar and dissolved in 10 mL of 6 M HCl before being heated at 125 ºC under microwave irradiation for 15 min. Upon completion, the reaction mixture was transferred to a round bottomed flask. HCl was removed under reduced pressure, and the residue was ultrasonicated in THF. p$\mathbf{E_{50}A_{50}}$ was recovered by filtration and dried in a vacuum oven overnight at 70 ºC. Yield: 82%.

Elemental analysis calcd. for p$\mathbf{E_{50}A_{50}}$: C 42.75, H 8.65, N 14.25%. Found: C 41,58, H 8.11, N 14.09%.

^{1}H-NMR (δ, 20 ℃, D_2O, 300 MHz): 0.8-1.2 (m, C(O)CH_2CH_3), 2.2-2.6 (m, C(O)CH_2CH_3), 3.0-4.0 (m, NCH_2CH_2N).

6.2.7.3. Poly(2-ethyl-2-oxazoline)$_{25}$-stat-poly(aziridinium chloride)$_{75}$

2.5 g p$\mathbf{E_{100}}$ (25.2 mmol) were added to a 20 mL microwave vial containing a stirring bar and dissolved in 10 mL of 6 M HCl before being heated at 125 ºC under microwave irradiation for 30 min. Upon completion, the reaction mixture was transferred to a round bottomed flask. HCl was removed under reduced pressure, and the residue was ultrasonicated in THF. p$\mathbf{E_{25}A_{75}}$ was recovered by filtration and dried in a vacuum oven overnight at 70 ºC. Yield: 85%.

Elemental analysis calcd. for **p$E_{25}A_{75}$**: C 33.72, H 8.43, N 14.30%. Found: C 34.43, H 8.13, N 14.65%.

^{1}H-NMR (δ, 20 ℃, D_2O, 300 MHz): 0.8-1.2 (m, C(O)CH_2CH_3), 2.2-2.8 (m, C(O)CH_2CH_3), 3.0-4.2 (m, NCH_2CH_2N).

6.2.7.4. Poly(aziridinium chloride)

2.5 g p**E**$_{100}$ (25.2 mmol) were added to a 20 mL microwave vial containing a stirring bar and dissolved in 10 mL of 6 M HCl before being heated at 125 ºC under microwave irradiation for 5 h. Upon completion, the reaction mixture was transferred to a round bottomed flask. HCl was removed under reduced pressure, and the residue was ultrasonicated in THF. p**A**$_{100}$ was recovered by filtration and dried in a vacuum oven overnight at 70 ºC. Yield: 96%.

^{1}H-NMR (δ, 20 ºC, D_2O, 300 MHz): 3.2-4.0 (m, NCH_2CH_2N).

6.2.7.5. Poly(2-nonyl-2-oxazoline)$_{75}$-stat-poly(aziridinium chloride)$_{25}$

2.5 g of p**N**$_{100}$ (12.7 mmol) and 10 mL of 6 M HCl were added to a 20 mL microwave vial containing a stirring bar. The vial was sealed with a septum and heated at 125 ºC for 30 min. Upon completion, the soluble contents were poured to a round bottomed flask. Insoluble contents were dissolved in DCM and added to the flask, upon which DCM was removed by freeze drying in liquid nitrogen. The flask contents were subsequently ultrasonicated in acetone and the product was recovered by filtration. Yield: 85%.

Elemental analysis calcd. for p**N**$_{75}$**A**$_{25}$: C 66.23, H 11.18, N 8.13%. Found: C 64.08, H 11.08, N 7.63%.

^{1}H-NMR (δ, 20 ºC, $CDCl_3$, 300 MHz): 0.8-1.0 (m, C(O)C_8H_{16}CH_3), 1.2-1.4 (m, C(O)CH_4C$_6H_{12}$CH_3), 1.4-1.8 (m, C(O)CH_2CH_2C$_7H_{15}$), 1.8-2.8 (m, C(O)CH_2C$_8H_{17}$) 3.0-4.8 (m, NCH_2CH_2N).

6.2.7.6. Poly(2-nonyl-2-oxazoline)$_{50}$-stat-poly(aziridinium chloride)$_{50}$

2.5 g of p**N**$_{100}$ (12.7 mmol) and 10 mL of 6 M HCl were added to a 20 mL microwave vial containing a stirring bar that was heated at 125 ºC for 80 min. Upon completion, the soluble contents of each vial were poured to a round bottomed flask. Insoluble contents were dissolved in DCM and added to the flask, upon which DCM was removed by freeze drying in liquid nitrogen. The flask contents were subsequently ultrasonicated in acetone and the product was recovered by filtration. Yield: 95%.

Elemental analysis calcd. for p**N**$_{50}$**A**$_{50}$: C 57.05, H 10.53, N 9.51%. Found: C 59.57, H 10.34, N 9.57%.

^{1}H-NMR (δ, 20 ℃, $CDCl_3$, 300 MHz): 0.8-1.0 (m, $C(O)C_8H_{16}CH_3$), 1.2-1.4 (m, $C(O)CH_4C_6H_{12}CH_3$), 1.4-1.8 (m, $C(O)CH_2CH_2C_7H_{15}$), 2.2-2.6 (m, $C(O)CH_2C_8H_{17}$), 2.6-4.8 (m, NCH_2CH_2N).

6.2.7.7. Poly(2-nonyl-2-oxazoline)$_{25}$-stat-poly(aziridinium chloride)$_{75}$

2.5 g of p**N$_{100}$** (12.7 mmol) and 10 mL of 6 M HCl were added to a 20 mL microwave vial containing a stirring bar that was heated at 125 ºC for 95 min. Upon completion, the soluble contents of each vial were poured to a round bottomed flask. Due to the solubility of p**N$_{25}$A$_{75}$** in water it was not necessary to dissolve reaction residues in DCM. The flask contents were subsequently ultrasonicated in acetone and the product was recovered by filtration. Before further use, the hydrolyzed polymers were dried in a vacuum oven overnight at 70 ºC. Yield: 91%.

Elemental analysis calcd. for p**N$_{25}$A$_{75}$**: C 49.71, H 9.21, N 12.89%. Found: C 53.56, H 10.27, N 9.82%.

^{1}H-NMR (δ, 20 ℃, D_2O, 300 MHz): 0.8-1.0 (m, $C(O)C_8H_{16}CH_3$), 1.2-1.8 (m, $C(O)CH_2C_7H_{14}CH_3$), 2.2-2.8 (m, $C(O)CH_2C_8H_{17}$), 2.8-4.4 (m, NCH_2CH_2N).

6.2.8 Plate preparation

Poly(2-oxazoline) samples of the various hydrolysis degrees were ground until a fine power was produced and weighed. **PP** was added to the sample in quantities such that the test polymer was present with a composition of 5/3/1% w/w. Subsequent to thorough mixing, three samples of 44.5 g were weighed from the bulk sample and added into stainless steel molds (150x150x2mm) before being spread evenly to ensure constant dimensions. Once prepared, the molds were placed into the platen press, where the oven had been pre-heated to 200 ºC, and were pressed under vacuum at 25 bar plten pressure for 15 minutes and cooled. The plates were then cut into smaller samples of 50x50x2mm and stored prior to biocidal testing. A blank set of reference plates containing only **PP** was additionally prepared according to this method.

6.2.9 Biocide Tests

Biocide tests of the ten series of test plates were carried out at HBICON GmbH in Bielefeld, Germany; study number AU/1107683. Tests were carried out in compliance

with ISO 22196:2007 employing *Escherichia coli* ATCC 25922, *Staphylococcus aureaus* ATCC 6538 P, *Candida albicans* ATCC 14053 *and Pseudomonas aeruginosa* ATCC 9027 as test organisms. For each series, three samples were tested by applying a defined suspension of each organism to the plate surface after washing of the samples. The number of colony forming units (CFUs) of each organism were: *E. coli* 1.4 E^6, *C. albicans* 6.8 E^4, *S. aureus* 3.3 E^4 and *P. aeruginosa* 1.5 E^5. In compliance with the standard, each sample was incubated for 24 hours at a temperature of 35 ºC. Once incubation was completed, each sample was rinsed in a sterilized saline solution and the number of remaining colony forming units determined. The average of the samples for each series was then used to calculate the reduction in biocidal activity of each organism using the formula:

$$\text{Reduction} = -\log\left(\frac{\text{average CFUs after 24 hours}}{\text{average initial CFUs}}\right) \qquad \textbf{Equation 6-2}$$

The overall biocidal activity of a series with each of the test organisms was determined based upon the values calculated.

6.3 Equipment

6.3.1.1. Biotage Initiator 8 Microwave Reactor

Gel and small-scale biocide syntheses were performed in the microwave reactor Initiator Eight from Biotage. The reactions were performed in sealed microwave-assisted synthesis process vials dedicatedly designed for the single-mode microwave system.

Figure 6-1: Initiator 8 microwave reactor from Biotage.

6.3.2 Anton Paar Masterwave Benchtop Microwave Reactor

Large scale polymer synthesis and hydrolysis was carried out in the Masterwave Desktop Reactor from Anton Paar. Reactions were carried out in a single Teflon vessel equipped with a stirrer capable of volumes up to 1 liter.

6.3.3 Laboratory Platen Press

To produce the biocide/PP compound plates, a Collin P 200 Laboratory Platen Press was used. The press is equipped with a vacuum pump and a water-cooling system nd was used with a temperature of 200 °C and max. 25 bars of pressure.

Figure 6-2: Collin Laboratory Platen Press.

6.3.4 NMR Spectroscopy

All NMR spectra were recorded on a Bruker Avance III 300 MHz NMR spectrometer. Polymer spectra were typically recorded with a minimum delay of 5 s; in general, a minimum number of 32 scans (^{1}H-NMR) was employed. As solvents, $CDCl_3$, DMSO-d_6 D_2O, and D_2O/DCl were used. The following peak shapes are indicated: s (singlet), d (doublet), t (triplet), m (multiplet). Residual solvent peaks were used for referencing purposes.

6.3.5 GPC Analysis

Average molecular weights in addition to the polydispersity indices were determined using gel permeation chromatography GPC. A mixture of $CHCl_3/Et_3N/^{iso}PrOH$ (94/4/2) was utilized as eluent. The GPC system consisted of a Merck Hitachi L-6000A pump, separation columns from Polymer Standards Service, 8\300 mm STV linear XL 5 µm-grade size, and a differential refractometer Waters 410 detector. Polystyrene standards from Polymer Standard Service were used for calibration.

6.3.6 Surface Energy Measurements

Contact angle measurements were recorded using a KRÜSS DSA100 automated goniometer (equipped with a CCD camera) under ambient conditions utilizing the sessile drop method. Deposition of test liquid droplets via micro syringes and the subsequent measurement of contact angles from the drop profile were performed automatically.

6.3.7 FT-IR Spectroscopy

IR spectra of the biocide containing compound plates were recorded an a Bruker Alpha FT-IR spectrometer equipped with ALPHA‘s Platinum ATR single reflection diamond ATR module in order to analyze the surface and near-surface regions.

6.3.8 Microanalysis

Scanning electron microscopy energy dispersive X-ray (SEM-EDX) measurements were carried out using a Tescan Vega 3 scanning electron microscope with an energy dispersive X-ray spectrometer (EDX Oxford Instruments INKAxact) attached. Electron energy levels were set to 20 kV.

6.3.9 Zeta Potential Measurements

Zeta potential measurements were conducted employing the electrokinetic surface analyzer SurPASS by Anton Paar; zeta potentials were calculated by the experimental streaming potential according to the Helmholtz-Smoluchowski equation.[151]

Reproducibility was tested utilizing two different specimens of each sample; zeta potential / pH correlations were fitted using 2nd order polynomial functions.

7 Appendix

7.1 Abbreviations

^{1}H NMR	Proton Nuclear Magnetic Resonance
ATR-IR	Attenuated total reflectance infrared spectroscopy
BisOx	Bis-functional oxazoline
Boc-AmOx	2-[*N*-Boc-5-aminopentyl]-2-oxazoline
CROP	Cationic Ring-Opening Polymerization
DDA	*N,N*-dimethyl dodecylammonium (chloride)
DCM	Dichloromethane
DMEM	Dulbecco's modified eagle medium
Dc=Ox	2-9'-Decenyl-2-oxazoline
EI	Ethylene imine
EtOx	2-Ethyl-2-oxazoline
% GI	% Growth inhibition
iPrOx	2-*Iso*-propyl-2-oxazoline
MeOx	2-Methyl-2-oxazoline
MeTsO	Methyl tosylate
MonOx	Monofunctional oxazoline
NonOx	*2*-Nonyl-2-oxazoline
PBO	Phenylene-bis(2-oxazoline)
PDI	Polydispersity Index
PP	Polypropylene
THF	Tetrahydrofuran
TMBOx	Tetramethylene-bis(2-oxazoline)

7.2 Gel Swelling Degrees

Table 7-1: Maximum swelling degrees of the 32 p**EtOx**$_m$-p**PhOx**$_n$-p**PBO**$_q$-based gels in water.

H_2O **MonOx**: **EtOx**: **PBO →** **PhOx ↓**	150:30	150:15	150:10	150:7.5	150:6	150:3	150:2	150:1.5
150:0	0.3	1.6	1.9	2.3	3.8	10.2	13.8	*
100:50	0.3	0.6	0.7	1.0	1.0	1.4	1.9	2.7
50:100	0.2	0.3	0.3	0.6	0.3	0.2	0.4	0.4
0:150	0.2	0.1	0.3	0.1	0.2	0.0	0.2	0.6

Table 7-2: Maximum swelling degrees of the 32 p**EtOx**$_m$-p**PhOx**$_n$-p**PBO**$_q$-based gels in ethanol.

EtOH **MonOx**: **EtOx**: **PBO →** **PhOx ↓**	150:30	150:15	150:10	150:7.5	150:6	150:3	150:2	150:1.5
150:0	0.0	1.4	1.5	1.7	4.1	7.1	8.8	*
100:50	0.0	0.6	1.1	1.4	2.0	4.5	6.2	11.7
50:100	0.0	0.3	0.7	0.7	1.3	2.2	2.5	6.8
0:150	0	0	0.1	0.1	0.2	0.7	0.7	0.7

Table 7-3: Maximum swelling degrees of the 32 p**EtOx**$_m$-p**PhOx**$_n$-p**PBO**$_q$-based gels in dichloromethane.

DCM **EtOx**: **PhOx** ↓	**MonOx**: **PBO** →	150:30	150:15	150:10	150:7.5	150:6	150:3	150:2	150:1.5
150:0		0.9	1.8	2.7	3.2	4.4	11.5	15.7	*
100:50		0.1	1.6	2.1	2.6	3.9	9.0	13.1	17.4
50:100		0.0	1.4	2.1	2.7	4.1	7.7	13.4	20.0
0:150		0.0	0.9	2.1	2.8	4.4	9.0	15.1	18.3

Compound Plate Contact Angle Data

Table 7-4: Contact angles of 95% PP / 5% **pE$_{100}$** in diiodomethane.

#	BD [mm]	θ(R) [°]	θ(L) [°]	θ(avrg.) [°]
1	4.394	64.7	57.4	61.1 ± 3.67
2	4.048	71.0	65.2	68.1 ± 2.90
3	4.105	70.8	66.0	68.4 ± 2.44
4	4.098	60.3	65.1	62.7 ± 2.37
5	4.285	67.0	54.1	60.5 ± 6.48
avrg.	4.186 ± 0.275	66.76 ± 8.96	61.56 ± 8.16	64.2 ± 6.77

Table 7-5: Contact ngles of 95% PP / 5% **pE_{100}** in water.

#	BD [mm]	θ(R) [°]	θ(L) [°]	θ(avrg.) [°]
1	3.218	87.8	86.0	86.9 ± 0.90
2	3.191	84.5	92.7	88.6 ± 4.07
3	3.310	87.5	86.2	86.8 ± 0.64
4	3.476	75.3	82.4	78.9 ± 3.59
5	3.395	84.0	81.2	82.6 ± 1.40
avrg.	3.318 ± 0.196	83.8 ± 8.33	85.7 ± 7.34	84.8 ± 6.53

Table 7-6: Contact angles of 95% PP / 5% **$pE_{75}A_{25}$** in diiodomethane.

#	BD [mm]	θ(R) [°]	θ(L) [°]	θ(avrg.) [°]
1	4.040	66.5	65.5	66.0 ± 0.51
2	4.014	65.2	73.3	69.2 ± 4.05
3	3.969	68.5	73.7	71.1 ± 2.59
4	3.905	71.0	71.4	71.2 ± 0.20
5	3.885	72.4	69.8	71.1 ± 1.32
avrg.	4.040	66.5	65.5	66.0 ± 0.51

Table 7-7: Contact angles of 95% PP / 5% **$pE_{75}A_{25}$** in water.

#	BD [mm]	θ(R) [°]	θ(L) [°]	θ(avrg.) [°]
1	3.231	90.9	90.9	90.9
2	3.179	96.0	84.1	90.1 ± 5.96
3	3.148	93.2	92.3	92.7 ± 0.45
4	3.151	96.8	86.7	91.8 ± 5.07
5	3.181	85.5	92.8	89.2 ± 3.69
avrg.	3.178 ± 0.055	92.5 ± 7.53	89.4 ± 6.24	90.9 ± 2.29

Table 7-8: Contact angles of 95% PP / 5% **$pE_{50}A_{50}$** in diiodomethane.

#	BD [mm]	θ(R) [°]	θ(L) [°]	θ(avrg.) [°]
1	3.816	68.3	77.8	73.0 ± 4.74
2	3.880	78.1	70.6	74.3 ± 3.76
3	3.886	73.4	74.4	73.9 ± 0.49
4	4.030	70.9	67.0	68.9 ± 1.94
5	4.103	73.6	77.2	75.4 ± 1.80
avrg.	3.943 ± 0.196	72.8 ± 5.98	73.4 ± 7.52	73.1 ± 4.08

Table 7-9: Contact angles of 95% PP / 5% **$pE_{50}A_{50}$** in water.

#	BD [mm]	θ(R) [°]	θ(L) [°]	θ(avrg.) [°]
1	3.111	88.5	95.5	92.0 ± 3.52
2	2.934	97.0	92.0	94.5 ± 2.50
3	3.189	82.5	87.9	85.2 ± 2.72
4	2.906	103.4	97.8	100.6 ± 2.80
5	2.894	102.8	106.1	104.5 ± 1.63
avrg.	3.007 ± 0.221	94.8 ± 15.06	95.9 ± 11.22	95.4 ± 12.35

Table 7-10: Contact angles of 95% PP / 5% **$pE_{25}A_{75}$** in diiodomethane.

#	BD [mm]	θ(R) [°]	θ(L) [°]	θ(avrg.) [°]
1	4.045	72.9	59.5	66.2 ± 6.73
2	3.903	73.5	68.8	71.2 ± 2.34
3	3.888	70.9	75.1	73.0 ± 2.07
4	3.942	68.8	76.4	72.6 ± 3.83
5	4.008	72.2	62.1	67.2 ± 5.05
avrg.	3.957 ± 0.111	71.7 ± 3.12	68.4 ± 12.43	70.0 ± 5.18

Table 7-11: Contact angles of 95% PP / 5% $\mathbf{pE_{25}A_{75}}$ in water.

#	BD [mm]	θ(R) [°]	θ(L) [°]	θ(avrg.) [°]
1	3.238	84.7	88.3	86.5 ± 1.80
2	3.350	86.0	73.7	79.8 ± 6.11
3	3.445	81.0	82.3	81.6 ± 0.65
4	3.455	82.3	83.4	82.8 ± 0.50
5	3.290	89.2	78.7	83.9 ± 5.25
avrg.	3.356 ± 0.156	84.6 ± 5.26	81.3 ± 8.94	82.9 ± 4.10

Table 7-12: Contact angles of 95% PP / 5% $\mathbf{pA_{100}}$ in diiodomethane.

#	BD [mm]	θ(R) [°]	θ(L) [°]	θ(avrg.) [°]
1	3.932	72.4	67.3	69.9 ± 2.51
2	3.995	70.1	68.0	69.1 ± 1.04
3	4.041	64.9	59.4	62.2 ± 2.73
4	4.059	65.5	59.8	62.6 ± 2.85
5	3.952	68.7	70.1	69.4 ± 0.69
avrg.	3.996 ± 0.090	68.3 ± 5.17	64.9 ± 8.18	66.6 ± 6.37

Table 7-13: Contact angles of 95% PP / 5% $\mathbf{pA_{100}}$ in water.

#	BD [mm]	θ(R) [°]	θ(L) [°]	θ(avrg.) [°]
1	3.232	88.4	78.6	83.5 ± 4.88
2	3.169	84.8	93.5	89.1 ± 4.34
3	3.091	92.1	85.1	88.6 ± 3.50
4	3.169	86.8	90.0	88.4 ± 1.61
5	3.069	92.8	91.3	92.1 ± 0.73
avrg.	3.146 ± 0.109	89.0 ± 5.65	87.7 ± 9.77	88.3 ± 5.07

Table 7-14: Contact angles of 95% PP / 5% **pN100** in diiodomethane.

#	BD [mm]	θ(R) [°]	θ(L) [°]	θ(avrg.) [°]
1	3.809	74.7	71.4	73.0 ± 1.68
2	3.771	74.2	73.4	73.8 ± 0.37
3	3.768	73.9	72.2	73.0 ± 0.84
4	3.868	72.3	63.2	67.8 ± 4.55
5	3.822	71.2	65.4	68.3 ± 2.91
avrg.	3.808 ± 0.068	73.2 ± 2.41	69.1 ± 7.44	71.2 ± 4.78

Table 7-15: Contact angles of 95% PP / 5% **pN100** in ethylene glycol.

#	BD [mm]	θ(R) [°]	θ(L) [°]	θ(avrg.) [°]
1	4.227	58.7	53.8	56.2 ± 2.45
2	4.596	51.5	37.6	44.5 ± 6.99
3	3.084	55.5	47.8	51.6 ± 3.88
4	4.466	57.1	46.2	51.7 ± 5.43
5	4.115	48.2	64.3	56.3 ± 8.07
avrg.	4.098 ± 0.983	54.2 ± 7.04	49.9 ± 16.33	52.1 ± 7.89

Table 7-16: Contact angles of 95% PP / 5% **$pN_{75}A_{25}$** in diiodomethane.

#	BD [mm]	θ(R) [°]	θ(L) [°]	θ(avrg.) [°]
1	3.806	77.3	63.8	70.6 ± 6.79
2	3.823	76.2	66.0	71.1 ± 5.10
3	3.770	71.7	73.3	72.5 ± 0.81
4	3.942	76.1	67.5	71.8 ± 4.27
5	4.055	63.0	64.0	63.5 ± 0.47
avrg.	3.879 ± 0.193	72.9 ± 9.69	66.9 ± 6.40	69.9 ± 5.97

Table 7-17: Contact angles of 95% PP / 5% **$pN_{75}A_{25}$** in ethylene glycol.

#	BD [mm]	θ(R) [°]	θ(L) [°]	θ(avrg.) [°]
1	4.388	50.1	49.6	49.9 ± 0.25
2	3.967	63.9	59.5	61.7 ± 2.20
3	4.199	58.7	64.2	61.4 ± 2.77
4	4.187	50.0	57.2	53.6 ± 3.64
5	3.999	63.0	59.5	61.3 ± 1.74
avrg.	4.148 ± 0.281	57.1 ± 11.12	58.0 ± 8.76	57.6 ± 9.02

Table 7-18: Contact angles of 95% PP / 5% **$pN_{50}A_{50}$** in diiodomethane.

#	BD [mm]	θ(R) [°]	θ(L) [°]	θ(avrg.) [°]
1	3.764	72.6	69.7	71.1 ± 1.44
2	3.865	70.2	70.9	70.6 ± 0.33
3	3.800	73.1	68.6	70.9 ± 2.23
4	3.602	73.1	76.3	74.7 ± 1.57
5	3.853	73.2	69.7	71.5 ± 1.77
avrg.	3.777 ± 0.174	72.5 ± 2.09	71.0 ± 4.99	71.7 ± 2.78

Table 7-19: Contact angles of 95% PP / 5% **$pN_{50}A_{50}$** in ethylene glycol.

#	BD [mm]	θ(R) [°]	θ(L) [°]	θ(avrg.) [°]
1	3.319	44.7	46.5	45.6 ± 0.88
2	4.665	48.6	42.8	45.7 ± 2.87
3	4.344	45.3	47.5	46.4 ± 1.14
4	3.559	58.7	51.3	55.0 ± 3.74
5	3.676	47.3	53.2	50.2 ± 2.99
avrg.	3.913 ± 0.933	48.9 ± 9.39	48.3 ± 6.72	48.6 ± 6.67

Table 7-20: Contact angles of 95% PP / 5% $\mathbf{pN_{25}A_{75}}$ in diiodomethane.

#	BD [mm]	θ(R) [°]	θ(L) [°]	θ(avrg.) [°]
1	3.861	73.5	74.0	73.7 ± 0.25
2	3.809	65.2	80.0	72.6 ± 7.37
3	3.793	75.4	77.6	76.5 ± 1.14
4	3.994	78.3	70.7	74.5 ± 3.77
5	3.904	72.6	71.2	71.9 ± 0.67
avrg.	3.872 ± 0.133	73.0 ± 7.97	74.7 ± 6.63	73.8 ± 2.94

Table 7-21: Contact angles of 95% PP / 5% $\mathbf{pN_{25}A_{75}}$ in ethylene glycol.

#	BD [mm]	θ(R) [°]	θ(L) [°]	θ(avrg.) [°]
1	4.132	62.3	51.7	57.0 ± 5.31
2	4.108	62.1	59.2	60.6 ± 1.44
3	4.378	63.1	50.7	56.9 ± 6.21
4	4.033	59.6	56.4	58.0 ± 1.62
5	4.069	56.9	47.2	52.0 ± 4.82
avrg.	4.144 ± 0.224	60.8 ± 4.19	53.0 ± 7.81	56.9 ± 5.11

Table 7-22: Contact angles of 100% PP in diiodomethane.

#	BD [mm]	θ(R) [°]	θ(L) [°]	θ(avrg.) [°]
1	3.433	64.3	56.7	60.5 ± 3.81
2	3.650	61.0	68.9	64.9 ± 3.92
3	3.712	53.2	75.1	64.2 ± 10.94
4	3.683	64.0	65.1	64.5 ± 0.52
5	3.844	61.4	63.8	62.6 ± 1.17
avrg.	3.664 ± 0.245	60.8 ± 7.37	65.9 ± 11.15	63.3 ± 3.01

Table 7-23: Contact angles of 100% PP in ethylene glycol.

#	BD [mm]	θ(R) [°]	θ(L) [°]	θ(avrg.) [°]
1	2.943	60.4	69.7	65.1 ± 4.65
2	3.257	62.0	74.2	68.1 ± 6.08
3	3.318	62.8	64.6	63.7 ± 0.90
4	3.330	69.0	66.6	67.8 ± 1.16
5	3.416	67.3	66.9	67.1 ± 0.20
avrg.	3.253 ± 0.300	64.3 ± 5.98	68.4 ± 6.10	66.4 ± 3.10

Table 7-24: Contact angles of 100% PP in water.

#	BD [mm]	θ(R) [°]	θ(L) [°]	θ(avrg.) [°]
1	3.258	92.2	81.6	86.9 ± 5.31
2	3.025	93.4	95.7	94.5 ± 1.18
3	3.160	94.8	94.2	94.5 ± 0.32
4	3.223	90.0	87.5	88.7 ± 1.25
5	3.029	98.9	86.5	92.7 ± 6.22
avrg.	3.139 ± 0.178	93.9 ± 5.50	89.1 ± 9.56	91.5 ± 5.73

7.3 Biocide Test Data

For all tables, the following abbreviations are used:

[1] Arithmetic mean; [2] Standard deviation; [3] Logarithmic reduction factor; [4] Standard deviation of the logarithmic reduction factor; [5] Bacterial suspension at t = 0. [A] The amount of residual microbes on samples that did not contain any microbes needed to be set to 1 for the subsequent calculations. [B] Logarithmic (relative) standard deviations were set to 0 if no microbes were found on any of the three samples.

Table 7-25: Antimicrobial tests in compliance with ISO 22196:2007 of the polymers **$pE_{100-25n}A_{25n}$** and **$pN100_{-25n}A_{25n}$** (n = 0-4) in compound plates (95% PP) against *E. coli* the initial concentration of the bacterial suspension being 1.40±0.10 10^6 colony forming units CFU. The quantity of residual microbes on the test samples was determined in triplicate after 24 h (entries #1-#3) and verified against a blank 100% PP plate.

	#1	#2	#3	Mean[1]	SD[2]	rel. SD[3]	lg RF[4]	lg SD(RF)[5]
Escherichia coli								
BS[6]	$1.3\cdot10^6$	$1.5\cdot10^6$	$1.4\cdot10^6$	$1.40\cdot10^6$	$1.00\cdot10^5$	0.07	0.00	0.00
PP	$7.0\cdot10^5$	$6.8\cdot10^5$	$8.2\cdot10^5$	$7.33\cdot10^5$	$7.57\cdot10^4$	0.10	0.28	0.16
pE_{100}	$5.8\cdot10^5$	$6.2\cdot10^5$	$3.2\cdot10^5$	$5.07\cdot10^5$	$1.63\cdot10^5$	0.32	0.44	0.65
$pE_{75}A_{25}$	$4.2\cdot10^5$	$3.8\cdot10^5$	$3.2\cdot10^5$	$3.73\cdot10^5$	$5.03\cdot10^4$	0.13	0.57	0.28
$pE_{50}A_{50}$	$1.0\cdot10^1$	0 (1)[A]	$1.4\cdot10^1$	8.33	6.66	0.80	5.23	1.05
$pE_{25}A_{75}$	0 (1)[A]	0 (1)[A]	0 (1)[A]	1.00	0.00	0.00	6.15	0.00[B]
pA_{100}	$1.0\cdot10^1$	0 (1)[A]	0 (1)[A]	4.00	5.20	1.30	5.54	1.26
$pN_{25}A_{75}$	0 (1)[A]	0 (1)[A]	0 (1)[A]	1.00	0.00	0.00	6.15	0.00[B]
$pN_{50}A_{50}$	0 (1)[A]	0 (1)[A]	0 (1)[A]	1.00	0.00	0.00	6.15	0.00[B]
$pN_{75}A_{25}$	$5.2\cdot10^5$	$2.4\cdot10^5$	$2.3\cdot10^5$	$3.30\cdot10^5$	$1.65\cdot10^5$	0.50	0.63	0.84
pN_{100}	$2.8\cdot10^5$	$1.9\cdot10^5$	$1.8\cdot10^5$	$2.17\cdot10^5$	$5.51\cdot10^4$	0.25	0.81	0.55

Table 7-26: Antimicrobial tests in compliance with ISO 22196:2007 of the polymers **$pE_{100-25n}A_{25n}$** and **$pN100_{-25n}A_{25n}$** (n = 0-4) in compound plates (95% PP) against *P. aeruginosa* the initial concentration of the bacterial suspension being 1.50±0.27 10^5 colony forming units CFU. The quantity of residual microbes on the test samples was determined in triplicate after 24 h (entries #1-#3) and verified against a blank 100% PP plate.

	#1	#2	#3	Mean[1]	SD[2]	rel. SD[3]	lg RF[4]	lg SD(RF)[5]
Pseudomonas aeruginosa								
BS[6]	$1.8\cdot10^5$	$1.4\cdot10^5$	$1.3\cdot10^5$	$1.50\cdot10^5$	$2.65\cdot10^4$	0.18	0.00	0.00
PP	$2.3\cdot10^5$	$1.9\cdot10^5$	$4.3\cdot10^5$	$2.83\cdot10^5$	$1.29\cdot10^5$	0.45	-0.28	0.41
pE_{100}	$4.2\cdot10^5$	$1.5\cdot10^5$	$1.8\cdot10^5$	$2.50\cdot10^5$	$1.48\cdot10^5$	0.59	-0.22	0.53
$pE_{75}A_{25}$	$9.8\cdot10^4$	$1.3\cdot10^5$	$1.5\cdot10^5$	$1.26\cdot10^5$	$2.62\cdot10^4$	0.21	0.08	0.07
$pE_{50}A_{50}$	$9.2\cdot10^3$	$7.5\cdot10^3$	$7.4\cdot10^3$	$8.03\cdot10^3$	$1.01\cdot10^3$	0.13	1.27	0.15
$pE_{25}A_{75}$	$5.0\cdot10^1$	$2.0\cdot10^1$	$4.0\cdot10^1$	$3.67\cdot10^1$	$1.53\cdot10^1$	0.42	3.61	0.37
pA_{100}	0 (1)[A]	0 (1)[A]	0 (1)[A]	1.00	0.00	0.00	5.18	0.00[B]
$pN_{25}A_{75}$	0 (1)[A]	0 (1)[A]	0 (1)[A]	1.00	0.00	0.00	5.18	0.00[B]
$pN_{50}A_{50}$	0 (1)[A]	0 (1)[A]	0 (1)[A]	1.00	0.00	0.00	5.18	0.00[B]
$pN_{75}A_{25}$	$1.0\cdot10^5$	$7.8\cdot10^4$	$1.0\cdot10^5$	$9.27\cdot10^4$	$1.27\cdot10^4$	0.14	0.21	0.11
pN_{100}	$4.3\cdot10^5$	$1.9\cdot10^5$	$2.1\cdot10^5$	$2.77\cdot10^5$	$1.33\cdot10^5$	0.48	-0.27	0.44

Table 7-27: Antimicrobial tests in compliance with ISO 22196:2007 of the polymers **$pE_{100-25n}A_{25n}$** and **$pN100_{-25n}A_{25n}$** (n = 0-4) in compound plates (95% PP) against *S. aureus* the initial concentration of the bacterial suspension being 3.27±0.40 10^4 colony forming units CFU. The quantity of residual microbes on the test samples was determined in triplicate after 24 h (entries #1-#3) and verified against a blank 100% PP plate.

	#1	#2	#3	Mean[1]	SD[2]	rel. SD[3]	lg RF[4]	lg SD(RF)[5]
Staphylococcus aureus								
BS[6]	$3.2\cdot10^4$	$3.7\cdot10^4$	$2.9\cdot10^4$	$3.27\cdot10^4$	$4.04\cdot10^3$	0.12	0.00	0.00
PP	$8.3\cdot10^4$	$9.3\cdot10^4$	$1.0\cdot10^4$	$6.20\cdot10^4$	$4.53\cdot10^4$	0.73	-0.28	0.77
pE_{100}	$6.7\cdot10^4$	$7.5\cdot10^4$	$8.9\cdot10^4$	$7.70\cdot10^4$	$1.11\cdot10^4$	0.14	-0.37	0.07
$pE_{75}A_{25}$	$9.8\cdot10^4$	$1.0\cdot10^5$	$8.9\cdot10^4$	$9.57\cdot10^4$	$5.86\cdot10^3$	0.06	-0.47	0.31
$pE_{50}A_{50}$	$5.8\cdot10^2$	$9.5\cdot10^2$	$3.6\cdot10^2$	$6.30\cdot10^2$	$2.98\cdot10^2$	0.47	1.71	0.58
$pE_{25}A_{75}$	$8.0\cdot10^1$	$1.3\cdot10^2$	$4.2\cdot10^2$	$2.10\cdot10^2$	$1.84\cdot10^2$	0.87	2.19	0.85
pA_{100}	$5.2\cdot10^2$	$6.2\cdot10^2$	$5.0\cdot10^2$	$5.47\cdot10^2$	$6.43\cdot10^1$	0.12	1.78	0.02
$pN_{25}A_{75}$	0 (1)[A]	0 (1)[A]	0 (1)[A]	1.00	0.00	0.00	4.51	0.00[B]
$pN_{50}A_{50}$	0 (1)[A]	0 (1)[A]	0 (1)[A]	1.00	0.00	0.00	4.51	0.00[B]
$pN_{75}A_{25}$	$5.0\cdot10^1$	0 (1)[A]	0 (1)[A]	$1.73\cdot10^1$	$2.83\cdot10^1$	1.63	3.28	1.12
pN_{100}	$3.8\cdot10^4$	$5.2\cdot10^4$	$4.0\cdot10^4$	$4.33\cdot10^4$	$7.57\cdot10^3$	0.17	-0.12	0.15

Table 7-28: Antimicrobial tests in compliance with ISO 22196:2007 of the polymers **$pE_{100-25n}A_{25n}$** and **$pN100_{-25n}A_{25n}$** (n = 0-4) in compound plates (95% PP) against *C. albicans* the initial concentration of the bacterial suspension being of 6.83±0.23 10^4 colony forming units CFU. The quantity of residual microbes on the test samples was determined in triplicate after 24 h (entries #1-#3) and verified against a blank 100% PP plate.

	#1	#2	#3	Mean[1]	SD[2]	rel. SD[3]	lg RF[4]	lg SD(RF)[5]
Candida albicans								
BS[6]	$6.7 \cdot 10^4$	$6.7 \cdot 10^4$	$7.1 \cdot 10^4$	$6.83 \cdot 10^4$	$2.31 \cdot 10^3$	0.03	0.00	0.00
PP	$9.8 \cdot 10^4$	$9.6 \cdot 10^4$	$1.1 \cdot 10^5$	$1.01 \cdot 10^5$	$7.57 \cdot 10^3$	0.07	-0.17	0.34
pE_{100}	$9.6 \cdot 10^4$	$9.8 \cdot 10^4$	$8.2 \cdot 10^4$	$9.20 \cdot 10^4$	$8.72 \cdot 10^3$	0.09	-0.13	0.45
$pE_{75}A_{25}$	$9.8 \cdot 10^4$	$9.4 \cdot 10^4$	$1.1 \cdot 10^4$	$6.77 \cdot 10^4$	$4.91 \cdot 10^4$	0.73	0.00	1.33
$pE_{50}A_{50}$	0 (1)[A]	$1.2 \cdot 10^2$	$8.0 \cdot 10^1$	$6.70 \cdot 10^1$	$6.06 \cdot 10^1$	0.90	3.01	1.43
$pE_{25}A_{75}$	0 (1)[A]	0 (1)[A]	0 (1)[A]	1.00	0.00	0.00	4.83	0.00[B]
pA_{100}	0 (1)[A]	0 (1)[A]	0 (1)[A]	1.00	0.00	0.00	4.83	0.00[B]
$pN_{25}A_{75}$	$6.0 \cdot 10^1$	$5.0 \cdot 10^1$	$2.0 \cdot 10^1$	$4.33 \cdot 10^1$	$2.08 \cdot 10^1$	0.48	3.20	1.15
$pN_{50}A_{50}$	$2.1 \cdot 10^2$	$5.0 \cdot 10^1$	$1.1 \cdot 10^1$	$9.03 \cdot 10^1$	$1.05 \cdot 10^2$	1.17	2.88	1.54
$pN_{75}A_{25}$	$5.8 \cdot 10^3$	$4.4 \cdot 10^3$	$1.4 \cdot 10^3$	$3.87 \cdot 10^3$	$2.25 \cdot 10^3$	0.58	1.25	1.24
pN_{100}	$2.9 \cdot 10^3$	$3.8 \cdot 10^3$	$3.4 \cdot 10^3$	$3.37 \cdot 10^3$	$4.51 \cdot 10^2$	0.13	1.31	0.60

Table 7-29: Antimicrobial tests of the polymer **$pN_{20}A_{80}$** in compound plates (95% PP) against *E. coli*: Incubation was performed twice; each incubation lasted 24 h. The initial concentration of the bacterial suspension was 5.43±1.14 10^5 colony forming units. The amount of residual microbes on the test samples was determined in triplicate after 24 h (entries #1-#3).

	#1	#2	#3	Mean[1]	SD[2]	lg RF[3]	SD lg RF[4]
Escherichia coli							
BS[5]	$6.7 \cdot 10^5$	$5.1 \cdot 10^5$	$4.5 \cdot 10^5$	$5.43 \cdot 10^5$	$1.14 \cdot 10^5$		
PP	$2.1 \cdot 10^7$	$2.1 \cdot 10^7$	$1.3 \cdot 10^7$	$1.83 \cdot 10^7$	$4.62 \cdot 10^6$	-1.524	0.081
pE_{100}	0 (1)[A]	0 (1)[A]	0 (1)[A]	1	0	5.729	0[B]

Table 7-30: Antimicrobial tests in compliance with ISO 22196:2007 of the polymer **$pN_{20}A_{80}$** in compound plates (95, 97, and99% PP) against *E. coli* with an initial concentration of the bacterial suspension of 1.40±0.27 10^5 colony forming units. The amount of residual microbes on the test samples was determined in triplicate after 24 h (entries #1-#3).

	#1	#2	#3	Mean[1]	SD[2]	lg RF[3]	SD lg RF[4]
Escherichia coli							
BS[5]	$1.3 \cdot 10^5$	$1.2 \cdot 10^5$	$1.7 \cdot 10^5$	$1.40 \cdot 10^5$	$0.27 \cdot 10^5$		
PP	$2.3 \cdot 10^7$	$2.1 \cdot 10^7$	$2.2 \cdot 10^7$	$2.20 \cdot 10^7$	$0.10 \cdot 10^7$	-2.201	0.079
5% $pN_{20}A_{80}$	0 (1)[A]	0 (1)[A]	0 (1)[A]	1	0	5.141	0[B]
3% $pN_{20}A_{80}$	0 (1)[A]	0 (1)[A]	0 (1)[A]	1	0	5.141	0[B]
1% $pN_{20}A_{80}$	0 (1)[A]	0 (1)[A]	0 (1)[A]	1	0	5.141	0[B]

7.4 NMR Spectra

pE_{100}

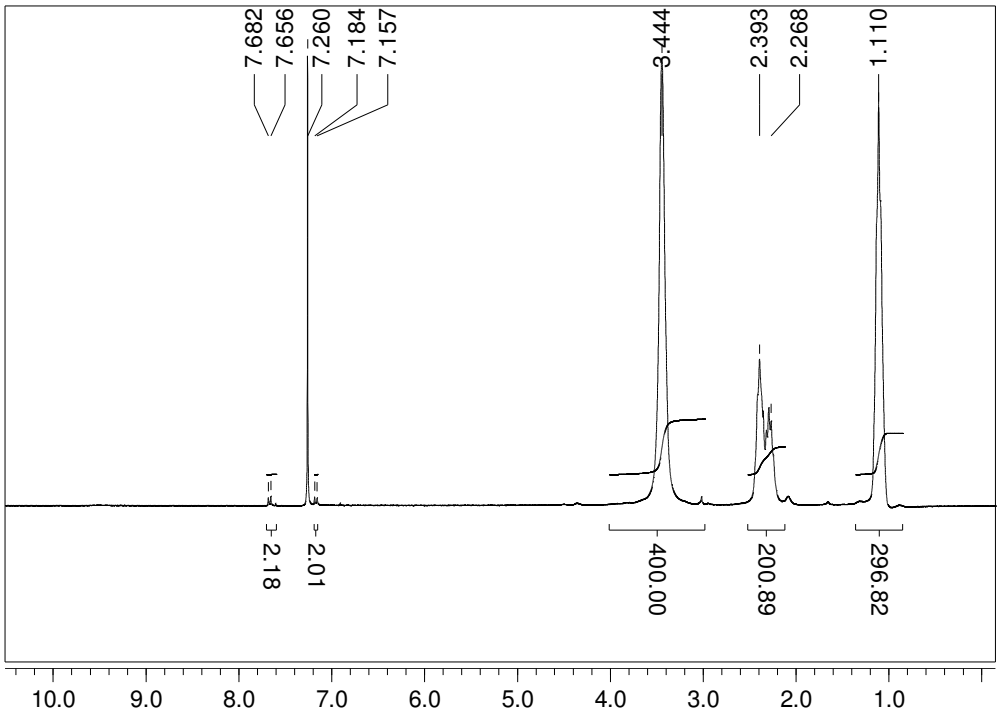

$pE_{75}A_{25}$

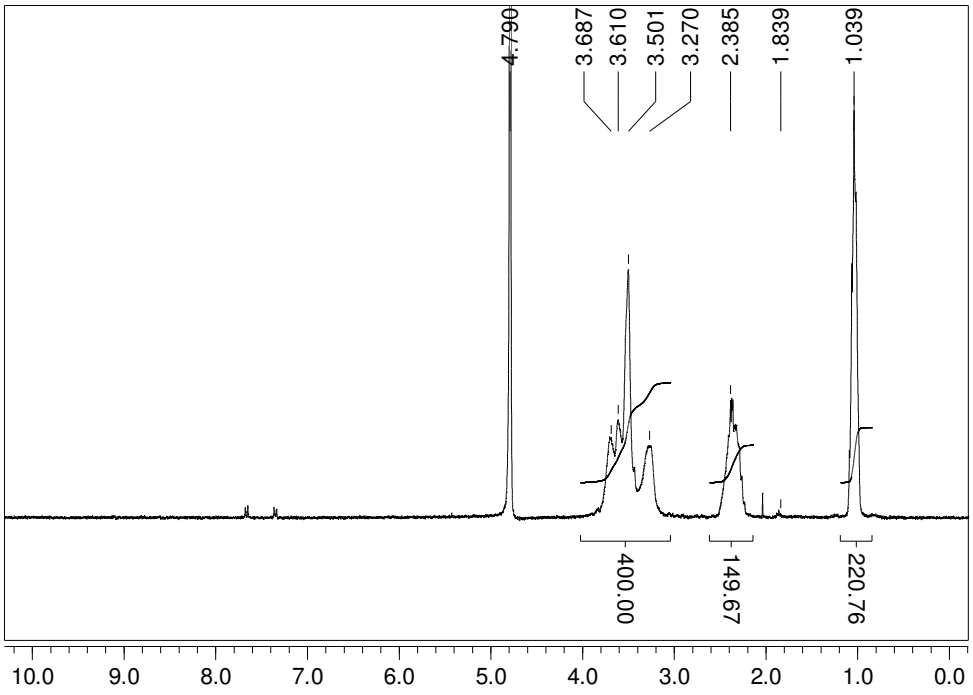

$pE_{50}A_{50}$

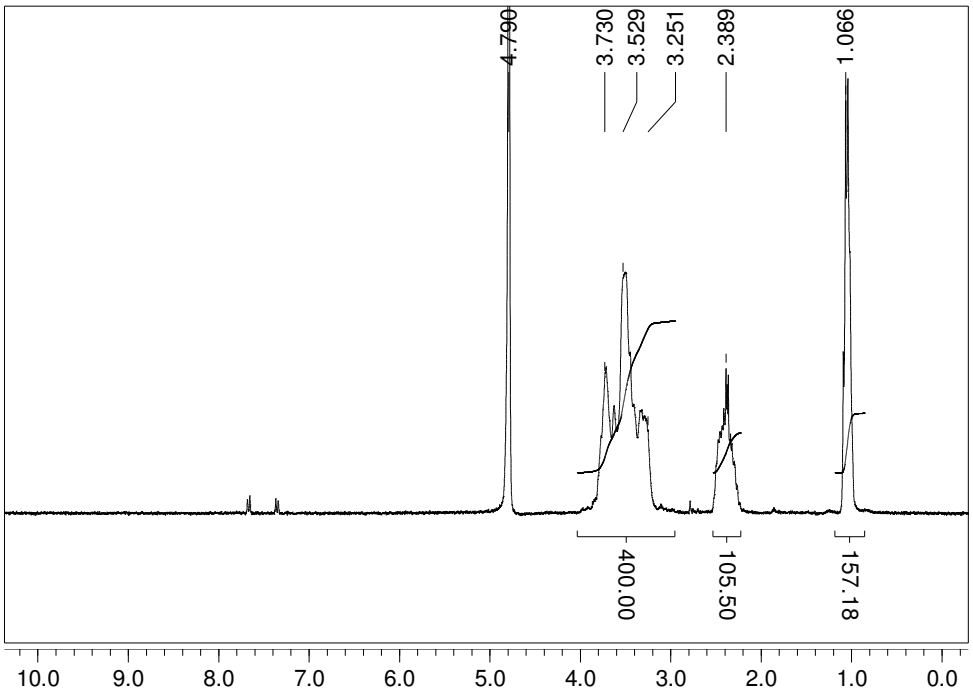

$pE_{25}A_{75}$

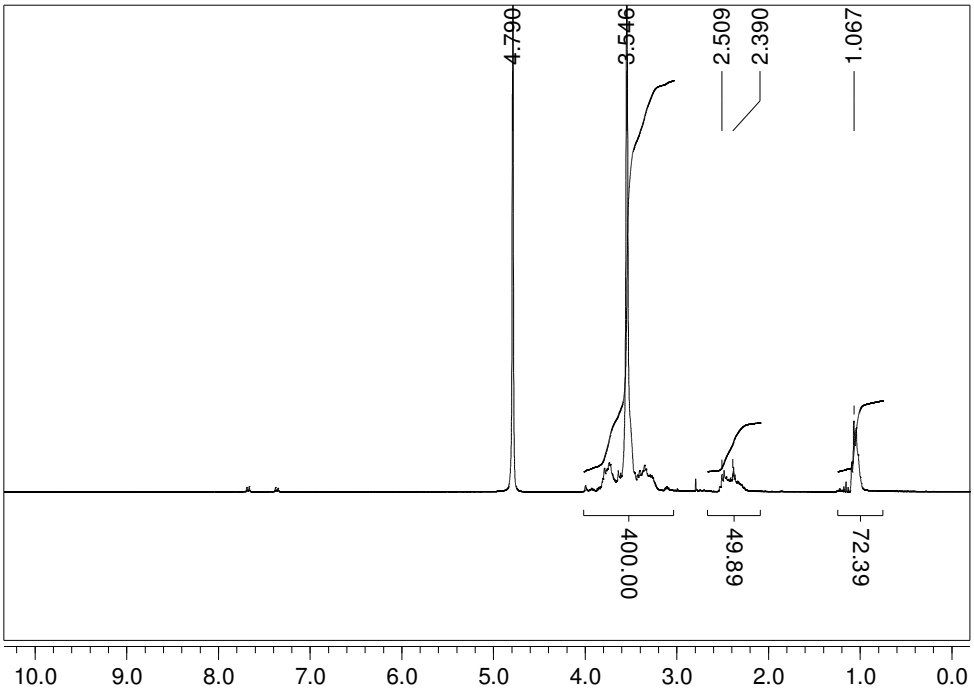

pA_{100}

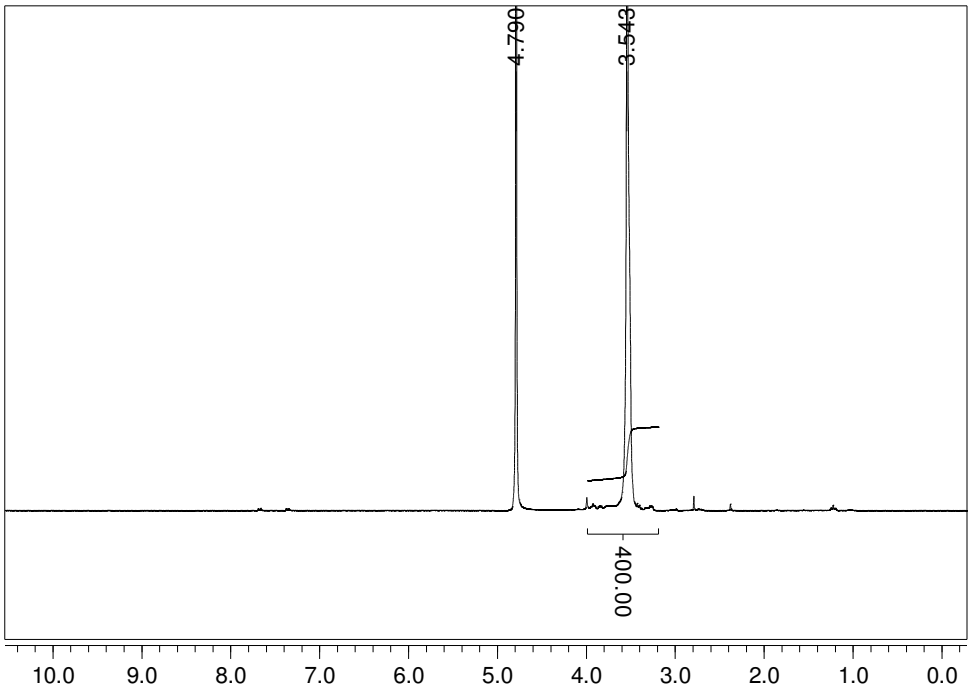
4.790
3.543
400.00
10.0
9.0
8.0
7.0
6.0
5.0
4.0
3.0
2.0
1.0
0.0

pN_{100}

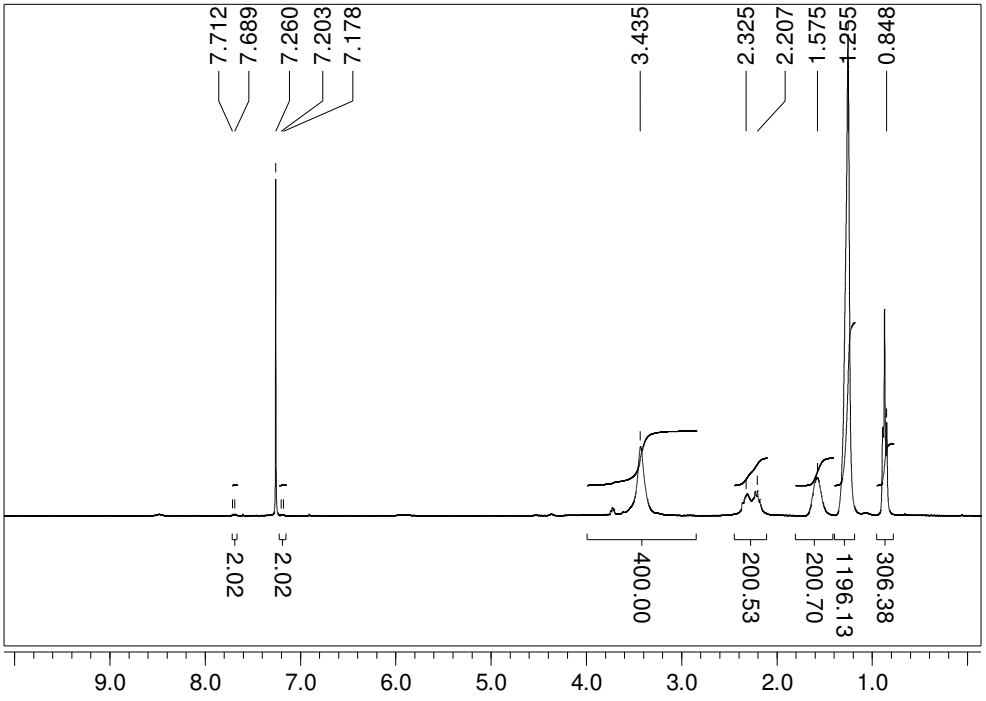
7.712
7.689
7.260
7.203
7.178
3.435
2.325
2.207
1.575
1.255
0.848
2.02
2.02
400.00
200.53
200.70
1196.13
306.38
9.0
8.0
7.0
6.0
5.0
4.0
3.0
2.0
1.0

$pN_{75}A_{25}$

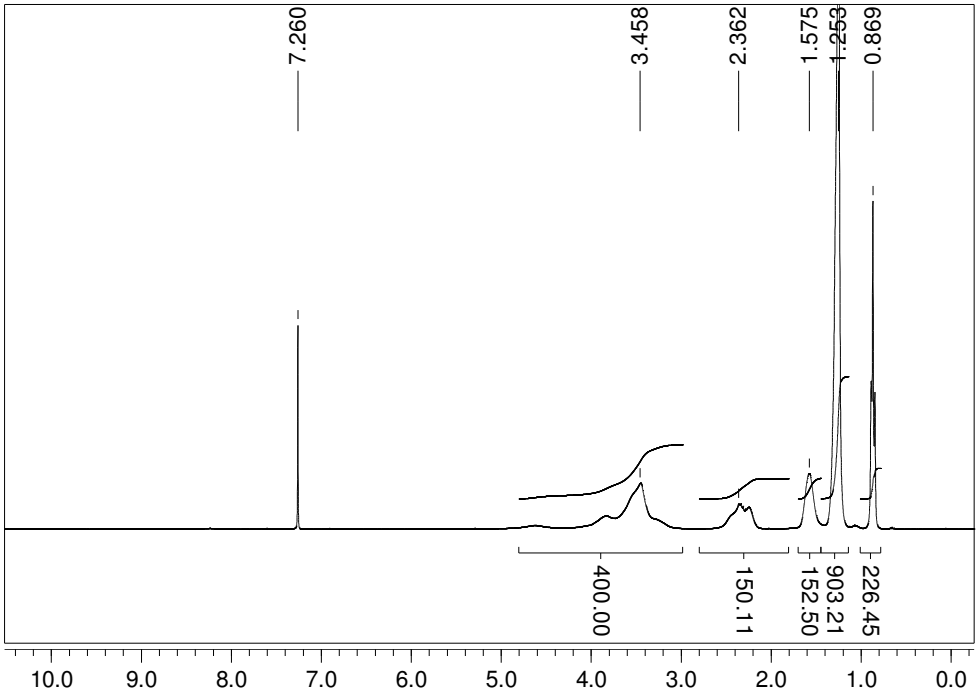

$pN_{50}A_{50}$

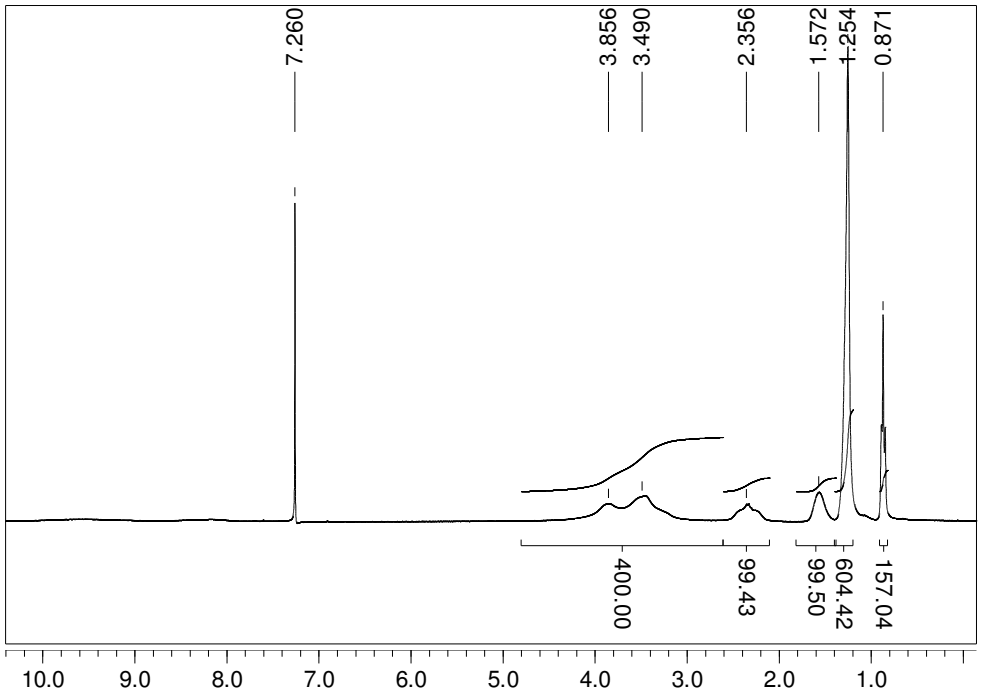

$pN_{25}A_{75}$

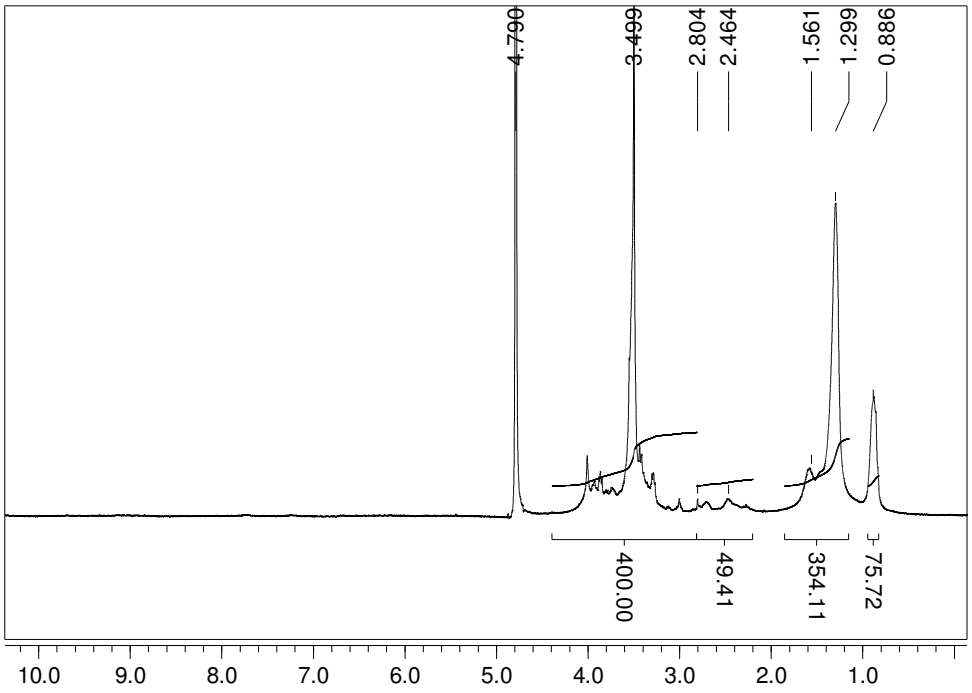
4.790
3.499
2.804
2.464
1.561
1.299
0.886
400.00
49.41
354.11
75.72
10.0
9.0
8.0
7.0
6.0
5.0
4.0
3.0
2.0
1.0

8 References

1) J.M. Colwill, J.M. Cultice, R.L. Kinse, *Health Affairs (Milwood)* **2008**, *77*, 232.

2) B.L. Plasssman, K.M. Langa, G.G. Fisher, S.G. Heeringa, D.R. Weir, M.B. Ofstedal, J.R. Burke, M.D. Herd, G.G. Potter, W.L. Rodgers, D.C. Steffens, R.J. Willis, R.B. Wallace, *Neuroepidemiology* **2007**, *29*, 125.

3) M.B. Brown, G.P. Martin, S.A. Jones, F.K. Akomeah, *Drug Delivery* **2006**, *13*. 175.

4) J. Panyan, V. Labhasetwar, *Adv. Drug Delivery Rev*. **2012**, *64*, 61.

5) K. Kataoka, A. Harada, Y. Nagasaki, *Adv. Drug Delivery Rev*. **2012**, *64*, 37.

6) A. Bianco, K. Kostarelos, M. Prato, *Curr. Opin. Chem. Biol*. **2005**, *9*, 674.

7) D. Schmaljohann, *Adv. Drug Delivery Rev*. **2006**, *58*, 1655.

8) Y. Qin, K. Park, *Adv. Drug Delivery Rev*. **2012**, *64*, 49.

9) S.R. Harris, E.J. Feil, M.T.G. Holden, M.A. Quail, E.K. Nickerson, N. Chantratita, S. Gardete, A. Tavares, N. Day, J.A. Lindsay, J.D. Edgeworth, H. de Lencastre, J. Parkhill, S.J. Peacock, S.D. Bentley, *Science* **2010**, *327*, 469.

10) L. Nordstierna, A.A. Abdalla, M. Masuda, G. Skarnemark, M. Nydén, *Prog. Org. Coat*. **2010**, *64*, 45.

11) E.-R. Kenaway, S.D. Worley, R. Broughton, *Biomacromolecules* **2007**, *8*, 1359.

12) N. Adams, U.S. Schubert, *Adv. Drug Delivery Rev*. **2007**, *59*, 1504.

13) R. Hoogenboom, *Macromol. Chem. Phys.* **2007**, *208*, 18.

14) R. Hoogenboom, *Angew. Chem. Int. Ed.* **2009**, *48*, 7978.

15) D. A. Tomalia, D. P. Sheetz, *J. Polym. Sci. Part A: Polym. Chem.* **1966**, *4*, 2253.

16) T. Kagiya, S. Narisawa, T. Maeda, K. Fukui, *J. Polym. Sci. Part B: Polym. Lett.* **1966**, *4*, 441.

17) W. Seeliger, E. Aufderhaar, W. Diepers, R. Feinauer, R. Nehring, W. Thier, H. Hellmann, *Angew. Chem. Int. Ed.* **1966**, *5*, 875.

18) T. G. Bassiri, A. Levy, M. Litt, *J. Polym. Sci. Part B: Polym. Lett.* **1967**, *5*, 871.

19) R. Hoogenboom, M.W.M. Fijten, U.S. Schubert, *J. Polym. Sci. Part A: Polym. Chem.* **2004**, *42*, 1830.

20) P. Buzin, G. Schwarz, H.R. Kricheldorf, *J. Polym. Sci. Part A: Polym. Chem.* **2008**, *46*, 4777.

21) S. Gabriel, *Chem. Ber.* **1889**, *22*, 1139.

22) R. Wiley, L.L. Bennett, *Chem. Rev.* **1949**, *44*, 447.

23) J.A. Frump, *Chem. Rev.* **1971**, *71*, 483.

24) H. Witte, W. Seeliger, *Liebigs Ann. Chem.* **1974**, 996.

25) H.-J. Krause, P. Neumann, Process for the preparation of 2-alkyl- and 2-alkenyl-oxazolines. EP 0315856 B1 (**1995**).

26) T. Bodner, L. Ellmaier, V. Schenk, J. Albering, F. Wiesbrock, *Polym. Int.* **2011**, *60*, 1173.

27) C.O. Kappe, *Angew. Chem. Int. Ed.* **2004**, *46*, 6250.

28) C. Ebner, T. Bodner, F. Stelzer, F. Wiesbrock, *Macromol. Rapid Commun.* **2011**, *32*, 254.

29) K. Kempe, C. R. Becer, U. S. Schubert, *Macromolecules* **2011**, *44*, 5825.

30) F. Wiesbrock, R. Hoogenboom, U.S. Schubert, *Macromol. Rapid Commun.* **2004**, *25*, 1739.

31) F. Wiesbrock, R. Hoogenboom, C.H. Abeln, U.S. Schubert, *Macromol. Rapid Commun.* **2004**, *25*, 1895.

32) F. Wiesbrock, R. Hoogenboom, M.A.M. Leenen, M.A.R. Meier, U.S. Schubert, *Macromolecules* **2005**, *38*, 5025.

33) F. Wiesbrock, R. Hoogenboom, M.A.M. Leenen, S.F.G.M. van Nispen, M. van der Loop, C.H. Abeln, A.M.J. van den Berg, U.S. Schubert, *Macromolecules* **2005**, *38*, 7957.

34) R. Hoogenboom, F. Wiesbrock, H. Huang, M.A.M. Leenen, H.M.L. Thijs, S.F.G.M. van Nispen, M. van der Loop, C.A. Fustin, A.M. Jonas, J.-F. Gohy, U.S. Schubert, *Macromolecules* **2006**, *39*, 4719.

35) R. Hoogenboom, F. Wiesbrock, M.A.M. Leenen, H.M.L. Thijs, H. Huang, C.-A. Fustin, P. Guillet, J.-F. Gohy, U.S. Schubert, *Macromolecules* **2007**, *40*, 2837.

36) S. Sinnwell, H. Ritter, *Macromol. Rapid Commun.* **2005**, *26*, 160.

37) S. Sinnwell, H. Ritter, *Macromol. Rapid Commun.* **2006**, *27*, 1335.

38) R. Hoogenboom, M.A.M. Leenen, F. Wiesbrock, U.S. Schubert, *Macromol. Rapid Commun.* **2005**, *26*, 1773.

39) R. Hoogenboom, F. Wiesbrock, M.A.M. Leenen, M.A.R. Meier, U.S. Schubert, *J. Comb. Chem.* **2005**, *7*, 10.

40) M. Lobert, H.M.L. Thijs, T. Erdmenger, R. Eckardt, C. Ulbricht, R. Hoogenboom, U.S. Schubert, *Chem. Eur. J.* **2008**, *14*, 10396.

41) M. Lobert, R. Hoogenboom, C.-A. Fustin, J.-F. Gohy, U.S. Schubert, *J. Polym. Sci. Polym. Chem.* **2008**, *46*, 5859.

42) R. Hoogenboom, M.W.M. Fijten, H.M.L. Thijs, B.M. van Lankvelt, U.S. Schubert, *Des. Monomers Polym.* **2005**, *8*, 659.

43) R. Hoogenboom, U.S. Schubert, *Green Chem.* **2006**, *8*, 895.

44) Y. Qiu, K. Park, *Adv. Drug. Delivery Rev.* **2001**, *53*, 321.

45) O. Wichterle, D. Lim, *Nature* **1960**, *185*, 117.

46) V. Percec, T.K. Bera , R.J. Butera , *Biomacromolecules* **2002**, *3*, 272.

47) F.C. Gaertner, R. Luxenhofer, B. Blechert, R. Jordan, M. Essler, *J. Controlled Release* **2007**, *119*, 291.

48) Y. Bae, S. Fukushima, A. Harada, K. Kataoka, *Angew. Chem. Int. Ed.* **2003**, *42*, 4640.

49) K. Y. Lee, D. J. Mooney, *Chem. Rev.* **2001**, *101*, 1869.

50) L. Brannon-Peppas, N. A. Peppas, *J. Controlled Release* **1989**, *10*, 5.

51) J. E. Puskas, Y. Chen, *Biomacromolecules* **2004**, *5*, 1141.

52) G. D. Prestwich, D. M. Marecak, J. F. Marecak, K. P. Vercruysse, M. R. Ziebell, *J. Controlled Release* **1998**, *83*, 93.

53) D. Campoccia, P. Doherty M. Radice, P. Brun, G. Abatabgelo, D. F. Williams, *Biomaterials* **1998**, *19*, 2101.

54) K. Knop, R. Hoogenboom, D. Fischer, U. S. Schubert, *Angew. Chem. Int. Ed.* **2010**, *49*, 6288.

55) K. Ulbrich, V. Subr, P. Podperova, M. Buresova, *J. Controlled Release* **1995**, *34*, 155.

56) Y. Chujo, K. Sada, K. Matsumoto, T. Saegusa, *Macromolecules* **1990**, *23*, 1234.

57) J. Rueda, R. Suica, H. Komber, B. Voit, *Macromol. Chem. Phys.* **2003**, *204*, 954.

58) J. C. Rueda, H. Komber, B. Voit, *J. Polym. Sci. Part A: Polym. Chem.* **2005***, 43,* 122.

59) Y.-H. Shin, S.-H. Yun, S.-H. Pyo, Y.-S. Lim, H.-J. Yoon, K.-H. Kim, S.-K. Moon, S.W. Lee, Y.G. Park, S.-I. Chang, K.-M. Kim, J.-H. Lim, *Angew. Chem. Int. Ed.* **2010**, *49*, 9689.

60) K. Kempe, A. Vollrath, H. W. Schaefer, T. G. Poehlmann, C. Biskup, R. Hoogenboom, U.S. Schubert, *Macromol. Rapid Commun.* **2010***, 21*, 1869.

61) I.C. Kwon, Y.H. Bae, S.W. Kim, *Nature* **1991**, *354*, 291.

62) M.N. Collins, C. Birkinshaw, *J. Appl. Polym. Sci.* **2008**, *109*, 923.

63) V. Percec, T.K. Bera, *Biomacromolecules* **2002**, *3*, 272.

64) H.S. Choi, T. Ooya, S. Sasaki, N. Yui, M. Kurisawa, H. Uyama, S. Kobayashi, *ChemPhysChem* **2004**, *5*, 1431.

65) Y. Chujo, K. Sada, T. Saegusa, *Polym. J*. **1993**, *25*, 599.

66) Y. Chujo, K. Sada, T. Saegusa, *Macromolecules* **1993**, *26*, 6320.

67) Y. Chujo, K. Sada, T. Saegusa, *Macromolecules* **1993**, *26*, 6315.

68) S.E. Kudaibergenov, Z.E. Ibraeva, N.A. Dolya, B.K. Musabaeva, A.K. Zharmagambetova, J. Koetz, *Macromol. Symp*. **2008**, *274,* 11.

69) Y. Murali Mohan, K.E. Geckeler, *React. Funct. Polym.* **2007**, *67*, 144.

70) I. Pantchev, R. Velichkova, L. Lakov, O. Peshev, E. Goethals, *Polymer* **1998**, *39*, 7089.

71) M. Nitschke, S. Zschoche, A. Baier, F. Simon, C. Werner, *Surf. Coat. Tech.* **2004**, *185*, 120.

72) A.E.-H. Ali, A.S. AlArifi, *J. Appl. Poly. Sci.* **2011**, *120*, 3071.

73) S. Francis, L. Varshney, K. Tirumalesh, *Radiat. Phys. Chem.* **2006**, *75*, 747.

74) Y.J.-J. Yuan, R.-H. Jin, *Langmuir* **2005**, *21*, 3136.

75) R.-H. Jin, Y. J.-J. Yuan, *Chem. Commun.* **2005**, 1399.

76) Y.J.-J. Yuan, R.-H. Jin, *J. Mater. Chem.* **2005**, *15*, 4513.

77) H. Kakuda, T. Okada, T. Hasegawa, *J. Phys. Chem. B* **2009**, *113*, 13910.

78) S. Navarro, A. Shkilnyy, B. Tiersch, A. Taubert, H. Menzel, *Langmuir* **2009**, *25*, 10558.

79) Y. Chujo, K. Sada, A. Naka, R. Nomura, T. Saegusa, *Macromolecules* **1993**, *26*, 883.

80) Y. Chujo, K. Sada, R. Nomura, A. Naka, T. Saegusa, *Macromolecules* **1993**, *26*, 5611.

81) Y. Chujo, K. Sada, T. Kawasaki, T. Saegusa, *Macromolecules.* **1990**, *23*, 2693.

82) Y. Chujo, K. Sada, T. Saegusa, *Macromolecules* **1990**, *23*, 2636.

83) D. Christova, R. Velichkova, E.J. Goethals, F.E. Du Prez, *Polymer* **2002**, *43*, 4585.

84) D. Christova, R. Velichkova, W. Loos, E.J. Goethals, F.E. Du Prez, *Polymer* **2003**, *44*, 2255.

85) C. Nardin, W. Meier, *Chimia* **2011**, *55*, 142.

86) J.C. Rueda, H. Komber, J.C. Cedron, B. Voit, G. Shevtsova, *Macromol. Chem. Phys.* **2003**, *204*, 947.

87) J.C. Cuggino, C.I. Alvarez Igarzabal, J.C. Rueda, L.M. Quinzani, H. Komber, M.C. Strumia, *Eur. Polym. J.* **2008**, *44*, 3548.

88) S.J. Kim, K.J. Lee, S.I. Kim, *J. Macromol. Sci. A* **2004**, *41*, 267.

89) S.J. Kim, K.J. Lee, I.Y. Kim, D.I. Shin, S.I. Kim, *J. Appl. Polym. Sci.* **2006**, *99*, 100.

90) H. Uyama, S. Kobayashi, *Chem. Lett.* **1992**, 1643.

91) G. David, B.C. Simionescu, A.-C. Albertsson, *Biomacromolecules* **2008**, *9*, 1678.

92) C.-W. Lee, H.-S. Park, M.-S. Gong, *Sensor Actuator B* **2005**, *109*, 256.

93) T.R. Dargaville, R. Forster, B.L. Farrugia, K. Kempe, L. Voorhaar, U.S. Schubert, R. Hoogenboom, *Macromol. Rapid Commun.* **2012**, *33*, 1695.

94) Y. Liang, T.W. Jensen, E.J. Roy, C. Cha, R.J. DeVolder, R.E. Kohman, B.Z. Zhang, K.B. Textor, L.A. Rund, L.B. Schook, Y.W. Tong, H. Kong, *Biomaterials* **2011**, *32*, 2004.

95) K. Zeng, Y. Liu, S. Zheng*., Eur. Polym. J.* **2008**, *44*, 3946.

96) A. Shkilnyy, R. Graf, B. Hiebl, A. T. Neffe, A. Friedrich, J. Hartmann, A. Taubert, *Macromol. Biosci.* **2009**, *9*, 179.

97) B. Unal, R.J. Klein, K.R. Yocca, R.C. Hedden, *Polymer* **2007**, *48*, 6077.

98) B. Unal, R.C. Hedden, *Polymer* **2009**, *50*, 905.

99) J. Ford, S. Yang, *Chem. Mater.* **2007**, *19*, 5570.

100) Y. Chujo, K. Sada, T. Kawasaki, T. Saegusa, *Polym. J.* **1992**, *24*, 1301.

101) S. Cesana, J. Auernheimer, R. Jordan, H. Kessler, O. Nyuken, *Macromol. Chem. Phys.* **2006**, *207*, 183.

102) Y.I.-H. Park, I.-S. Han, D.-K. Kim, T. Saegusa, *Angew. Makromol. Chem.* **1991**, *190*, 165.

103) Y. Chujo, Y. Yoshifuji, K. Sada, T. Saegusa, *Macromolecules* **1989**, *22*, 1074.

104) D.T. Glatzhofer, M.J. Erickson, R. Frech, F. Yepez, J.E. Furneaux, *Solid State Ionics* **2005**, *176*, 2861.

105) M. Chanda, G.L. Rempel, *Ind. Eng. Chem. Res.* **2003**, *42*, 5647.

106) G.V.N. Rathna, *J. Mater. Sci. Mater. Med.* **2008**, *19*, 2351.

107) K. Na, S. Kim, B. K. Sun, D. G. Woo, H.-M. Chung, K.-H. Park, *Biotechnol. Lett.* **2007**, *29*, 1447.

108) A. Richter, A. Janke, S. Zschoche, R. Zimmermann, F. Simon, K.-J. Eichorn, B. Voit, D. Appelhans, *New J. Chem.* **2010**, *34*, 2105.

109) T.E. Zewert, M.G. Harrington, *Electrophoresis* **1999**, *20*, 1339.

110) C.M. Homenick, H. Sheardown, A. Adronov, *J. Mater. Chem.* **2010**, *20*, 2887.

111) C.-H. Wang, G.-H. Hsiue, *J. Poly. Sci. Part A: Polym. Chem.* **2002**, *40*, 1112.

112) C.-H. Wang, G.-H. Hsiue, *Biomacromolecules* **2003**, *4*, 1487.

113) C.-H. Wang, G.-H. Hsiue, *J. Contr. Rel.* **2005**, *108*, 140.

114) X. Wang, X. Li, Y. Li, Y. Yhou, C. Fan, W. Li, S. Ma, Z. Fan, Z. Huang, N. Li, Z. Liu, *Acta Biomaterialia* **2011**, *7*, 4149.

115) S.C. Lee, S.W. Kang, C. Kim, I.C. Kwon, S.Y. Jeong, *Polymer* **2000**, *41*, 7091.

116) C. Kim, S.C. Lee, S.W. Kang, I.C. Kwon, S.Y. Yeong, *J. Polym. Sci. Part B: Polym. Phys.* **2000**, *38*, 2400.

117) C.-H. Wang, Y.-S. Hwang, P.-R. Chiang, C.-R. Shen, W.-H. Hong, G.-H. Hsiue, *Biomacromolecules* **2012**, *13*, 40.

118) M. Pulkkinen, J.J. Palmgren, S. Auriola, M. Malin, J. Seppälä, K. Järvinen, *Rapid Commun. Mass Spectrom.* **2008**, *22*, 121.

119) S.B. Lee, R.R. Koepsel, S.W. Morley, K. Matyjaszewski, Y. Sun, A.J. Russell, *Biomacromolecules* **2004**, *5*, 877.

120) Z. Cheng, X. Zhu, Z.L. Shi, K.G. Neoh, E.T. Kang, *Ind. Eng. Chem. Res.* **2005**, *44*, 7098.

121) G.J. Gabriel, A. Som, A.E. Madkour, T. Eren, G.N. Tew, *Mater. Sci. Eng.* **2007**, *57*, 28.

122) J.A. Lichter, K.J. Van Vliet, M.F. Rubner, *Macromolecules* **2009**, *42*, 8573.

123) J.C. Tiller, C.-J. Liao, K. Lewis, A.M. Klibanov, *Proc. Natl. Acad. Sci.* **2001**, *98*, 5981.

124) G. Seyfriedsberger, K. Rametsteiner, W. Kern, *Eur. Polym. J.* **2006**, *42*, 3383.

125) A.M. Klibanov, *J. Mater. Chem.* **2007**, *17*, 2479.

126) N. Pasquier, H. Keul, E. Heine, M. Moeller, *Macromol. Biosci.* **2008**, *8*, 903.

127) O. Toke, L. Cegelski, J. Schaefer, *Biochim. Biophys. Acta* **2006**, *1758*, 1314.

128) K.A. Brodgen, *Nat. Rev. Microbiol.* **2005**, *3*, 238.

129) H. Sato, J.B.J. Feix, *Biochim. Biophys. Acta* **2006**, *1758*, 1245.

130) P. Gilbert, L.E. Moore, *J. Appl. Microbiol.* **2005**, *99*, 703.

131) S.J. Ludtke, K. He, W.T. Heller, T.A. Harroun, L. Yang, H.W. Huang, *Biochemistry* **1996**, *35*, 13723.

132) K.J. Hallock, D.K. Lee, A. Ramamoorthy, *Biophys. J.* **2003**, *84*, 3052.

133) H.W. Hwuang, *Biochemistry* **2000**, *39*, 8347.

134) F.Y. Chen, M.T. Lee, H.W. Hwuang, *Biophys. J.* **2003**, *84*, 3751.

135) H. Steiner, D. Andreu, R.B. Merrifield, *Biochim. Biophys. Acta.* **1988**, *939*, 260.

136) E. Gazit, A. Boman, H.G. Boman, Y.Shai, *Biochemistry* **1995**, *34*, 11479.

137) Y.Shai, *Biochim. Biopolymers* **2002**, *66*, 236.

138) K. Lienkamp, A.E. Madkour, A. Musante, C. F. Nelson, K. Nüsslein, G.N. Tew, *J. Am. Chem. Soc.* **2008**, *130*, 9836.

139) S. Colak, C.F. Nelson, K. Nüsslein, G.N. Tew, *Biomacromolecules* **2009**, *10*, 353.

140) G.J. Gabriel, J.A. Maegerlein, C.F. Nelson, J.M. Dabkowski, T. Eren, K. Nüsslein, G.N. Tew, *Chem. Eur. J.* **2009**, *15*, 433.

141) C.J. Waschinski, V. Herdes, F. Schueler, J.C. Tiller, *Macromol. Biosci.* **2005**, *5*, 149.

142) C.J. Waschinski, J. Zimmermann, U. Salz, R. Hutzler, G. Sadowski, J.C. Tiller, *Adv. Mater.* **2008**, *20*, 104.

143) V.G. Correia, V.D.B. Bonifacio, V.P. Raje, T. Casimiro, G. Moutinho, C. Lobato da Silva, M.G. Pinho, A. Aguiar-Ricardo, *Macromol. Biosci.* **2011**, *11*, 1128.

144) Y.-J. Lu, K.-C. Wei, C.-C. M. Ma, S.-Y. Yang, J.-P. Cha, *Colloids Surf. B* **2012**, *89*, 1.

145) J. Suh, H.-J. Paik, B.K. Hwang, *Bioorg. Chem.* **1994**, *22*, 318.

146) O. Boussif, F. Lezoualc'h, M. A. Zanta, M.D. Mergny, D. Schermann, B. Demeneix, J.-P. Behr, *Proc. Natl. Acad. Sci. USA* **1995**, *92*, 7297.

147) E. Occhiello, M. Morra, G. Morini, F. Garbassi, D. Johnson, *J. Appl. Polym. Sci*. **1991**, *42*, 2045.

148) W. Paulus, Microbiocides for the Production of Materials - A Handbook, 1st edition, Chapman & Hall, London 1993.

149) N.T. Reichmann, A. Gründling, *FEMS Microbiol. Lett.* **2011**, *319*, 97.

150) B.R. Kim, J.E. Anderson, S.A. Mueller, W.A. Gaines, *Water Res* **2002**, *36*, 4433.

151) A. Sze, D. Erickson, L. Ren, L. Dongqing, *J. Colloid Interface Sci*.**2003**, *261*, 402.